COOPERATIVE RESEARCH REPORT

NO. 165

CURRENT METER DATA QUALITY

https://doi.org/10.17895/ices.pub.7957

ISBN 978-87-7482-630-9

ISSN 2707-7144

International Council for the Exploration of the Sea
Palægade 2-4, 1261 Copenhagen K
Denmark

May 1989

TABLE OF CONTENTS

PREFACE

High quality measurements, together with an understanding of the associated uncertainties, are essential for any scientific activity. Measurements provide both an initial inspiration for a theory or model and, separately, a test of its validity. Oceanographic measurements are additionally precious, being both difficult and expensive to obtain, so the extra efforts to minimize the potential for errors and to extract the maximum information from the measurements, commensurate with their quality, are judicious. To achieve these aims discussion sessions on data processing procedures and techniques are invaluable; with the bonus that the papers, if published in one volume, will provide a useful reference source both for novices and those not directly involved in the data processing.

Such a discussion is particularly timely for recording current meter data. These instruments have been deployed extensively over the past 20 years in studies of the temporal variability of the dynamics of oceans and continental shelf seas. For continental shelf seas these studies have led to a better understanding of their large scale depth-averaged response to tidal and wind forcing. Now, however, three-dimensional models are being developed of small scale processes, for instance of fronts of the vertical structure of currents and of circulation. All require more precise current measurements and usually involve the extraction of a weaker signal from a more energetic record. Developments in deep sea oceanography require similar improvements in accuracy and data quality. Over the period current meters have improved technically and new, remote, techniques are now being developed, particularly HF radar backscatter measurements of surface currents and acoustic doppler backscatter measurements of current profiles, both with their own data processing problems.

A session on current meter data quality was therefore convened at the ICES Statutory Meeting held in Bergen, Norway, in October 1988, succeeding previous similar sessions on CTD data quality in 1985 and 1987. This forms part of a continuing drive by the Hydrography Committee of ICES to disseminate information and to promote the exchange of ideas on data processing procedures and techniques with, in this case, additional objectives concerning the assessment of current meter data quality (for instance when banking data) and the improvement of the quality and the improvement of the quality of future measurements. The seven papers presented to the session fall broadly into two categories although there is some overlap - firstly those predominantly on the data processing procedures followed at various laboratories and secondly those on current meter intercomparisons (one of the few relatively objective methods of obtaining an indication of current meter data quality). Four papers are in the first category - on experiment design and data processing strategy, by Howarth; two on laboratory data processing procedures, for the Fisheries Research Laboratory, Lowestoft, by Medler and for the Scottish Marine Biological Association, Oban, by Griffiths & MacDougall; and finally on data banking, important for preserving the value of the data, by Rickards. Three papers are in the second category and cover intercomparisons of a wide variety of instruments from Aanderaa type to vector averaging current meters (Read et al. and Smith & Lawrence, including HF radar) to acoustic doppler current profilers (Østerhus & Golmen).

To conclude I have jotted some personal reflections on the session, in no particular order:-

No current meter is exempt from problems however good its reputation.

Accurate recovery from instrumental errors for any instrument in which internal computation is executed, for instance vector averaging current meters, is usually impossible.

Intercomparisons always raise doubts about records which otherwise would have been deemed to be of good quality.

Scatter plots are invaluable when determing data quality (both one component plotted against another recorded by the same instrument and one instrument against another). 'Banana' shaped plots should be viewed with distrust, unless independently corroborated.

With each analysis technique applied to the data further information on data quality is gained.

More effort needs to be given to developing error analysis procedures.

Scientists regard most commercial instrument manufacturers with deep suspicion, particularly if the manufacturer holds a monopoly. This is fostered by the difficulty of holding a meaningful two-way conversation with the manufacturer.

Much hope for future measurements is being placed on two particular instruments - a vector averaging electo-magnetic current meter and an acoustic doppler current profiler.

Regrettably there was a lack of papers devoted to deep sea concerns - the session was dominated by continental shelf seas.

The value, importance and relevance of such sessions.

M.J. Howarth

March 1989

CURRENT METER DATA PROCESSING

M.J. Howarth
Proudman Oceanographic Laboratory, Bidston Observatory,
Birkenhead, Merseyside, L43 7RA, U.K.

1. INTRODUCTION

Recording current meters have made the acquisition of current measurements in shelf seas and the deep ocean relatively easy. Reliable instruments are available from manufacturers at an affordable price which can be moored in the sea in a routine fashion and which, in most cases, on recovery are full of data. The data can then be transferred to a computer, processed and converted into believable currents in engineering units without too much difficulty. However, unless more thought and care has been applied to these procedures than is implied in the above outline, the meaning which can be attached to the resulting numbers is debatable and will probably have been completely lost if the measurements are referred to at a later date - a waste of effort and money.

In this paper I shall describe a complete scheme for acquiring meaningful current data - experiment design, instrument preparation and data processing. The twin aims of the scheme are ease of application without skimping, since time and manpower are always in demand, and data quality. Data quality not only includes trapping errors but, more importantly, trying to reduce their occurrence since in most cases it is difficult, if not impossible, to recover from serious or frequent errors in a manner in which doubts about the data content do not remain. The scheme has been designed with Aanderaa type current meters and shelf sea deployments in mind. However, each experiment is different and so for each type emphasis may need changing, more care in one aspect or less in another. In conclusion, the extension to more advanced instrumentation and new methods of current measaurement are discussed.

2. EXPERIMENT DESIGN

The first step, requiring some knowledge of the sea's dynamics, is to formulate realistic objectives (scientific or engineering). Following from these the experiments design parameters are estimated - where and when the measurements are to be made, the range of speeds anticipated, the required accuracy of the measurements and the space and time scales of the dynamics. The space scales determine the horizontal and vertical separation of the instruments, although an additional constraint is the (small) number of current meters usually available.

In this respect, recording current meters are far from ideal instruments since, although time variations are well measured, spatial variations are sparsely sampled. The time scales fix both the duration of the measurements and the sample interval, from the longest and shortest periods of interest, respectively. The sample interval should be shorter than half the shortest period of interest whilst the energy associated with periods shorter than this should be negligible. This presents a difficulty because of the wide range of periods encountered in the sea, from surface waves (1-20s) to a year and longer. Since to sample at a rate which would include all is beyond the capacity of currently available data loggers, several sampling schemes have been devised which utilize a relative energy minimum at periods from minutes to hours (between surface waves and turbulence on the one hand and internal motion, storms and tides on the other). Basically either the data are recorded frequently (1-2 Hz) in bursts with quiescent periods in between or the measurements are averaged before recording. Two common methods in the latter category are firstly to average the speed over the sample interval and record a spot direction and secondly vector averaging. In the former scheme, the times associated with the speed and direction measurements are different. This can easily be rectified by combining the average of two consecutive directions with the appropriate speed, or vice versa. More seriously, the radically different time constants of the speed and direction measurements lead to near surface measurements being badly corrupted by wave energy (Beardsley et al., 1981). In vector averaging the sensors are sampled rapidly (1-2 Hz), east and north components calculated and the results averaged over a sample interval. This scheme averages out wave energy satisfactorily when the speeds are measured as two orthogonal components (Weller and Davis, 1980).

Briefly, regarding sensors, their design, especially of speed sensors, has taxed many people and been the source of many papers (for instance papers in Dobson et al., 1980). Although the design of a sensor to measure steady horizontal currents accurately, applying one of many possible methods, is relatively easy, major difficulties occur when high frequency energy is significant - turbulence, high frequency mooring motion, and particularly wave orbital velocities, all of which inherently also involve vertical motion. Then the design of the sensors becomes more critical and in practice a more sophisticated (and expensive) current meter is necessary, for which the choice is very restricted. Because of waves, this particicularly applies to measurements in shallow seas and near to

the sea surface where vector averaging current meters with fast response linear sensors become obligatory. In these cases, alternative approaches not involving moored instrument should also be considered.

The appropriate current meter, which must also be reliable, robust and affordable, is then chosen, based on the above constraints on sensors, logger/battery capacity and sampling scheme. The mooring can now be designed. The first objective of the mooring is to survive so that the equipment is present at recovery. Conditions at sea are hostile - storms, corrosion, great pressures at depths - particularly for near surface measurements with an added complication in shelf seas and at the shelf edge of trawlers, and to some extent shipping. It is imprudent to expect 100% equipment recovery, let alone 100% data recovery - redundancy must be designed into the experiment both in terms of the number of moorings and meters and also in terms of the methods of recovery. When planning mooring positions it is not possible to deploy moorings anywhere, especially in shelf seas - not only are there physical constraints - depth, current strength, suitability of the sea bed (for instance sand-waves, steep slopes, sediment strength), extent of surface waves, proneness to marine fouling - but also human constraints - shipping lanes, oil rigs, pipelines, submarine cables, military reasons, areas/times of frequent trawling.

The overall accuracy of the measurements does not just depend on the attributes of the current meter in isolation, however well the sensors behave in laboratory tests, but more significantly on the meter's behaviour in the sea, as a unit with the mooring, where in addition the motion is always more chaotic than in the laboratory. Unfortunately there is no absolute standard against which a current meter can be tested, the best that can be done is to gain a feeling for its merit through intercomparisons at sea. Moorings pose two areas for concern. Firstly, the presence of the meter and of the mooring will locally alter the flow and, maybe, the Earth's magnetic field. Secondly, moorings are flexible and as such are unable to keep a meter stationary, fixed relative either to the sea surface or, more commonly, to the sea bed. Moorings move at high frequencies, through eddy shedding, strumming, the meter 'porpoising', or through wave action, and at low frequencies, deforming in response to the drag of the current. The effect of surface wave motion is greatest if the mooring has a surface buoy or if its sub-surface buoy is close to the surface, any such motion being transmitted down throughout the entire mooring (Gould and Sambuco, 1975). Surface waves make the measurement of currents close to the sea surface particularly

difficult not only being an integral part of the interpretation of the measurements, but also hindering the deployment of the meter with respect to the desired frame of reference and providing a difficult environment for the sensors to measure.

Mooring deformation can have two effects on data quality. Firstly, the wire will no longer be vertical, tilting the meter. This not only reduces the measured speed by the cosine of the angle but, more significantly, once narrow bounds are exceeded causes erroneous direction measurements, both by compasses and flux gate magnetometers. Secondly, the meter can be moved a significant distance vertically, especially in the deep sea where although currents may be weak the wire length is long. The interpretation of measurements is then complicated since the meter may have sampled different regimes at different times. The low frequency mooring deformation for a given current profile is relatively easy to predict with simple computer programs once the size, weight/buoyancy and drag coefficients of the meters, buoys and wires are known. Hence moorings can easily be designed with the appropriate stiffness provided by sufficient buoyancy, bearing in mind the size of anchor this entails and the breaking strain of the wire. It is advisable to fit at least one of the meters on each mooring with a pressure sensor, to record any vertical movement of the meter and to show when the meter was deployed and recovered and whether the mooring had been moved.

Deploying current meters in isolation severely limits the value of the resulting data. To interpret the data so that the sea's dynamics can be understood and predicted (the essence of any scientific or engineering application) the context of the time series measurement (of a two-dimensional vector at a single point in a three-dimensional and time varying world) needs establishing. Movement in the sea is driven by four forces - tide, wind, pressure gradient and density gradient - with the sea's reponse affected by the Earth's gravity and rotation by the sea's shape, by the water density profile, and by friction (both internal and at the sea bed). Information about these, particularly about the driving forces, is necessary, and can be obtained either from other agencies or as part of the experiment - for instance density measurements using a CTD or conductivity and temperature sensors fitted to the current meters, and measurements of the local wind, waves or sea surface elevations.

3. INSTRUMENT PREPARATION

Instrument preparation has two facets - calibrations and checks. The purpose of calibrations is to establish the factors needed to convert the data recorded by an instrument into engineering units, whilst the purpose of checks is primarily

to ensure, before deployment, that the meter is functioning and, secondly, that the calibration equations appear reasonable. The frequency of calibrations depends on the sensor, and particularly on its stability, for instance, for a rotor, the ratio of current speed to revolutions per second should not change with time. For many current meters the direction sensor has the greatest need of calibration since deviations of less than 1^0 from linear will corrupt an estimate of the mean current in an area of strong tidal currents (Gould, 1973). Aanderaa type current meters should have their compasses calibrated before each deployment, at least, and preferably after recovery at 10^0 intervals and at 1^0 intervals through the 'dead-space' formed by the terminals. The calibration is then most easily applied by creating an array converting every possible meter reading into a direction in degrees. Such a calibration is not difficult to do and the equipment can be readily constructed. However, calibrations are time-consuming and tedious and of little value unless both designed and executed with great care and attention to detail.

In vector averaging current meters the calibrations are applied internally, since the current is sensed frequently and the components calculated and averaged. The calibration constants themselves, particularly for direction, are often less accessible, being part of the software or hardware. The calibration of new remote sensing current meters, for instance HF radar and ADCPs, is often not possible since the current of a volume, not a point, is measured, and in a sense is not meaningful because the relationship of current strength to frequency shift is fixed a priori. Here only intercomparisons are possible. Calibrations, particularly over a period of time, together with evaluations and intercomparisons, are part of the process whereby confidence in an instrument is established. Evaluations involve both studying the literature and detailed laboratory tests carried out, once only perhaps, when a new type of instrument has been purchased. Even more so than for calibrations, the laboratory tests are expensive to conduct and require time, great care and attention to detail (for instance, Appell et al., 1983). For a speed sensor, for instance, the tests might incorporate a tow tank or flume test in uni-directional flow, as for a calibration, and also varying the heading and azimuth of the flow relative to the meter and a combination of a uni-directional flow and sinusoidal motion and establishing the time constants of the sensors.

After fully preparing an instrument for deployment it is wise to check that all aspects function, preferably at the expected working temperature - that each sensor works and that data are being rercorded. For the latter, a short segment

of data should be recorded on the working tape and translated - the small loss in data capacity will be more than compensated for by an increase in reliability. The sensors can be subject to simple tests, for instance determining the zero offsets for e-m or acoustic current meters by immersing them in a bucket of water or checking that rotor bearings are not sticking or, if necessary, that the meter balances by immersing it in a tank of sea water.

4. DATA PROCESSING

To process a current meter record more information than just the logged data is needed. The calibration constants, magnetic deviation and certain times are essential (see below), whilst the time, position and meter height or depth identify the record and descriptions of the meter, mooring and of the meter's condition on recovery are invaluable when assessing the quality of the data. The position fixes the water depth, which should also be measured at deployment and recovery, and, with time, the magnetic deviation (all direction sensors refer to the Earth's magnetic field). By storing the relevant information in a computer file and using it as the only source of data for the programs executed during data processing, mistakes can be reduced and the archival of the measurements facilitated. To interpret the current measurements in terms of dynamics other observations are also needed, as described earlier.

From the start and stop times of the meter and its sampling interval the number of scans can be estimated and compared with the actual number recorded and thence the timing error calculated. For most combinations of sample interval and duration two estimates of the number of scans should be the same, since quartz crystal clocks are typically rated at $\pm$ 2 seconds/day. However, scans can easily be added or lost both through logger or battery malfunctions and during translation, in which case an independent elapsed time or scan counter channel is invaluable to identify where any such glitches have occurred. Different methods of analysis can accommodate different levels of timing error - for most (including tidal analysis) $\pm$ 2 seconds/day is adequate whilst when low pass filtering even quite gross errors have little effect. The meaningful record lasts from the end of the deployment to the start of the recovery. It is beneficial to record the time the meter goes into and comes out of the water, events which can often, but not always, be identified in the record by a change in temperature, pressure or speed and unambiguously in a conductivity measurement (zero in the air). Since meters are frequently started sometime (days) before deployment it is often useful to identify a scan at a specified time an hour or so before deployment by spinning the rotor or cooling the temnperature sensor.

In outline, the basic steps in processing before the data are available for further analysis are:-

1. translation of the data so that it can be put into a computer
2. store the meaningful data in a computer file
3. check
4. edit
5. apply calibrations
6. plot
7. further checks and edits
8. simple statistics
9. archive.

Advances in technology are tending to simplify the process. For instance, it is relatively easy and quick to extract data from a solid state memory (as opposed to magnetic tape or a cassette) and store it on floppy disc (amalgamating steps 1 and 2); high powered graphics workstations make short work of steps 3 and 4 combined; vector averaging current meters, by their nature, apply calibrations internally, abolishing 5. However, not all advances are beneficial - the individual data values are tending to become less accessible, particularly for data assessment purposes. For instance, in any procedure involving internal averaging the accuracy of a sample may be diminished by a few erroneous values in a way which is not always easy to detect and which can only be edited by replacing the whole sample.

Timing checks have already been mentioned. Since current meter data (even when recorded by reliable meters) are noisy, simple checks applied to the data are usually sufficient - upper and lower bounds, detection of spikes and of constant values (especially zeroes). Two useful aids for determing the boundary between acceptable and unacceptable are histograms of the values and of their first differences and straightforward time series plot. Whether values deemed to be in error should be edited or flagged is to some extent a matter of choice although for any analysis which requires a uniformly spaced time series (filtering, spectral analysis but not least squares fits) editing is essential. Values should be edited only as a last resort by as simple a procedure as possible, for instance by linear interpolation. Difficulties arise if a significant proportion of values require editing, when some <u>a priori</u> knowledge is useful, and the procedure is then often iterative. For instance, in shelf seas the dominance of the tides can be applied if gaps longer than an hour need editing.

Plotting is a most important stage since this allows the ready comprehension of a large set of numbers (several thousand) leading to a rapid assessment of data quality and content. For checking the data, stacked time series plots and scatter plots (particularly good for directions) are invaluable. Other plots (histograms, cumulative frequency, progressive vector diagram, feather of stock plots) in general are more biased towards data content. This is also summarized by the calculation of simple statistics - the maximum and minimum value, mean, directional stability (Ramster et al., 1978), standard deviation and variance ellipse both for the data as observed and after low pass filtering, to remove tidal and internal energy. At this stage, the data can be checked further for consistency against expected values or neighbouring or previous measurements and further edited if necessary. Only then can the data be archived.

5. FURTHER ANALYSIS

To obtain a more detailed and quantitative understanding of the measurements and to relate them to theory, further analysis is necessary. In general, this is not a routine procedure, but requires careful thought and tailoring for each experiment. However, whatever analysis is carried out, the results should first be considered in relation to the information it contains concerning data quality. A wide range of techniques are available most of which are fairly easy to program, at least in a rudimentary fashion, with the aid of standard mathematical software packages such as NAG and IMSL. Three broad approaches are available - to study the variations either in time, in frequency or in space. Some techniques are reasonably standard, notably filtering, tidal analysis (for instance, Pugh, 1987), rotary spectral analysis (Mooers, 1973), least squares fits, regression analysis, principal component analysis and analysis for extremes (Pugh, 1987). Low pass filters are applied to remove high frequency energy, for instance tides in the study of meteorological forcing, and band-pass filters to study inertial and internal motion. In shelf seas, where tidal currents tend to dominate, tidal analysis (response or harmonic) is essential both for the study of tides per se and also so that residuals can be calculated when studying non-tidal motion, particularly with periods shorter than one day. Both aspects (the amplitudes and phases of the tidal constituents and the tidal residuals) provide fertile ground for data quality assessment. The vector nature of currents should be incorporated into the analysis procedure as far as possible - for instance, rotary spectral analysis - and results presented accordingly, for instance tidal or variance ellipses.

6. REMOTE MEASUREMENT TECHNIQUES

The content of this paper applies equally to new, remote, techniques for measuring currents such as HF radar surface current measurement (Prandle, 1987) and acoustic doppler current profilers (see Pinkel's chapter in Dobson et al., 1980). However, a few comments can be made. Firstly, these techniques acquire large volumes of data so that data processing procedures must be automated, with a consequent reduction in the emphasis on checking and editing. Secondly, the spatial coverage of the meaasurements is much greater, entailing different methods of presentation and analysis for the full benefit to be reaped. Thirdly, the measurements are qualitatively different from those by recording current meters, since average current in a volume is measured, not the current at a given point, and, therefore, probably better suited for comparison with numerical model predictions. Finally, for ship-mounted current profilers, neither the position nor the time of measurement is fixed, again suggesting that numerical model predictions will be more closely incorporated in the analysis of the measurements.

REFERENCES

Appell, G.F., Moorey, K.A. and Woodward, W.E. 1983. A framework for the laboratory testing of Eulerian current measuring device. IEEE Journ. of Oceanic Engineering, OE-8(1):2-8.

Beardsley, R.C., Boicourt, W.C., Huff, L.C., McCullough,J.R. and Scott, J. 1981. CMICE: A near-surface current meter intercomparison experiment. Deep-Sea Res., 28A(12):1577-1603.

Dobson, F., Hasse, L., and Davis, R. 1980. Air-Sea Interaction. New York:Plenum. 801 pp.

Gould, W.J. and Sambuco, E. 1975. The effect of mooring type on measured values of ocean currents. Deep-Sea Res., 22:55-62.

Gould, W.J. 1973. Effects of non-linearities of current meter compasses. Deep-Sea Res., 20:423-427.

Halpern, D., Weller, R.A.,Briscoe, M.G., Davis, R.E., and McCullough, J.R. 1981. Intercomparison tests of moored current measurements in the upper ocean. Journ. of Geophys.Res., 86(C1):419-428.

Mooers, C.N.K. 1973. A technique for the cross spectrum analysis of pairs of complex time series, with emphasis on properties of polarized components and rotational invariants. Deep-Sea Res., 20:1129-1141.

Prandle, D. 1987. The fine-structure of nearshore tidal and residual circulations revealed by HF radar surface current measurements. Journ. of Phys. Oceanography, 17(2):231-245.

Pugh, D.T. 1987. Tides, surges and mean sea level: a handbook for engineers and scientists. Chichester: John Wiley. 472 pp.

Ramster, J.W., Hughes, D.G. and Furnes, G.K. 1978. A 'steadiness' factor for estimating the variability of residual drift in current meter records. Deutsch. Hydrogr. Zeitschr., 31(6)230-236.

Weller, R.A. and Davis, R.E. 1980. A vector measuring current meter. Deep-Sea Res., 17(7A):565-582.

PROCEDURES FOR PROCESSING CURRENT METER RECORDS AT LOWESTOFT

K.J. Medler
Ministry of Agriculture, Fisheries and Food
Directorate of Fisheries Research
Fisheries Laboratory
Lowestoft, Suffolk NR33 OHT, England

INTRODUCTION

The Fisheries Laboratory has been deploying current meters in the European shelf seas for approximately twenty years. For the last ten years, moorings have been established in the deep waters of the North Atlantic Ocean. During this time, the facilities for processing records from the meters have changed considerably and the present system, using a HP1000 minicomputer, was initiated during 1983. This is a considerable improvement on the previous system, which used a remote mainframe, since it not only allows closer operator control but also provides much needed graphics facilities.

This paper outlines the procedure for processing current meter records on this system, beginning with the calibration of the meter sensors. Instances of meter malfunction, which result in data being rejected, are given.

CALIBRATION

No matter how much data is collected by an instrument, its value amounts to little if careful calibration of the sensors has not been predetermined. This is especially so with a current meter compass, since a small error in direction can lead to the calculation of misleading residuals (Gould, 1973; Talbot, 1977). Consequently, instruments are calibrated carefully before deployment, using a table which rotates both clockwise and anticlockwise and is fitted with cradles to enable up to four meters to be calibrated at one time. The meter rotors are made to rotate so as to simulate working conditions. Readings are made at ten degree intervals, during two clockwise and two anticlockwise rotations of the table. Further details of the calibration table are given by Talbot and Baxter (1975).

A calibration is accepted only if the range of values at each direction is not greater than four degrees, but it is usually no more than two degrees. If the range is greater than four degrees the calibration is repeated. If it again fails this criterion the meter compass is replaced.

Each meter is calibrated twice with individual instruments occupying different cradle positions and the calibration applied is a mean of these two calibrations. A comparison is made with previous calibration results to look for conformity or to identify occasions when changes appear to have occurred.

No individual calibration of the speed sensor is made. The speed sensors of some Aanderaa RCM4S (paddle-wheel type) and Plessey Mo21F meters have been calibrated using the tow tank facility at IOS, Wormley and the results of these tests have been used to modify the values of speed coefficients provided by the manufacturer. In fact, these tests showed that the appropriate values of speed coefficients for use with the RCM4S were closer to those cited by the manufacturer for their older RCM4 instrument.

Thermistors are fitted to most instruments and these are calibrated in a Guildline constant temperature bath. Platinum resistance thermometers are incorporated to calibrate high-resolution thermistors.

Pressure sensors, fitted to a few meters, are calibrated using a dead weight tester (Medler and Pearson, 1985).

DATA PROCESSING

Although a few recent meter acquisitions have a solid-state memory, eighty percent of the meters record on 1/4 inch magnetic tape. These are read using a Brennell tape deck coupled to an Applied Microsystems tape reader. The data are written to an Apricot personal computer and then transferred to the Hewlett Packard 1000 minicomputer. Once there, the instrument coded data are converted to real units, applying the compass corrections in the process. A listing of the data in both instrument and real units is obtained to enable the record to be scrutinized, amendments to be decided upon and timing discrepancies calculated. Amendments, for example the deletion of observations at the start and end of the record, are made before converting speed and direction to east and north components. These components are calculated after the two directions recorded at the start and end of the speed sampling interval are meaned. Very little smoothing of the data is undertaken by the processing programs. There is an option to impose a limitation on the amount of change in direction which may occur between adjacent readings at speeds greater than 21 cm s^{-1}; specifically a change in direction greater than 45^0 is smoothed and flagged. This is a legacy from some

20 years ago when meter compasses were probably less reliable and its use is being reviewed. Smoothing of directions is also invoked when a compass "gap" reading is recorded.

Speeds, directions, east and north components are plotted by computer to enable further examination of each record. These plots, with the previously described listings, are the principal method of validating data. They help to identify abnormal speeds, erratic directions and poorly-defined tidal streams. Further amendments are made if necessary.

Final versions of the records are archived on half-inch tape, together with a log-sheet file which details mooring identifier, latitude and longitude, meter height above seabed, etc.

In most instances, the need is for records of non-tidal flow and this is obtained at present by applying a Gaussian filter to the data (similar to Schmitz, 1974).

DATA LOSS

As explained previously, current meter records are validated by examination of listings and large-scale plots of the data. Over the years, this has identified a number of instances when a meter has malfunctioned, resulting in a loss of data:

A) Rotor turning, but either a breakdown of magnetic coupling between rotor and follower or reed switch fails to register rotations.

B) Rotor not turning, fouled with weed. From the time series of speed, the gradual accumulation of weed is often apparent.

C) Directions not being resolved. This could result from a stiff meter suspension or a meter being fouled by its mooring wire. Readily seen in impellor systems such as those fitted to Plessey meters, since the reverse rotor counter will operate if the instrument is not aligned into the flow.

D) Compass sticking. This may occur if the meter is inclined too far from the horizontal plane and can be a problem in fast tidal streams when in-line instruments are used. Usually obvious in the listing.

E) Worn compass. Some directions become repetitive, usually apparent from listing.

F) Non linearity of compass. Usually seen from the "scatter" plot of east v north components.

G) Encoder fault, when pin(s) stick. This is often manifest by the appearance of the value of the pin(s) in the listing (e.g., 0, 256, 512, 768 or 1023). Printing the value from the reference channel is useful in these instances since it too usually suffers.

H) Underrated power supply. Usually induces the same effect as G), but often shows in the compass channel first because of the extra current drain during clamping.

I) Electronic failure, (e.g., dry joints, circuitry broken). This does not always produce a total loss of data. A dry joint in the tapehead circuit may result in data not being written to tape when the tape is transported. This is usually seen by the absence of a signal when the tape is translated and by having less data than expected. Plessey Mo21F meters have a signal counter fitted. This can be useful when seeking occasions when the meter may have stopped, since if the circuitry dies the counter resets to zero.

J) Poor quality recording tape. Indicated by the appearance of suspect data at regular intervals.

Table 1 lists the frequency of these malfunctions in deployments since 1983. In many instances (e.g., malfunction A) only part of a record is lost, but in some instances (e.g., a meter being fouled by its mooring wire) no useful data will result. Partial loss of speed registration was particularly troublesome during 1986 and 1987 and affected many records from Plessey Mo21F current meters. The fault often occurred intermittently during the record and it was difficult to reproduce in the workshop. Eventually, the problem was traced to the reed switch fitted to these instruments. These have now been replaced and this particular malfunction has not recurred.

CASE STUDIES

Some meter malfunctions are readily seen from listings of the data, for example when rotations of the impellor of a Plessey Mo21F meter fails to register. Other evidence of poor performance is better detected when the data are plotted.

i) Stiff meter suspension. Figure 1 shows an extract from a Plessey Mo21F instrument which appeared to record sensible speeds and directions. A closer look, however, indicated that the current speed had to reach approximately 30 cm s^{-1} before the instrument changed its direction (from SW to NE and vice versa). The effect is most clearly seen in the time series of east and north components, where "spikes" indicate periods when the current had dropped to a minimum and was beginning to accelerate again before the instrument swung.

The diagnosis was confirmed by examination of the meter suspension.

ii) Directions not being resolved. One mooring in the Irish Sea during 1987 had a Plessey Mo21F and a Valeport BFM208 meter separated by 3 m. Both meters gave full records of twenty-eight days. Residuals calculated for these records are shown in Figure 2a,b, and clearly indicate that one of the instruments did not perform adequately. The "scatter plot" of east v north components for each instrument appear in Figure 2c, d. Both are questionable. The distribution recorded by meter 749 (Figure 2d) is clearly spurious, but had not been seen before in MAFF records and cannot be explained. The "scatter plot" from the Valeport meter 287 (Figure 2c) suggests that directions recorded on the WSW tidal stream are slightly too large. A correction to these directions was made empirically, and by adjustment of the form

$$\text{direction} = \text{direction} - 8^0$$
$$\text{for } 225^0 < \text{direction} < 315^0$$

gave a linear "scatter plot" (Figure 2e). It also resulted in a residual which was in very good agreement with that of meter 749 (Figure 2f). Although the residuals from this meter may be considered unreliable in view of earlier remarks, the SSW flow is in agreement with that obtained from a third meter on this mooring at 43 m depth (not shown).

iii) A third case study thought to show the result of excess tilt on an in-line instrument is illustrated by two meters positioned 3 m apart on Irish Sea mooring 87W5. When this mooring was recovered the subsurface buoy and both meters were on the sea bed. The data prior to the collapse of the meter-wire appeared sound, but the residuals from the in-line RCM4S and the A-frame-mounted Mo21F were markedly different during the final six day (Figure 3). A comparison of histograms of directions for the first 22 and final 6 days (Figure 4) shows that the Aanderaa instrument recorded significantly more values to the WSW than the Mo21F. A possible explanation is that the sinking of the subsurface buoy was gradual and that the increasing tilt was sufficient to exceed the capability of the in-wire instrument while the Mo21F continued to operate normally on its A-frame suspension.

iv) Compass non-linearity. Recently acquired "vector averaging" meters of both Valeport and Aanderaa manufacture have been deployed in a trial basis. Some of the records obtained produced "scatter plots" which suggest a lack of linearity in the compass directions. A typical example from a Valeport meter is shown in Figure 5. Insufficient use of these meters makes for caution, but the relatively

high proportion of records from these instruments which produce suspicious "scatter plots" is noteworthy. Details of the experiences of other users with these types of meters would be welcome. Read et al. (1988) describe one instance in which the apparent error was corrected with a relatively small correction, within the calibration tolerance of the compass.

SUMMARY

The method by which current meter records are processed at the MAFF Fisheries Laboratory has evolved during the past twenty years. In addition to describing this method, four case studies have been presented which indicate some of the instrument malfunctions which have occurred. It is difficult to define guidelines by which a record may be judged sound or invalid, each record having to be carefully scrutinized. Consideration was given to having the validation process an integral part of the processing suite of computer programs, but it was deemed impossible in view of the nature of the causes of unacceptable data. However, the present system does allow changes to be made if such changes result in an improvement. It is intended to replace the Gaussian filter by the "HILOW" filter (Cartwright, 1983) during 1988, since the latter has a better characteristic. Examination of current meter records using a tidal analysis program may assist in identifying suspect data and it is hoped to incorporate this shortly. A particular cause for concern is the possible error in compass direction which will produce significant errors in the residual flow, especially when it is perpendicular to the tidal current. It should also be noted that in two of the four case studies an indication of a meter malfunction was first apparent only because a second instrument was located within 3 m of it.

REFERENCES

Cartwright, D.E. 1983. On the smoothing of climatological time series, with application to sea level at Newlyn. Gepphys. J.R. astr. Soc., 75: 639-658.

Gould, W.J. 1973. Effects of non-linearities of current meter compasses. Deep-Sea Res., 20(4):423-427.

Medler, K.J. and Pearson, N.D. 1985. Calibration of the Guildline model 8705 digital CTD: effects of temperature on the pressure transducer. ICES, Doc. C.M.1985/C:14, 5 pp. (mimeo.)

Read, J.W., Medler, K.J. and Jones, S.R. 1988. Intercomparison of Valeport BFM208, Aanderaa RCM4S and Plessey Mo21F current meters in the Irish Sea (see this volume).

Schmitz, W.J. Jr. 1974. Observations of low frequency current fluctuations on the continental slope and rise near site D. Journ.Mar.Res., 32:233-251.

Talbot, J.W. and Baxter, G.C. 1975. The direction calibration of Plessey current recording meters. Fish. Res. Tech. Rep., MAFF Direct. Fish. Res., Lowestoft, (12):10 pp.

Talbot, J.W. 1977. The dispersal of plaice eggs and larvae in the Southern Bight of the North Sea. ICES, J.Cons.int.Explor.Mer, 37(3):221-248.

Table 1. Number of records affected by meter malfunction from deployment since 1983.

Exercise identifier	Malfunction code										Total
	A	B	C	D	E	F	G	H	I	J	
Sellafield, Irish Sea, 1983-1987	5		3						1		9
Selsey Bill, Engl.Channel,1985		2									2
Irish Sea, 1984-1985	2										2
Irish Sea, 1986	18		4				3				25
Irish Sea, 1987	13	3	3	1		3					23
North Sea, 1987						1					1
Irish Sea, 1988		2				1					3
Porcupine Bank, 1983-1984				N O N E							-
Charcot-Theta Gap, 1983-1984											-
Iberia Abyssal Plain, 1984-1985	1						1	2			4
Rockall, 1985-1986								6			6
Porcupine Bank, 1986-1987				N O N E							-
East Greenland, 1986-1987				N O N E							-
Neads 6, 1983-1984	1										1
Neads 6, 1984-1985								1			1
Neads 6, 1985-1986									1		1
Neads 6, 1986-1987				N O N E							-

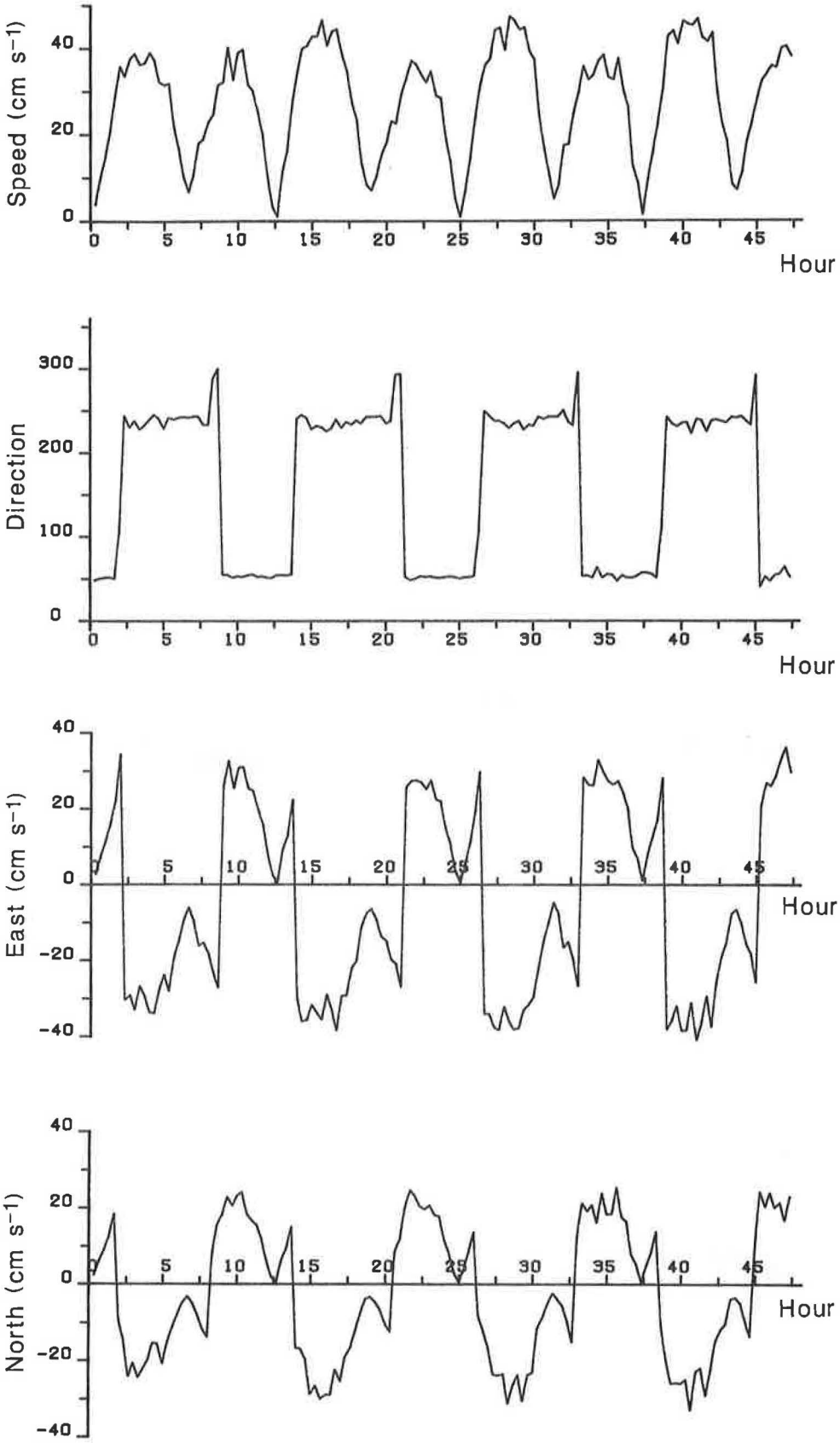

Figure 1. Speed, direction and east and north components from a current meter record which suffers from a stiff suspension.

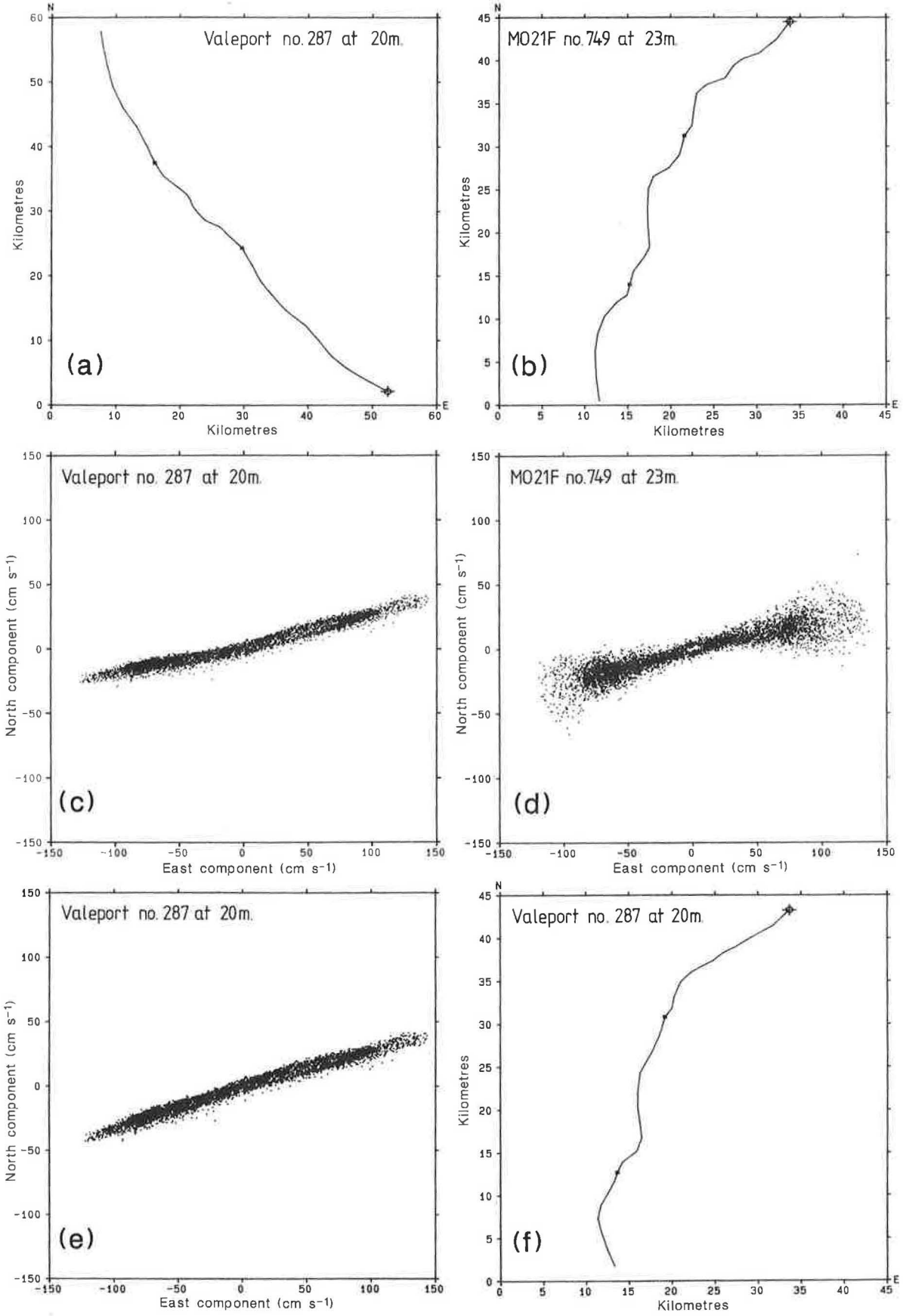

Figure 2a, b Progressive vector diagram of residuals from meter 287 and meter 749;
2c, d "Scatter plot" of east v north components, meter 287 and meter 749;
2e, f "Scatter plot" of east v north components and progressive vector diagram of residuals from meter 287 after 8 degree correction to the WSW directions.

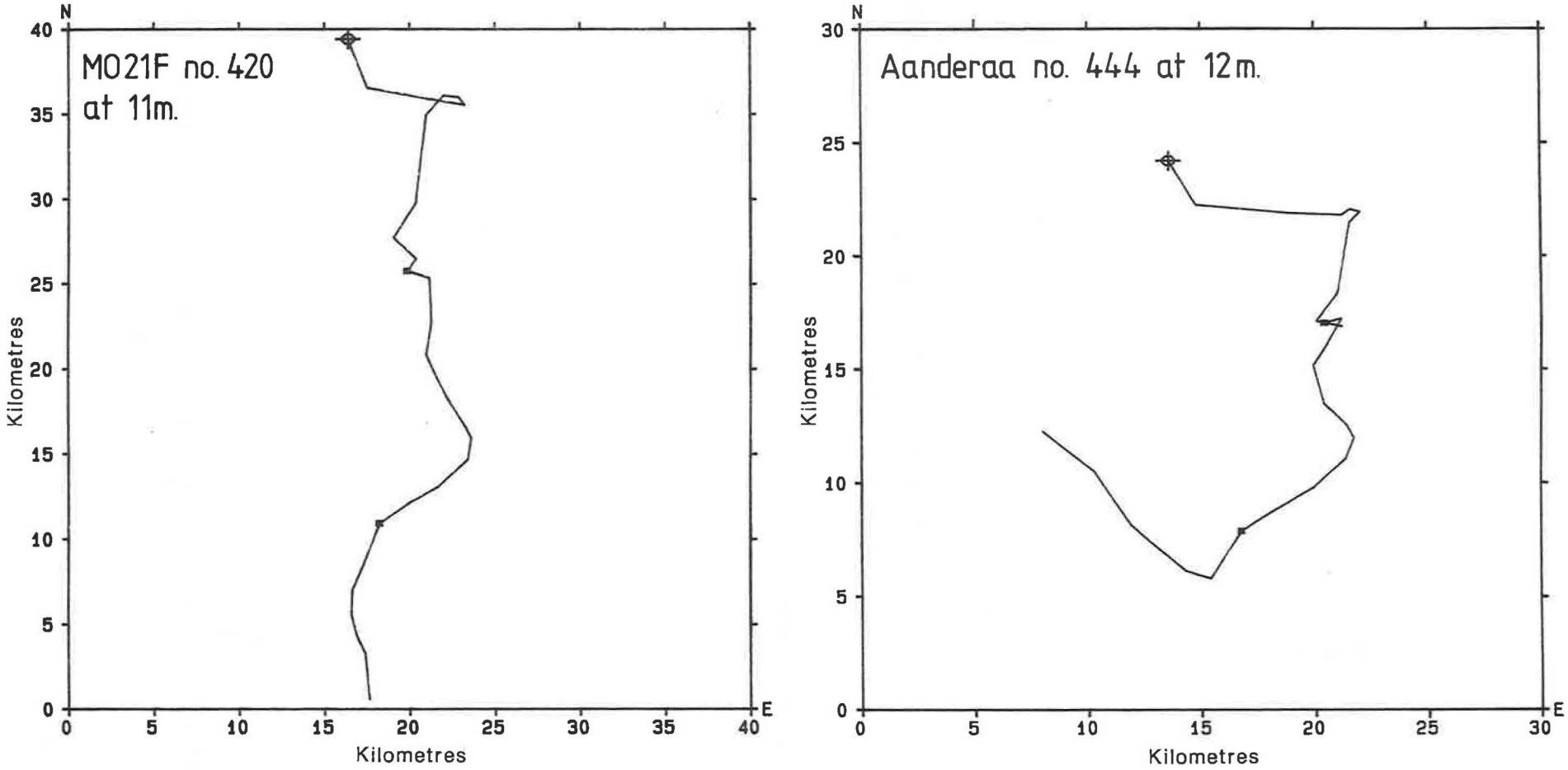

Figure 3. Progressive vector diagram of residuals from meter 420 and meter 444.

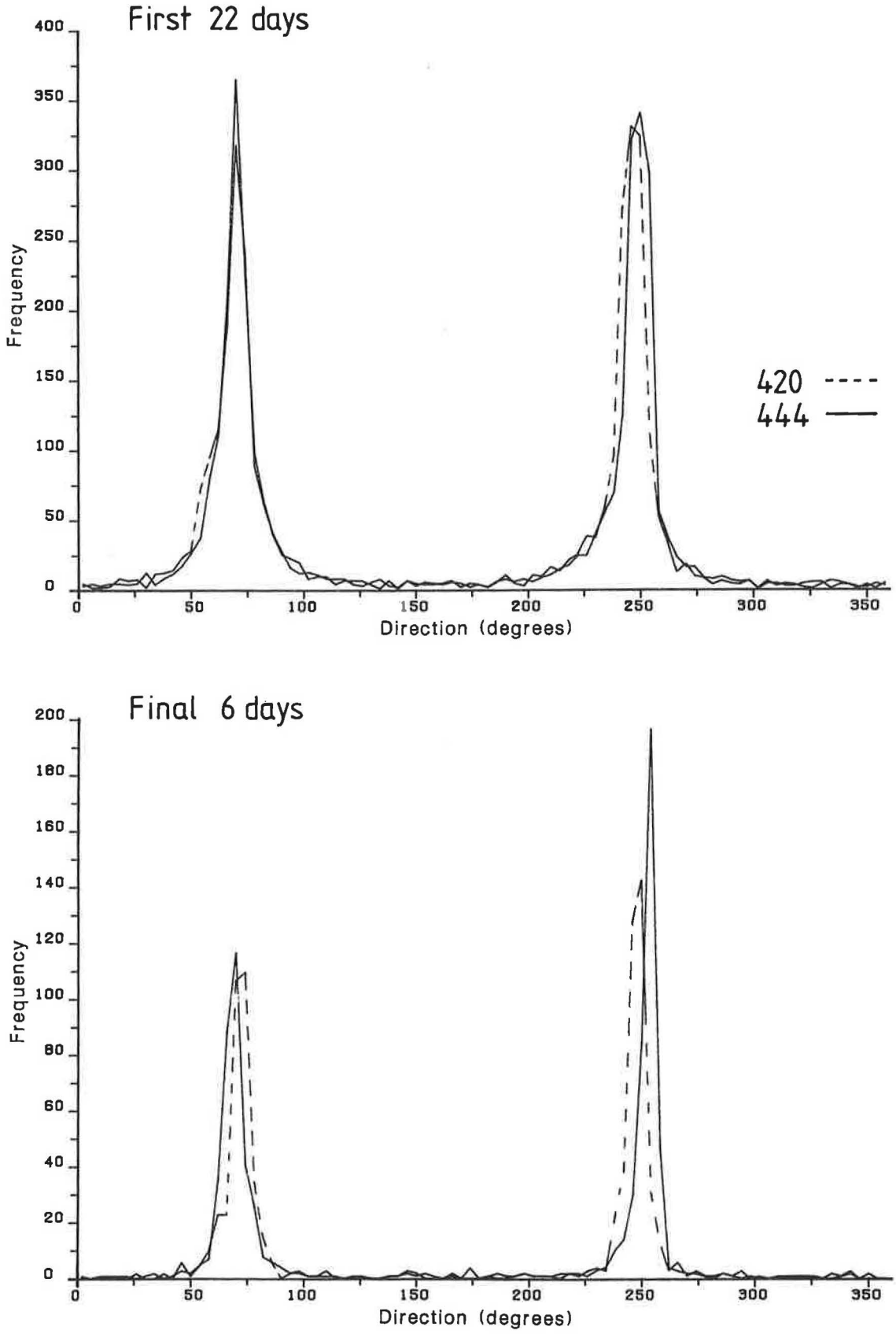

Figure 4. Frequency of current direction during the first 22 and final 6 days of records from meter 420 and meter 444.

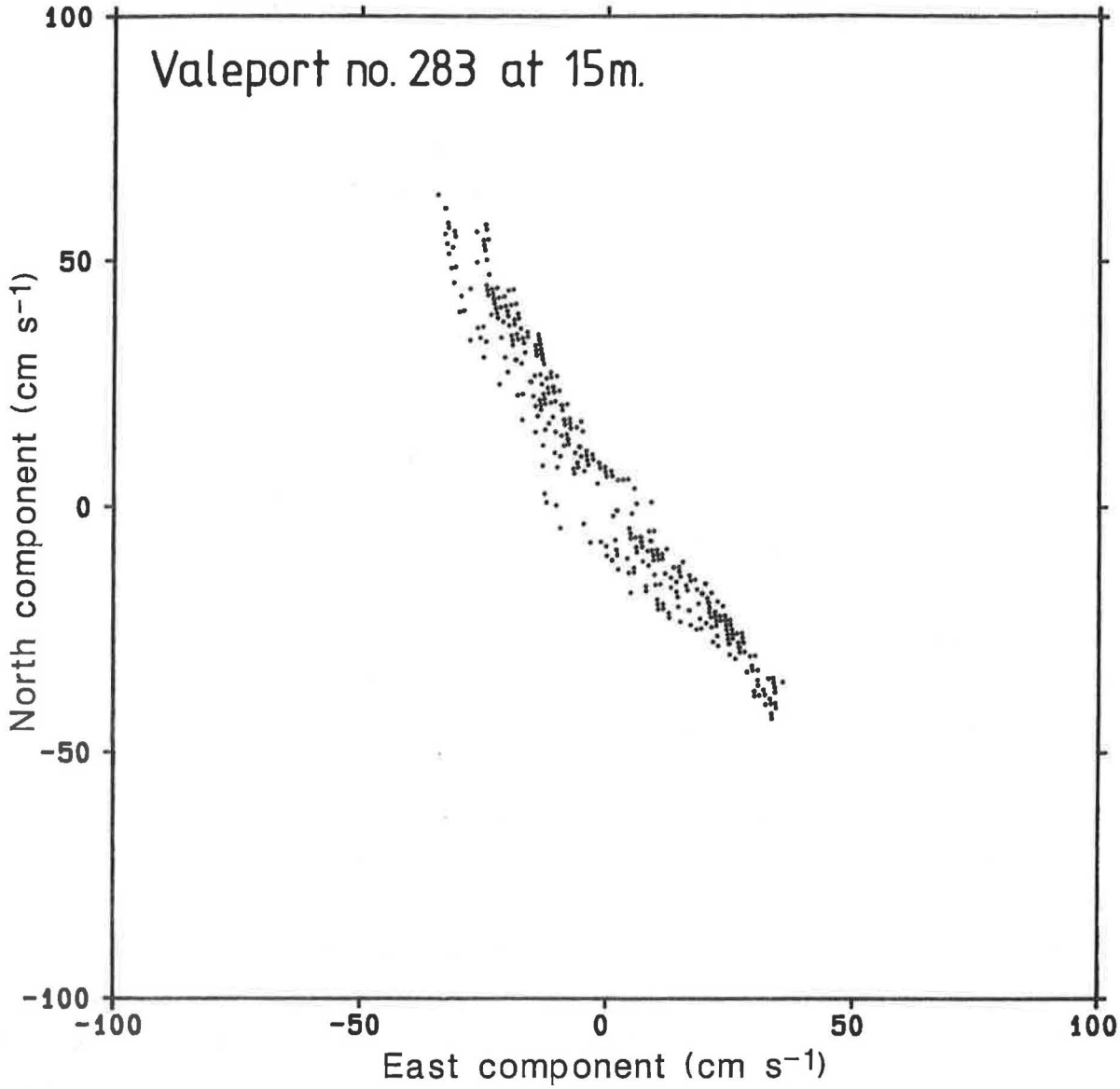

Figure 5. "Scatter plot" of east v north components, Valeport meter 283.

CURRENT METER USE AND ANALYSIS AT SMBA, OBAN

C.R. Griffiths and N. MacDougall
Scottish Marine Biological Association
P.O. Box 3, Argyll PA34 4AD, Scotland

INTRODUCTION

The SMBA Marine Physics Group still relies heavily on recording current meters to carry out its own research (and contracts). In addition, a service is provided for the rest of the laboratory. Activities can range from an hour's survey in a local sea loch to a six month deployment in the Rockall Channel.

In the last year there have been 42 mooring deployments. Over 10 years of current meter data were collected. Of the 84 current meters deployed only 3 were lost. A further 2 records were lost due to instrument malfunction.

The bulk of the work is done by RCM4/5s using both rotor systems. An increasing amount of work is being done by Interocean Electromagnetic 54 current meters.

Other instruments that have been deployed include the Bell Acoustic current meter, the Ocean Surface Current Radar (OSCR: Griffiths et al. 1985). More recently the RD Instruments Acoustic Doppler Current Profiler (ADCP) mounted on RRS Challenger has been used. Software is still to be developed to analyse this data. One Aanderaa RCM7 has recently been purchased.

BASIC-PROCESSING

The Aanderaa tapes are read into a PDP 11/23 mini computer using the X-talk terminal emulator package. The data is then plotted, a wild point searching program is run on the data, with the channels treated separately. No automatic editing is allowed, this is in part due to the fact that the speed and direction should be treated together. The wild point program is similar to the 'Turkey 53H' procedure which uses a Hanning smoothing filter. This routine is described by Otnes & Enochson (1978). The procedure uses the fact that the median is a robust estimator of the mean. In the case of a systematic error occurring in one or more channels in the data a subroutine is written to correct these. Any changes made to the data are recorded.

A calibration file is then created for each meter deployed. This will contain the relevant mooring information, times (GMT), local magnetic deviation and the calibrations for the individual sensors. A third order polynomial is used for the temperature, a linear relationship is used for the other sensors except direction.

The speed calibration includes the rotor count setting. The direction calibration consists of a look-up table, nominally every 30^0 although special emphasis is given to the dead space, 355^0 to 5^0. On input to the calibration program this look-up table is filled out using linear interpolation to produce a direction for every value. This table is checked to test that the direction spacing falls within given limits. The speed is calibrated from the average of adjacent values. The speed value is now centred in time to correspond with the spot measurement of the compass.

The program outputs the calibrated data in a standard SMBA format of time (GMT), day number, year, east and north components (true), temperature, and pressure and conductivity if fitted. If required the two latter can be converted to depth and salinity using equations from Saunders & Fofonoff (1976) and UNESCO (1981), 1983) respectively. Each calibrated data file is titled with a two line header. This contains the SMBA sequential mooring number and the instrument's serial number as well as all the relevant mooring information. The FORTRAN format of the data, the interval and number of scans are also included.

The calibration program also outputs basic statistics of the record, a table of daily means including the stability factor (Ramster et al. 1978), and a file used to plot histograms for the individual values of the various channels. A file to control all the plotting routines is the final output.

The data from the S4 is down loaded via an RS232 interface. The data is reformatted into the SMBA standard format. No additional calibrations are performed. The direction is corrected for the magnetic deviation, any timing error is corrected assuming a linear drift.

A Standard set of plots and tables is included in Appendix 1.

All calibrated data is banked with MIAS.

FURTHER ANALYSIS

Prior to any further analysis the data is reduced to hourly values. The data is prefiltered to avoid aliasing and hourly values are obtained using linear or cubic spline interpolation depending on the original interval.

The filter used is a general purpose filter known as HILOW, Cartwright (1980). This is applied again to produce long-period and tidal components. These time series are plotted and the basic statistics are derived. In certain cases the eddy kinetic energy will be derived from the long-period data (Dickson et al., 1986).

Routines are available to perform harmonic and spectral analyses for the various parameters. In the case of currents, the harmonic ellipse properties are computed along with rotary spectra. The harmonic constituents are chosen in accordance with the interval and the duration of the record. Related constituents can be included in the analysis. Errors can be calculated from the residual spectrum. As the harmonic analysis routine (T.I.R.A.) uses least squares, gaps in the record do not present a problem.

An extreme analysis package is being written. In the first instance the hourly tidal residual speeds are plotted on various probability scales. The desired return value is extrapolated from the distribution providing the best fit. The method will be extended to analyse current vectors combining both predicted and residual components (Carter et al., 1987; Pugh, 1987).

BASIC PROCEDURES

Prior to each deployment the Aanderaas are serviced in accordance with the manufacturer's manual. The meters are then run with tapes that have been degaussed on site. Calibrations are then performed as necessary. This test tape is then translated. This provides a good check of the instrument and the tape which is to be deployed.

More emphasis is put on the compass calibration than any other sensor. The SMBA has no facilities to calibrate the speed sensor although a zero check is performed on the S4. However, the two tank facilities at IOSDL have been used from time to time. The average calibration for the old rotor system is 3.3 and 40.0

with an average visual threshold of 2.7 cm/s. Only one new rotor system has been calibrated with values of 2.2, 46.2 and 3.5, respectively.

All relevant times are recorded during deployment and recovery of each mooring. These are checked with the data and then used to determine the start and end times of the record. The meters are checked over on recovery to see that the rotor is moving freely, there is no wear on the gimbal, and that the vane or fin have not been damaged. Any fouling is also recorded on the mooring sheets.

The calibrations for each Aanderaa deployment and the raw data plots are filed away. The minimum speed value is recorded as well as the performance of the compass dead space. It has proved useful to have a readily accessible case history for each instrument.

For any given deployment some initial research must be done to estimate the maximum speeds to be encountered. This will enable the rotor count to be set correctly as well as providing an upper speed limit for the design of the mooring. The rotor count will also be dependent on the interval set. The choice of interval will be limited by the expected duration of the deployment, even more so when, as a precaution, the expected duration is doubled. This will then allow for any delay in recovery. From experience it is best not to aim for a full tape from each deployment. It is quite common for a deterioration to occur in tape head and/or encoder performance. Once logging errors appear, the loss in data quality increases rapidly.

If the maximum observed current occasionally exceeds the given full scale, value data are not lost as the count is reset and then starts again. These values will appear in the wild point analysis and can be corrected during the editing stage. To discard such values would certainly underestimate any extreme values derived.

Moorings are designed using the SHAPE program developed at IOSDL (Barber, 1971) with the aim of minimising the knockdown of the instrument string in accordance with the specification of the instruments used. If the instrument is not gimballed or automatically tilt compensated then any knockdown will reduce the observed speed, though the proximity of the subsurface sphere to the sea surface can have the opposite effect with certain instruments. The compass will have a tilt limit for correct operation. In higher latitudes the angle of the earth's magnetic dip should also be considered. This is essentially a unidirectional phenomenon as illustrated by the first figure in Appendix II. This scatter plot

is from an S4 meter moored 2 m below the mean trough level; another S4 a further 3 m down on the same surface tail showed no such features on the scatter plot. The mooring was stiffened and redeployed at the same site off Flamborough Head and this time the scatter plot of the near surface S4 showed no such peculiarities.

Nonetheless this problem needed further investigation, especially as the instruments are usually deployed in a vector average mode. As with the compass calibration, no later corrections can be applied if the data is recorded in this mode.

The next figure in Appendix II shows the result of a simple tow experiment. The point of interest is the noise induced in the compass heading when a near-northerly flow was simulated, compared to the other cardinal points. Further tests are needed and firmware modifications are being discussed. Interocean recommend that at sites where magnetic inclinations of 70^0 (e.g., Oban) or more are expected, the mooring should be designed to prevent tilts exceeding 5 degrees.

ASSESSMENT OF DATA QUALITY

Many of the points already mentioned will contribute to the assessment of the data quality from a given instrument. Comparisons are frequently made between nearby instruments, especially meters on the same string. The Harmonic Analysis results are useful not only for comparisons with nearby meters and/or models, but also in determining if the measured residual is in any way distorted due to instrument malfunction. This is particularly true if a given site has been occupied on more than one occasion.

REFERENCES

Carter, D.J.T., Loynes, J. and Challenor, P.G. 1987. Estimates of extreme current speeds over the continental slope off Scotland. Inst. Oceanogr. Sci. Rep. No.239, 143 pp.

Cartwright, D.E., A. Edden, Spencer, R. and Vassie, J.M. 1980. The tides of the northeast Atlantic Ocean. Phil Trans. Roy. Soc. London, 298, 1436: 87-139.

Dickson, R.R., Gould, W.J., Griffiths, C.R., Medler, K.J. and Gmitrowicz, E.M. 1986. Seasonality in currents of the Rockall Channel. Proc. Roy. Soc. Edinburgh, 888: 103-125.

Griffiths, C.R., Booth, D.A., Eccles, D. and Bennett, F.D.G. 1985. Comparison of near-surface currents measured by Acoustic and Electromagnetic current meters with HF Radar current measurements. Int. Council Explor. Sea, Doc. C.M.1985/C:25 (mimeo).

Pugh, D.T. 1987. Tides, Surges and Mean Sea-Level. New York: John Wiley & Sons.

Ramster, J.W., Hughes, D. and Furnes, G. 1978. Steadiness factor for estimating the variability of residual drift in current meter records. Deutch. Hydrogr.Zeitschr., 31, H.6.

Saunders, P.M. and Fofonoff, N.P. 1976. Conversion of pressure to depth in the Ocean. Deep-Sea Res., 23.

UNESCO. Technical papers in Marine Science, Nos. 37 (1981) and 44 (1983).

Raw data time series

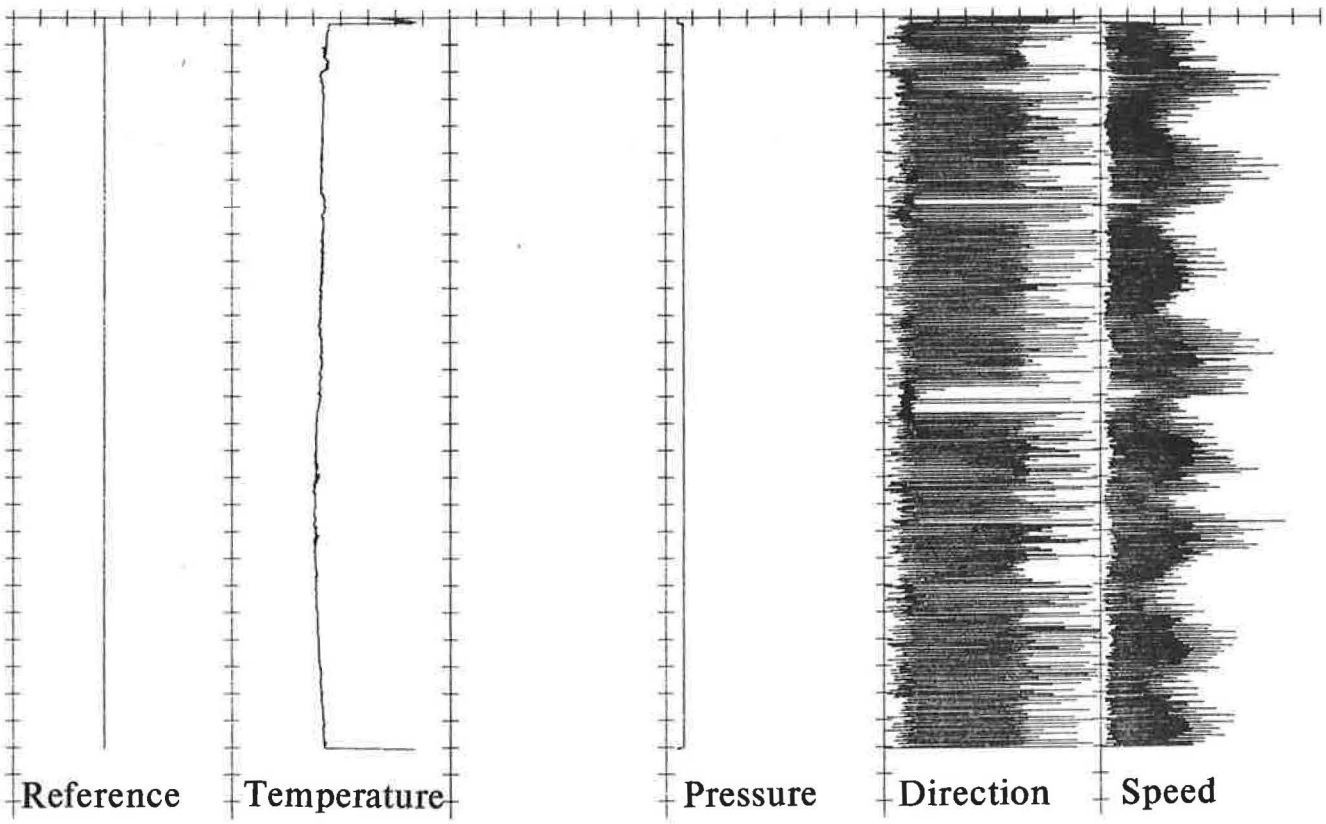

Raw data histograms

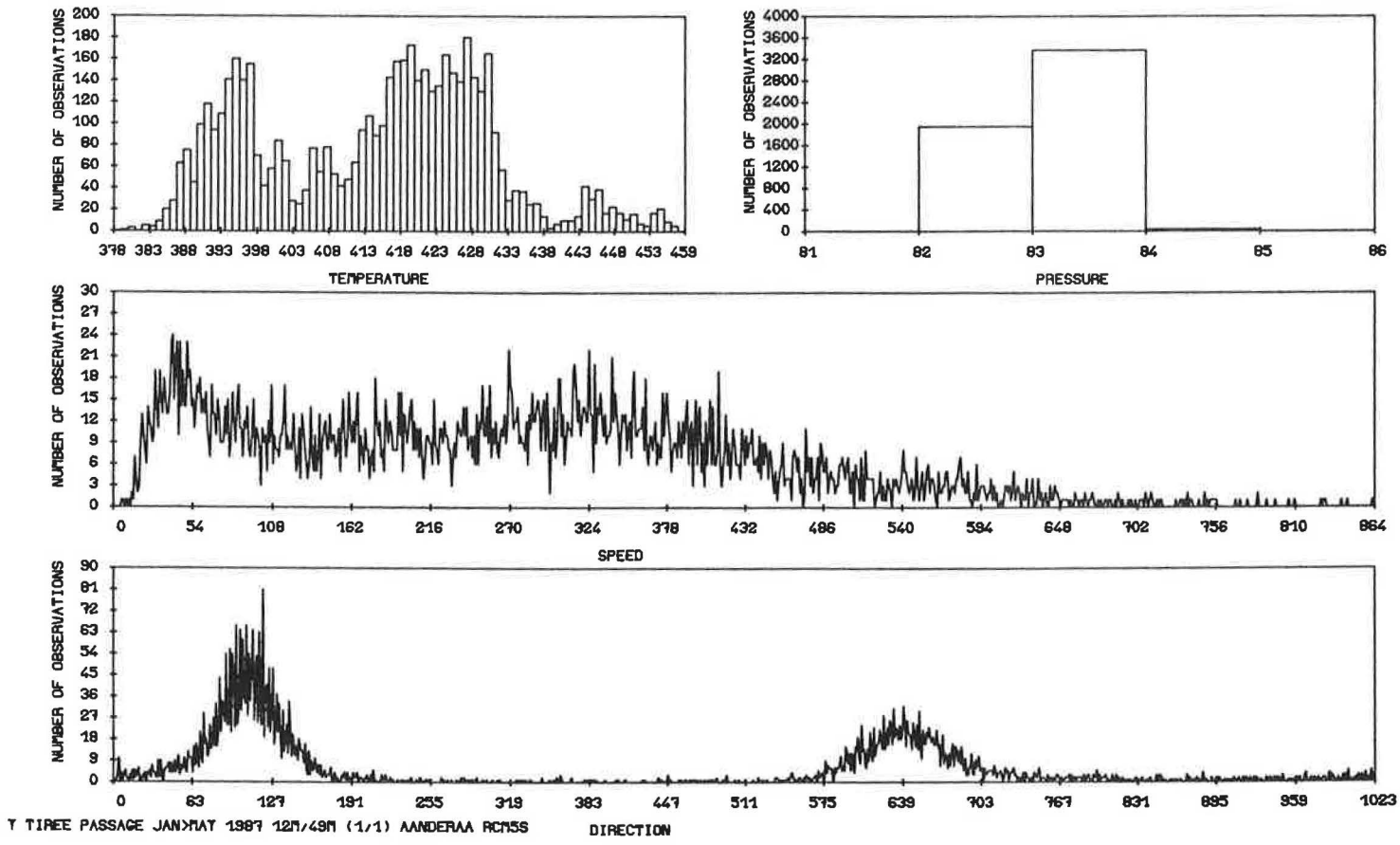

Y Tiree Passage Jan-Feb 1987 12m/49m (1/1) Anderaa RCM5s

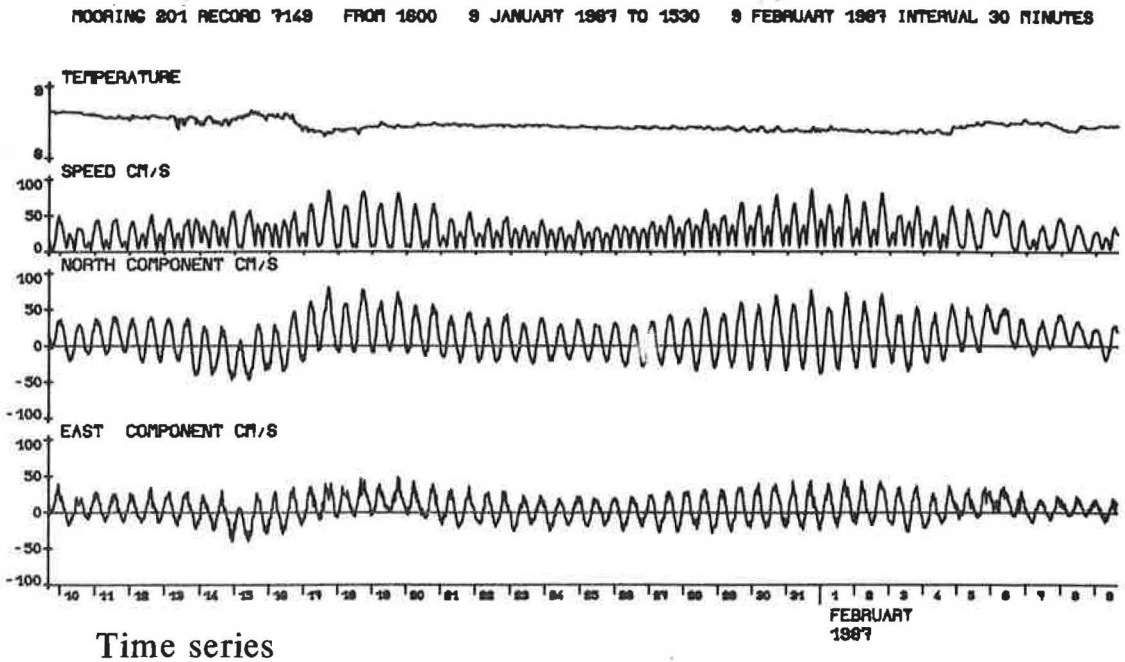

Time series

Progressive Vector Diagram

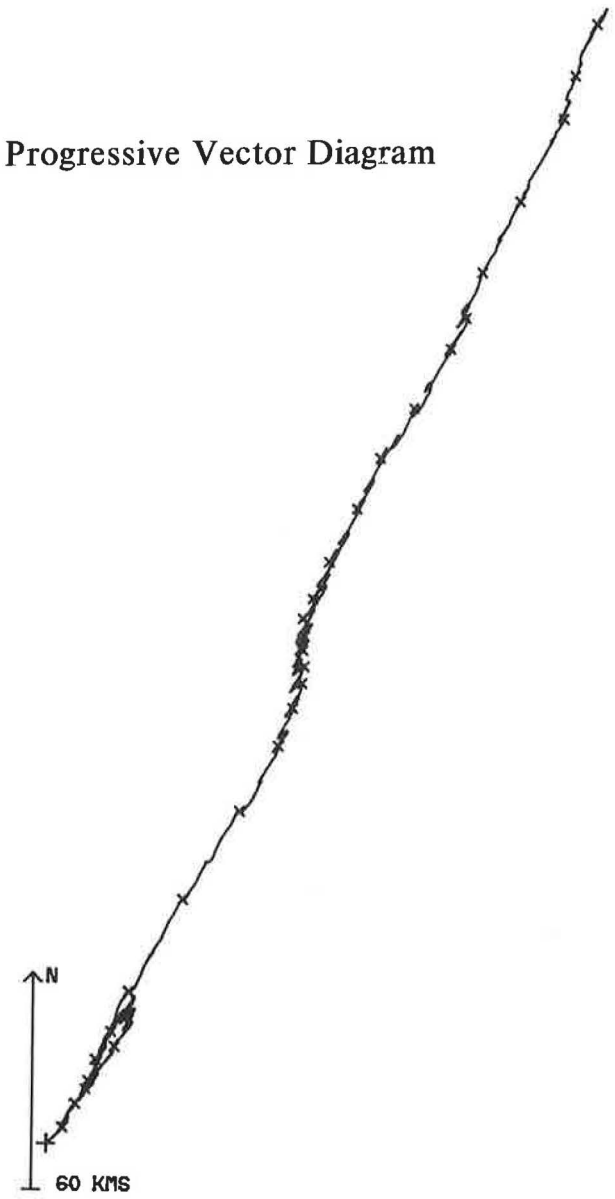

Scatter plot

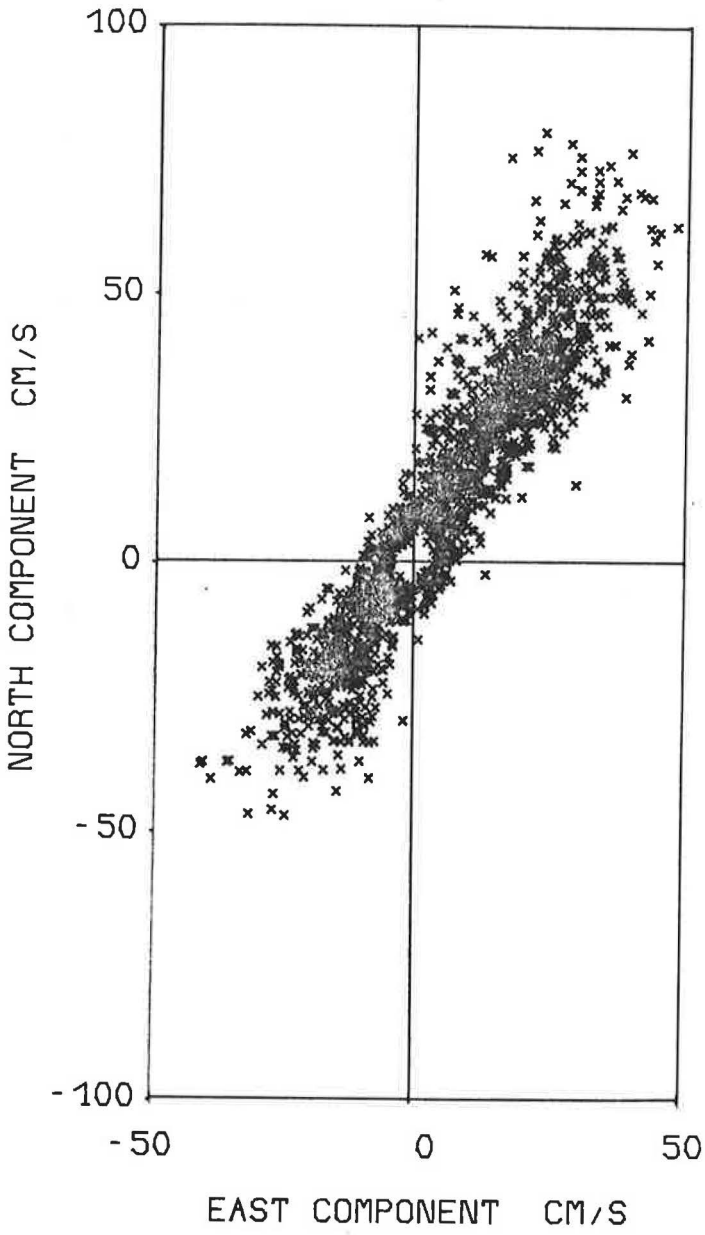

MOORING 201

Location	Tiree Passage
Position	N 56 37.6 W 6 23.2
Aims	W. of Scotland shelf dynamics
Meter No.	7149
Meter type	Aanderaa RCM5s
Water depth (m)	49
Height a.s.f. (m)	12
Posn. in sequence	1/1 BOTTOM
Rotor count (& max cm/s)	4 107.72cm/s
Sampling interval (mins)	30
Timing error	-0.16 sec/day (slow)
Data channels	4 Temp,Pres,Speed,Direction
Start of good data	1600 9 January 1987 (9)
End of good data	1530 9 February 1987 (40)
Duration of data (approx.)	31 days
Constancy factor (%)	87.5
S.Dev of daily means (cm/s)	East 5.9 North 10.1
Magnetic deviation (W -ve)	W 10.4

	Mean	S.Dev	Max	Min
Speed	28.1	17.8	86.5	2.9
Speed bits			820	17
Dirn. bits			1023	2
East comp.	5.7	16.5	48.9	-40.1
North comp.	11.7	25.8	80.3	-47.2
Temperature	7.4	0.2	8.0	6.9

Subsequent analysis: Harmonic,spectral,Hi & Lo pass filters

Comments: ALL recovered in good condition, 100 % data return, deep water pressure sensor used.

7149.201 Y TIREE PASSAGE JAN>FEB 1987 12M/49M (1/1) AANDERAA RCM5S

Daily Means	EAST	NORT	SPED	TEMP
10/ 1/87	3.95	7.54	19.38	7.88
11/ 1/87	6.67	14.44	22.24	7.71
12/ 1/87	4.97	9.14	23.35	7.70
13/ 1/87	4.66	4.83	27.99	7.60
14/ 1/87	-3.04	-8.31	26.82	7.53
15/ 1/87	-9.28	-13.85	28.57	7.77
16/ 1/87	0.93	2.22	26.83	7.63
17/ 1/87	12.45	28.43	37.13	7.11
18/ 1/87	16.69	29.64	37.71	7.20
19/ 1/87	17.72	28.33	35.86	7.31
20/ 1/87	12.41	20.76	29.48	7.36
21/ 1/87	4.42	11.91	25.78	7.36
22/ 1/87	2.85	7.90	24.50	7.33
23/ 1/87	0.38	5.08	22.68	7.33
24/ 1/87	-0.67	5.10	20.78	7.29
25/ 1/87	0.51	4.31	20.19	7.26
26/ 1/87	-0.75	-0.47	22.60	7.24
27/ 1/87	0.32	6.38	27.24	7.25
28/ 1/87	3.29	6.85	31.19	7.24
29/ 1/87	5.49	11.92	33.41	7.19
30/ 1/87	8.94	17.26	36.26	7.16
31/ 1/87	7.40	16.30	37.69	7.13
1/ 2/87	10.61	15.74	37.00	7.16
2/ 2/87	11.54	18.79	36.71	7.10
3/ 2/87	4.94	9.91	31.11	7.11
4/ 2/87	4.63	14.16	29.83	7.12
5/ 2/87	11.79	22.35	29.08	7.40
6/ 2/87	14.03	26.96	31.58	7.46
7/ 2/87	3.36	13.34	19.13	7.43
8/ 2/87	6.58	16.97	19.21	7.23

STABILITY FACTOR= 87.48% OVER 30 DAYS

EAST COMPONENT MEAN= , 5.59 DEVIATION OF DAILY MEANS= 5.92

NORT COMPONENT MEAN= , 11.80 DEVIATION OF DAILY MEANS= 10.07

APPENDIX 2

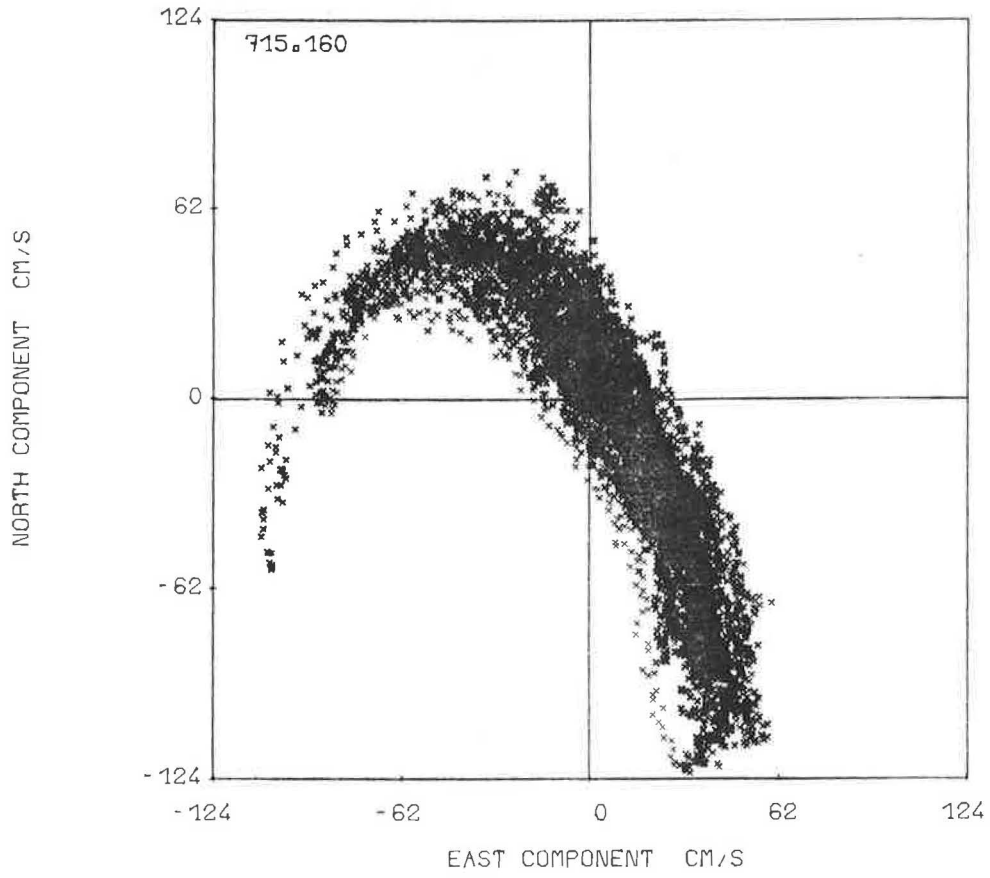

MOORING 160 RECORD 715 FROM 2102 30 JULY 1985 TO 1612 21 AUGUST 1985 INTERVAL 5 MINUTES

S4 TOWED BEHIND SEOL MARA USING 3 FLOATS 15 APRIL 88

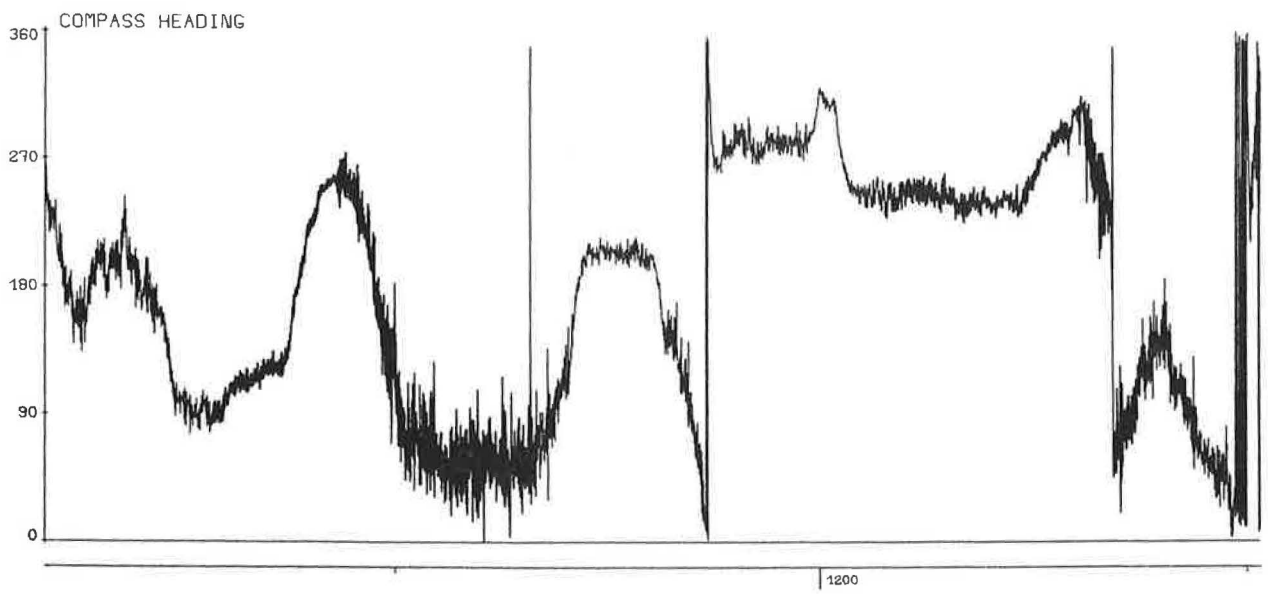

MOORING 222 RECORD 958 FROM 1141 15 APRIL 1988 TO 1210 15 APRIL 1988 INTERVAL 29 SECONDS

THE UK NATIONAL OCEANOGRAPHIC DATA CENTRE - CURRENT METER DATA QUALITY CONTROL AND BANKING

L. J. Rickards
Marine Information and Advisory Service
Proudman Oceanographic Laboratory
Bidston Observatory, Birkenhead
Merseyside L43 7RA UK

INTRODUCTION

The Marine Information and Advisory Service (MIAS) was set up in 1976 by the Natural Environment Research Council to establish a national archive of oceanographic data and to serve as a focal point for the provision of advice and information about the sea, particularly on waves, currents, sea temperatures/salinities, and sea levels.

There are two aspects to the service:

i) An Advisory and Enquiry Service which is based at the Deacon Laboratory of the Institute of Oceanographic Sciences, Godalming, Surrey, UK.

ii) A Data Banking Service which acts as the UKs National Oceanographic Data Centre and is located at the Proudman Oceanograhic Laboratory, Bidston Observatory, Birkenhead, UK.

As the UKs National Oceanographic Data centre, MIAS has three main functions:

i) to create, develop, and maintain a National Oceanographic Data Bank,

ii) to make oceanographic data available in a useful form to industry, research workers, and local and central government departments,

iii) to collaborate with other data centres in the international exchange of oceanographic data.

The UK National Oceanographic Data Bank was created to protect the long-term value of oceanographic data and to make the data readily available in a form convenient to users. It also provides a research facility in its own right, by bringing together into the same common system and format a wide range of data from many different sources.

To be fully effective, an oceanographic data bank must be viewed as more than simply a collection of numerical values; these must also be qualified by additional information concerning methods of measurement and subsequent data processing. It is neither desirable nor practicable to bank data simply because they have been collected, and standards need to be imposed on the quality and long-term value of the data that are accepted.

DATA SCOUTING AND CURRENT METER INVENTORY

An essential prerequisite to the data banking activities themselves is a detailed knowledge of the oceanographic data that are available from UK organizations. To this end, a data scout is employed to visit groups involved in oceanographic work, not only to ascertain their data holdings and future plans but also to gain familiarity with their techniques of data collection and processing. The information obtained during the 'data scouting' work is collated into the form of a catalogue or inventory. The MIAS current meter inventory contains over 6,000 entries for current meter series collected by UK laboratories. Of these, nearly 5,000 series have returned data; for the remainder the meters have either been lost or malfunctioned so no data are available. MIAS hold 3,500 data series (i.e., 70% of that available) from 40 laboratories; this comprises approximately 4,500 months of data. A limited amount of non-UK current meter data from international projects such as JONSDAP'76 and JASIN78 is also held.

Each current meter deployment known to MIAS is accorded a unique reference number within the current meter inventory and described in the following terms:

* geographic location - latitude, longitude, and sea floor depth
* meter height above the sea floor
* start date/time of the data series and duration in days or hours
* interval in seconds between individual records within the series
* instrument type
* source laboratory
* reference identified by which the series is known at the source laboratory
* confidentiality restrictions on access to the data, if any
* parameters measured
* whether data have been acquired/banked by MIAS.

DATA QUALITY CONTROL AND BANKING

Data are rarely considered for banking until they have first been quality controlled, analyzed and worked up by their originator, and it is expected that prior to submission to MIAS:

i) all relevant corrections have been applied to the data

ii) the data have been fully checked for quality and pre-edited for errors such as spikes and constant values

iii) all data are expressed in oceanographic units

iv) the appropriate qualifying information has been documented.

MIAS can do little to improve the basic quality of the data it receives - this is dependent on the person collecting the data and on his standards of measurement, calibration, and processing. Indeed, the data originator is relied upon to provide as clean and as well documented a version of his data as is possible. It is, therefore, important that he is given sufficient time to work up his data to this standard before handing it to MIAS. MIAS is not in a position to edit or modify original data nor can it ever hope to fully validate data, i.e., prove that it is an accurate representation of the conditions being measured. However, it does screen data before loading it onto the Data Bank to check that:

i) the data conform to the format specified for it by the originator,

ii) values of individual variables fall within an acceptable range,

iii) sufficient documentation is collated with the data,

iv) when plotted out the data exhibit reasonable oceanographic characteristics

As data are acquired by MIAS in a wide range of different formats the first task on receipt of each data accession is to reformat those data into a common input form so that it can be processed by the MIAS software. The series header qualifying information and the data cycles themselves are then screened for obvious errors. Automatic checks are carried out to ensure that, for example, latitude and longitude are within sensible ranges, that the start date of the series precedes the end date and that the dates are within acceptable ranges. General checks are carried out with regard to units and corrections (for example, whether current directions are in ^{0}true or magnetic, whether current directions are constrained between 0^{0} and 360^{0}, whether pressure data have been converted to metres of water and whether pressure data have been corrected for atmospheric pressure). The series header information is inspected to check that related information is consistent, for example: depths of meter and sea bed; times for mooring deployment/recovery and start/end of the data series; length of record or number of data cycles, and the cycle interval, the clock error and the period over which the data were collected.

In acquiring data for banking it is essential that sufficient documentation is also acquired describing conditions under which the data were collected and their quality. The aim of this documentation is to ensure that the data can be used with confidence by scientists or engineers other than those responsible for the original data collection, processing, and quality control. The information required to ensure that the data are adquately qualified is set out in Table 1. Unless collated fully at the outset, this documentation may be difficult to obtain in years to come and may even get lost, thereby seriously limiting the long-term value of the data.

Data cycles are inspected, using a graphics workstation, via time series plot presentations of all parameters measured plus north and east velocity components. Checks are made to ensure that the data are free from spikes, gaps, spurious data at the start and end of the record and other irregularities (for example, missing data or long strings of constant values). In addition, current vector scatter plots are produced; these may show larger than anticipated centre holes, abnormal asymmetry in the tidally dominated regimes, gaps where a range of speeds or directions are not registered due to meter malfunctions, or preferential directions where the compass was not functioning correctly.

Comparisons are made between data from meters on the same rig - by overlaying the plots on the workstation and by comparing the maximum and minimum values of individual parameters. Similar comparisons are also made between data from neighbouring current meter moorings. In addition to comparing parameter ranges, the orientation and rotation of the tidal ellipse are compared, both for meters on the same rig and for meters on neighbouring rigs. Where possible, checks are carried out to ensure the characteristics of the data set are consistent with the known distribution of tidal current speeds and directions in UK waters. Careful attention is paid to the time channel, where it is present. Automatic checks are used to ensure that the time channel progresses forwards at equal intervals - problems have been encountered with time channels which jump backwards by a number of hours. In addition, the sampling interval is checked in conjunction with the number of data cycles in the series and the start/end time of the series. This is particularly useful when the time channel has not been supplied with the data.

Data values which are thought to be suspect are flagged by MIAS. Where a large number of data points appear suspect, a cautionary document will be stored alongside the data series describing the problem. After screening the data

cycles and header information, any problems encountered with the data are discussed with the data originator and, if necessary, warning documents are stored with the data itself.

CONCLUSIONS

The success of the data banking system is dependent not only on its ability to store data safely but also on its ability to retrieve that data in a suitable form. The MIAS Data Banking Service answer a number of requests for current meter data every year from government laboratories, university research workers and industry. Most of these requests relate specifically to data services with requirements ranging from standard plot presentations or data cycles on tape to more comprehensive reports.

Such an oceanographic data bank should benefit both the scientific and industrial community, and, in particular, it should serve to:

i) encourage research workers to edit and document their data to a standard that enables it to be used effectively by others rather than just as input to their own studies,

ii) ensure that data may be made rapidly available on demand,

iii) ensure that data are available in a single format rather than a multiplicity of different formats,

iv) provide a research facility in its own right, particularly for climatic and synoptic studies,

v) safeguard the data both for short- and long-term use and so protect the considerable investment that is being made, in terms of both effort and money, in the collection of oceanographic data.

TABLE 1 DOCUMENTATION REQUIRED WITH DATA FOR BANKING

General/Identification of Data

* Name of laboratory/organisation responsible for data collection, processing and on whose behalf the data were collected
* Short term restrictions or confidentiality
* Purpose for which the data were collected
* Originator's identifiers/reference numbers for the data
* Dates and times of start and end of useable data
* Precise time interval between successive data cycles in the series

Observation site

* Sea area and name of site
* Latitude and longitude and method of position fixing
* Depth of sea floor and method of measurement
* For shallow water, tidal range (MHWS-MLWS) and strength of currents, if known
* Comments on the environment/geography of the site and any factors which may make the data untypical of the general area

Platform/Instrumentation/Recording System

* Name and type of observing platform/mooring
* Instrument description including instrument name, manufacturer and model and principle of measurement (for each sensor)
* Instrument modifications and their effect on the data
* Accuracy, resolution and response range of individual sensors
* Method of sampling and recording
* Description of instrument mounting/mooring
* Instrument depth below sea level or height above sea bed
* Method and frequency of instrument/recording system calibration

Data sampling, processing and quality control

* Original sampling scheme and its relation to the final processed data for each parameter, including for example,
    - Type of sampling (eg instantaneous, averaged, burst recording)
    - Sensing interval of meter (raw data)
    - Duration of individual sample (raw data)
    - Number of raw data samples used in processed value
    - Nominal interval of processed data
    - Methods of averaging, filtering or compression
* Data processing procedures including methods used in deriving processed values
* Criteria and procedures used for the editing and quality control/ assessment of the data

Data History/Quality

* Dates and times of each individual deployment and recovery
* Assessment of performance, condition on recovery and any malfunctions of instrument/recording system and platform
* Time, nature and outcome of service visits to the observation site
* Data quality and any known errors or uncertainties in the data
* Report on corrections applied to the data including treatment of errors (particularly timing errors) or system malfunctions
* Any special non-routine analyses and examinations carried out on suspect data or on extreme events
* Other sources of data or interpolations used to infill gaps in data sequences
* Any additional item or event that may have affected the data or have a bearing on the subsequent use of the data, for example, effects of near surface buoyancy, sea state, fouling, knockdown etc.

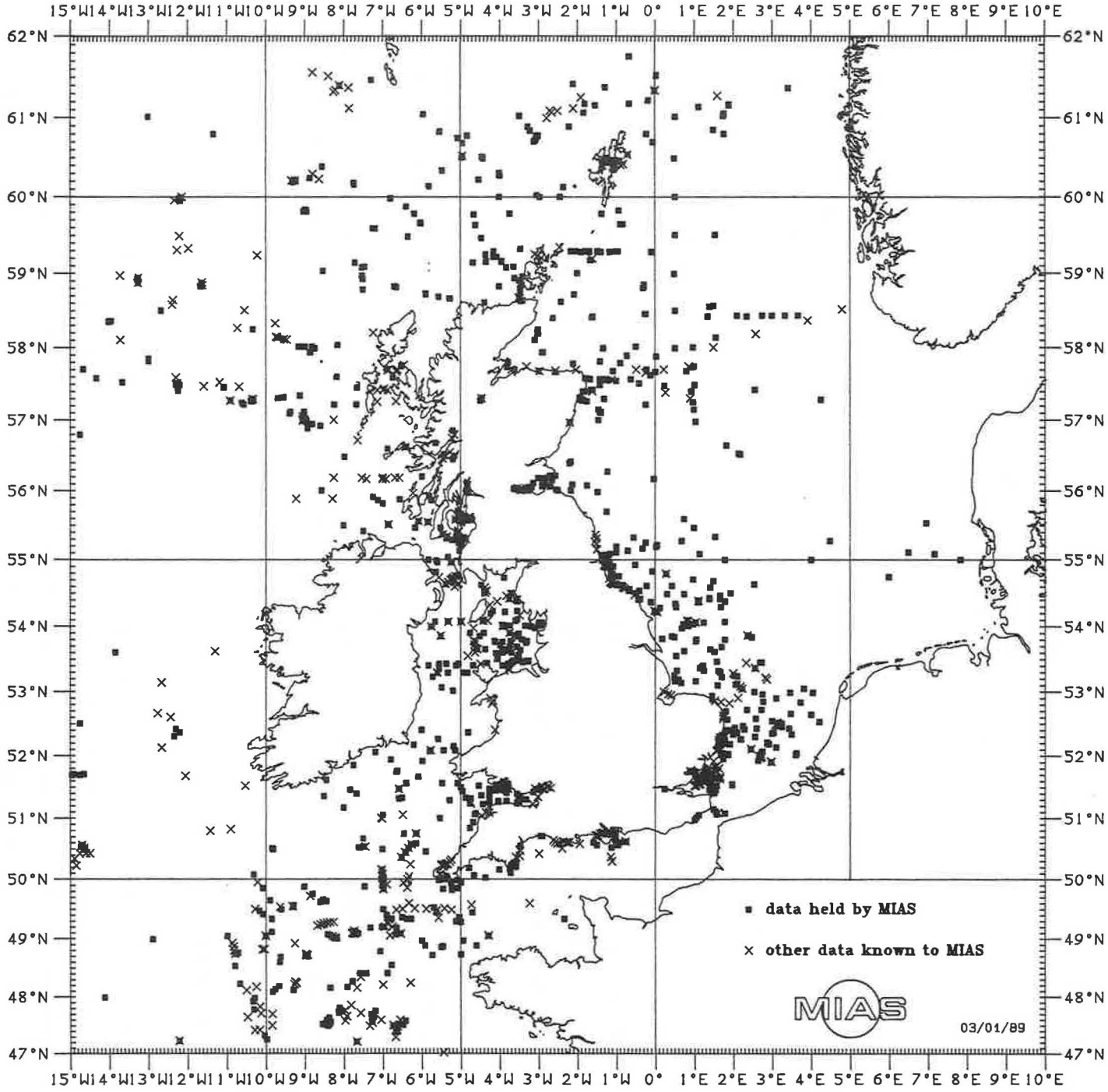
INVENTORY SOURCE = United Kingdom
15°W 14°W 13°W 12°W 11°W 10°W 9°W 8°W 7°W 6°W 5°W 4°W 3°W 2°W 1°W 0° 1°E 2°E 3°E 4°E 5°E 6°E 7°E 8°E 9°E 10°E
62°N
61°N
60°N
59°N
58°N
57°N
56°N
55°N
54°N
53°N
52°N
51°N
50°N
49°N
48°N
47°N
data held by MIAS
other data known to MIAS
MIAS
03/01/89

INTERCOMPARISONS OF VALEPORT BFM208, AANDERAA RCM4S AND PLESSEY M021F CURRENT METERS IN THE IRISH SEA

J.W. Read, K.J. Medler and S.R. Jones
Ministry of Agriculture, Fisheries and Food
Directorate of Fisheries Research
Fisheries Laboratory
Lowestoft, Suffolk NR33 OHT, England

INTRODUCTION

During the second half of 1986, the need to increase stocks of instruments for use in the Irish and North Seas led to the decision, based on bench and towing tank trials, to purchase 12 Valeport BFM208 recording current meters. These were delivered in the spring of 1987, and during June and July of that year eight moorings were laid in the eastern Irish Sea, of which three incorporated closely-spaced pairs of instruments (Figure 1). On one mooring a BFM208 and a M021F were compared, with an RCM4S and M021F pairing on the other two moorings; instruments were spaced 1 metre apart in all cases. These moorings were recovered in August 1987, after a deployment of 41 days.

The moorings were of conventional "U" design consisting of a toroidal surface marker anchored to the sea bed, a 150 m ground line and an instrument wire supported by an Aberglen CB200 subsurface buoy of 200 kg buoyancy. The M021F meters were hung from "A" frames attached to the instrument wire and the Aanderaas and Valeports were fitted "in line". The data interval in each instrument was 10 minutes.

INSTRUMENTATION

The Plessey M021 recording current meter has been in use by MAFF for some twenty years and has been extensively altered internally to use solid state circuitry for the encoding of the data rather than the electro/mechanical system originally fitted. Aanderaa compasses, thermistors and tape drive components have also been fitted, but the hydrodynamic outline of the original meter remains. The first MAFF conversion of the M021 to solid state circuitry is described in Read et al., 1981; the latest version, bearing the "F" suffix, was used in this comparison.

The Valeport BFM208 is a new development of a long line of instruments; it reads the compass and rotor every 5 seconds, applies calibration figures, and converts to a northing and an easting, which are summed until, at a preset interval the north/east pair are logged into solid state memory, together with a similarly averaged and corrected third channel sensor. During laboratory and towing tank trials it performed well and, although all 12 instruments had to have factory modifications after purchase, all deployments so far have produced full records. These instruments are fitted with 6-bit compasses, giving a resolution of $\pm$ 2.8 degrees, so that to get an acceptable calibration a computer-controlled version of the Lowestoft compass calibration table (Talbot and Baxter, 1975) has been developed to look for and position the boundaries of the compass sectors. From this information, new Vector "look-up tables" will be produced for inserting into the calibration ROM of the instrument. The results referred to in the present report have, however, been produced by a temporary method of applying calibration figures after the meter has been recovered.

The Aanderaa RCM4 has been in general use for many years but was originally considered to have limited usefulness in shelf seas areas because of the response of its Savonious rotor to turbulent flow. The introduction of the "S" version of the instruments, fitted with the "paddle wheel" rotor and shield, was the manufacturer's attempt to rectify that shortcoming. It was claimed to be capable of improved response in turbulent flows and is the version used in this comparison.

RESULTS

All the records considered in this report have been processed by standard Lowestoft methods (Medler, 1988) and the main items of comparison have been the unfiltered time series of speed, scatter plots and the filtered Progressive Vector Diagrams (PVD). The speed time series for a representative 3-day period (Figure 2) show clearly that the M021F consistently records speeds that are about 8% lower at the tidal maximum than those of both the RCM4S and the Valeport; second, with its "paddle wheel" rotor there is no sign of the problem of "rotor pumping" at slack water, associated with the earlier Aanderaa rotors, when used in a shelf sea's environment (Ramster and Howarth, 1973).

The mooring at position X5 ($53^0$39.9'N, $4^0$38.4'W) produced usable records of 41 days duration (39 after filtering) from a sampling depth of 12 metres for the M021F and 13 metres for the BFM208. The residuals [Figure 3(a)] compare well, with an exercise mean vector of 52 km 108^0 for the M021F and 59 km 115^0 for the

BFM208. The difference between these figures is accounted for largely by their behaviour between days 20 and 30 when the BFM208 indicated a larger southerly component than the M021F. Since examination of the wind data from Valley (Anglesey) shows that there was no obvious difference in the wind during this period, the cause of the discrepancy is unknown.

The scatter plots from these instruments compare well [Figure 3(b)] except that the BFM208 shows a clearly slimmer "tail" at large eastward speeds. The mooring at position W5 ($53^0$46.8'N, $4^0$39.9'W) incorporated an M021F at 11 metres and an RCM4S at 12 metres and apparently produced 27.5 days of data before the subsurface buoy collapsed, but the last 800 readings (5.5 days) were later deleted from both records when it became obvious that the records of the RCM4S were affected by the increasing tilt as the buoy began to sink.

The PVDs (Figure 4) show that the RCM4S indicated a residual in the same direction as the M021F but only approx. 60% of its length, with exercise mean vectors of 28 km 176^0 for the M021F and 17 km 170^0 for the RCM4S. A study of the scatter of 10-minute values (Figure 5) shows that for large westward speeds the scatter produced by the RCM4S is "hooked". This is a similar feature to that found in some BFM208 records before individual compass calibrations were applied and prompted us to try altering the RCM4S compass calibration by -2^0 in the area 225 to 315^0. This has a minor effect on smoothing out the hook [Figure 5(c)] but brings the PVD significantly closer to that indicated by the M021F [Figure 5(b)]. A post-cruise compass calibration of the M021F indicated that no change in its compass response had taken place during the deployment, but we were unable to check the RCM4S as the meter had been damaged and had leaked when the rig collapsed.

Another interesting effect discovered during investigation of this pair was the inconsistent response of the speed sensors to increasing and decreasing speeds. Figure 6 shows that, compared with the RCM4S, the M021F reads low on increasing speeds and high during decreasing flows. The composite [Figure 6(c)] indicates that as the larger proportion of all values lie above the line, an increase in the speed coefficients for the RCM4S could improve the test results. This was done, for the purposes of the present investigation [Figure 6(d)], but the change produced no further improvement in the match of the PVDs and, since the

different behaviour of the two instruments may be a real reflection of (for example) a different response to turbulence, it was concluded that altering these coefficients in the routine analysis of data was neither practical nor justified.

The mooring at position U5 (53^0 43.1'N, 4^0 38.7'W) matched an M021F at 24 metres with an RCM4S at 25 metres and produced record lengths of 40 days from each instrument. The PVDs compare well (Figure 7) with exercise mean vectors of 102 km 240^0 for the M021F and 110 km 232^0 for the RCM4S, and the scatter plots are also closely matched, though perhaps with some signs of "hooking" in the RCM4S at large westward speeds, as before.

DISCUSSION

Three pairs of instruments have been compared. Two (RCM4S and M021F) are well established in shelf sea's work but have recently been modified, the M021F to overcome lack of spare parts and unreliability and the RCM4S to rectify the well documented overrunning problem in shelf sea's use. The BFM208 is a new development from an established manufacturer, with several novel features.

From the comparison of the recorded speeds the RCM4S and BFM208 match closely, suggesting that the RCM4S rotor modification has successfully overcome the problems associated with these instruments in the past. The fact that the M021F recorded speeds different to those of the others at certain phases of the tide might be thought to reflect that it was the only instrument of the three to incorporate a reverse rotor-sensing counter, which was incorporated during the rebuilding because of the suspicion that in turbulent flow any rotation of the impellor (forwards or backwards) would register as a forward count. However, this explanation is discounted by the fact that an 8% discrepancy is observed in the upper range of speeds when no reversal of the rotors is likely; thus, the cause of the differential is regarded as being unknown at present.

The difference in the PVD's at W5 (RCM4S vs M021F) could not be explained or back-corrected after deployment due to the severe damage sustained by the RCM4S on that deployment. However, the fairly minor "adjustment" of adding a -2^0 correction to a 90^0 sector on the RCM4S illustrates once again how critical compass accuracies are in deriving residuals, particularly when the main tidal stream is at right angles to the residual flow direction, as in this case (Gould, 1973).

MAFF calibrates all RCM4S and M021F current meter compasses at 10^0 intervals with the criterion that the 8 readings recorded at each direction-interval must fall within a 4^0 band (Talbot and Baxter, 1975). This gives a calibration accuracy of $\pm 2^0$, so that the -2^0 adjustment described above is within the tolerance of the calibration. A further point that should be remembered is that the compass calibrations which we apply take account only of the "static" errors, and do not correct for errors in the alignment of the meter into the flow. Directional accuracy figures that Aanderaa Instruments quote for the RCM4S are speed-related, presumably with this dynamic error in mind, and even the best compass resolutions quoted are $\pm 5^0$. Thus, once again the -2^0 adjustment is justified.

CONCLUSIONS

This intercomparison exercise has been based on very few pairs of instruments so that our conclusions cannot be regarded as being firm. The exercise should also be regarded as an exploration of sources of error in current meter records rather than as a guide to correcting these since, whether the corrections are within calibration-tolerance or not, we will rarely have adjacent pairs of current meters to determine the appropriate correction to apply in a particular instance.

However, the comparison has shown once again that the validity of residuals calculated from data collected by recording current meters depends, above all else, on the accuracy of the direction measurement. The calibration of a direction sensor improves the measurement of that parameter because the manufacturer's accuracy figures include errors in that sensor, but also included is the accuracy to which the instrument aligns itself into the current, and this cannot easily be improved upon or even measured. If the overall accuracy to which these meters measure the direction of the current is typically $\pm 5^0$ then all the differences in performance of these instruments could be within that tolerance. The differences in speed measurement may reflect real differences in the ways in which the different speed sensors respond to the current but their effects on the residual current vector is small.

REFERENCES

Gould, W.J. 1973. Effects of non-linearities of current meter compasses. Deep Sea Res., 20: 423-427.

Medler, K.J. 1988. Procedures for processing current meter records at Lowestoft. ICES Doc. C.M.1988/C:6.

Ramster, J.W. and Howarth, M.J. 1973. A detailed comparison of the data recorded by Aanderaa Model 4 and Plessey MO21 recording current meters at two shelf sea's locations with strong tidal currents. ICES Doc. C.M.1973/C:3, 22 pp.

Read, J.W., Thomas, M.R., and French, J. 1981. A solid state current meter conversion. IERE Conf.Proc., 51:181-188.

Talbot, J.W. and Baxter, G.C. 1975. The direction calibration of Plessey recording current meters. Fish. Res. Tech. Rep., MAFF Direct. Fish. Res., Lowestoft, (12):10 pp.

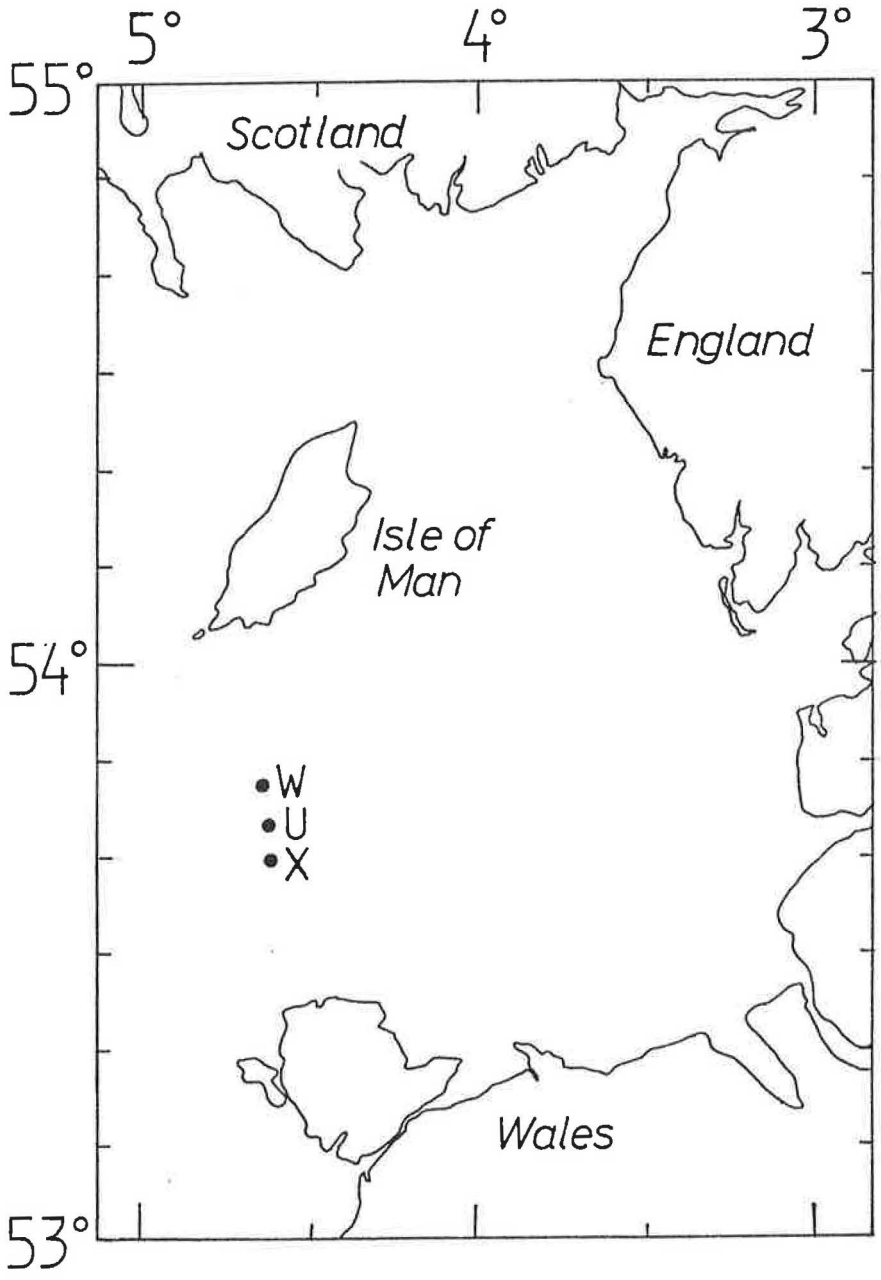

Figure 1. Positions of moorings under discussion.

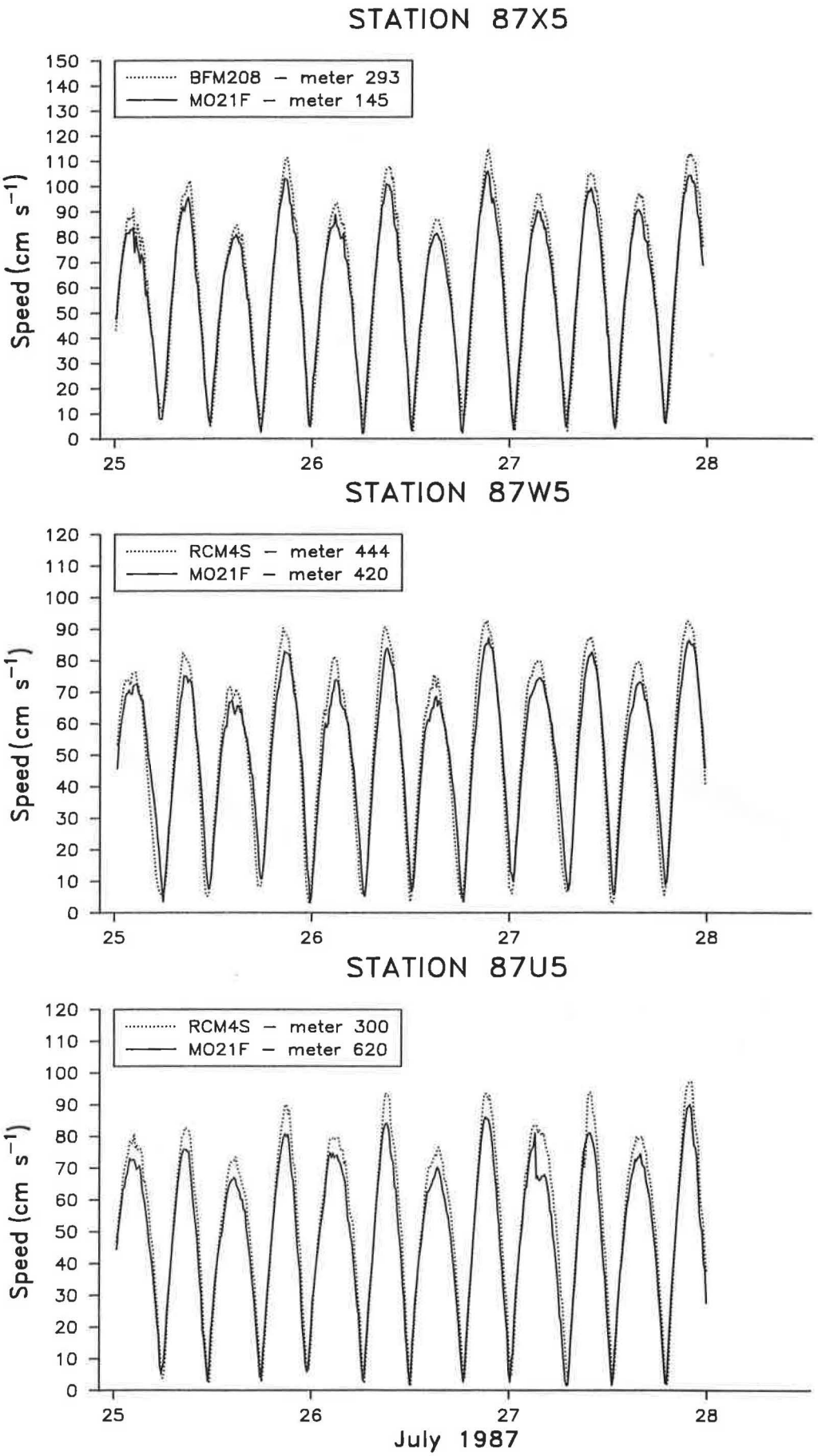

Figure 2. Speed vs time plot for each meter pair for a representative three-day period.

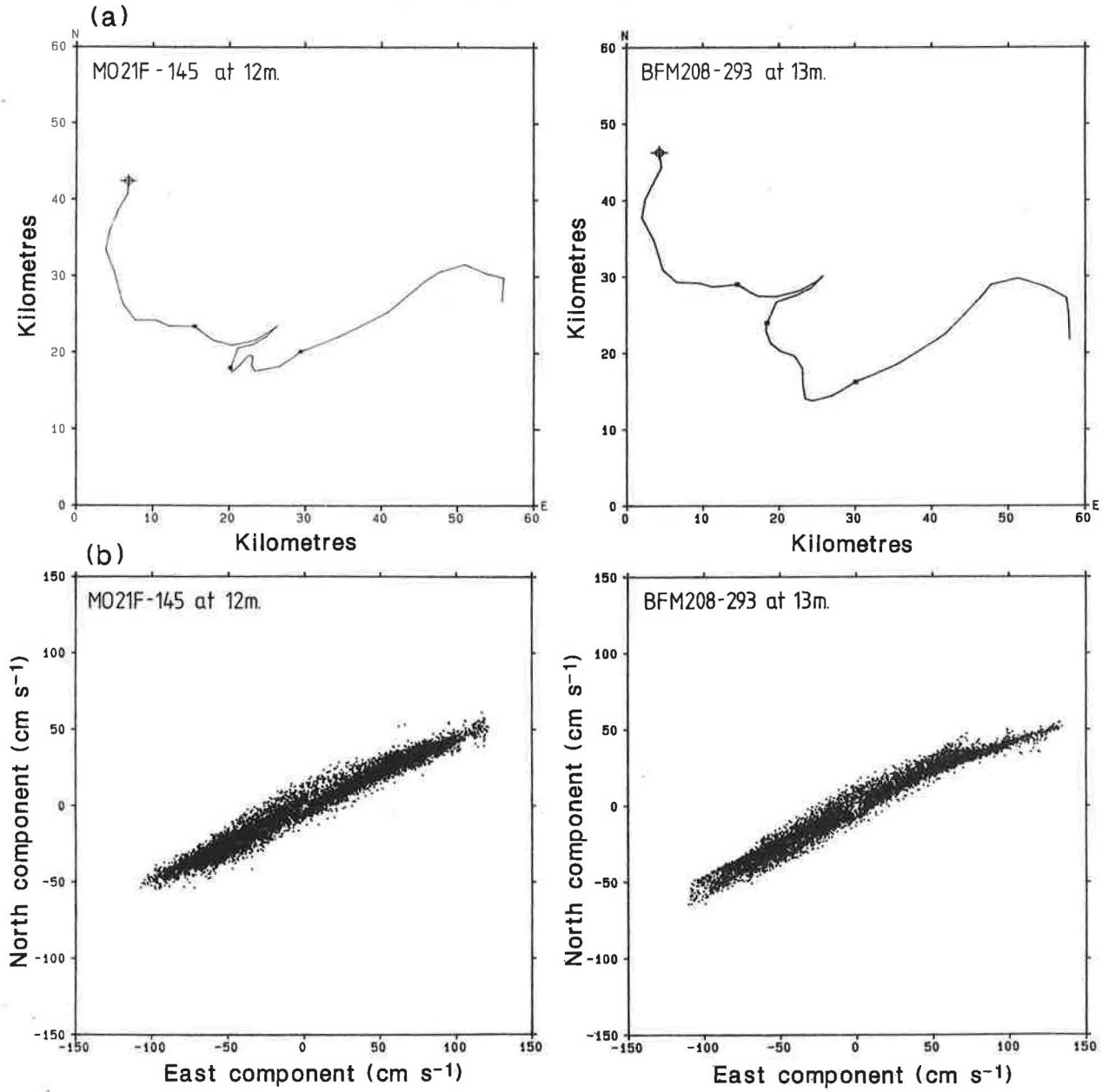

Figure 3. (a) Progressive vector diagrams from the meter pair at mooring X5. (b) Scatter diagrams from the meter pair at mooring X5.

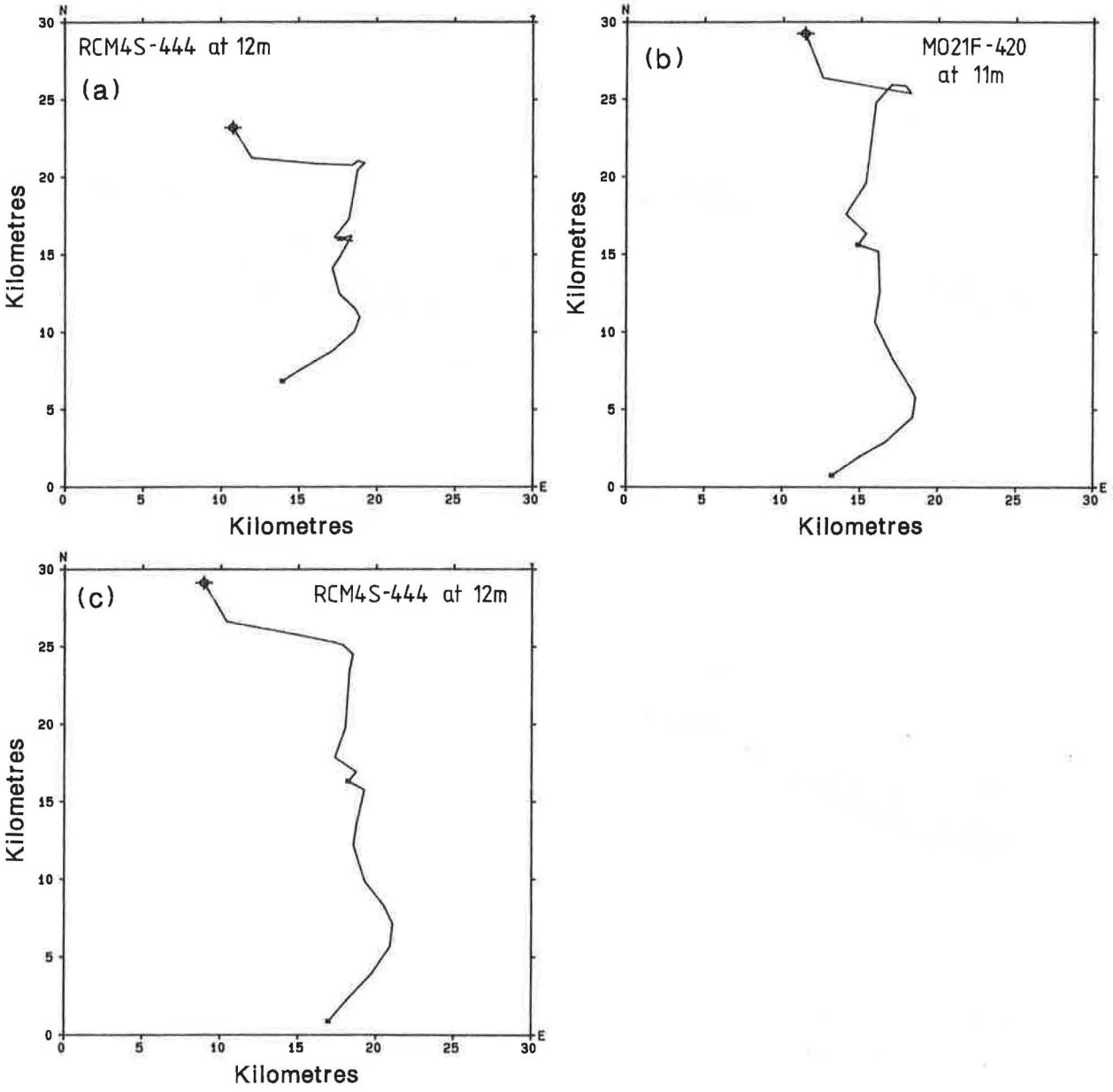

Figure 4. Progressive vector diagrams from the meter pair at mooring W5: (a) Aanderaa RCM4S before adjustment; (b) Plessey M021F; (c) Aanderaa RCM4S after adjustment of compass correction between 225° and 315°.

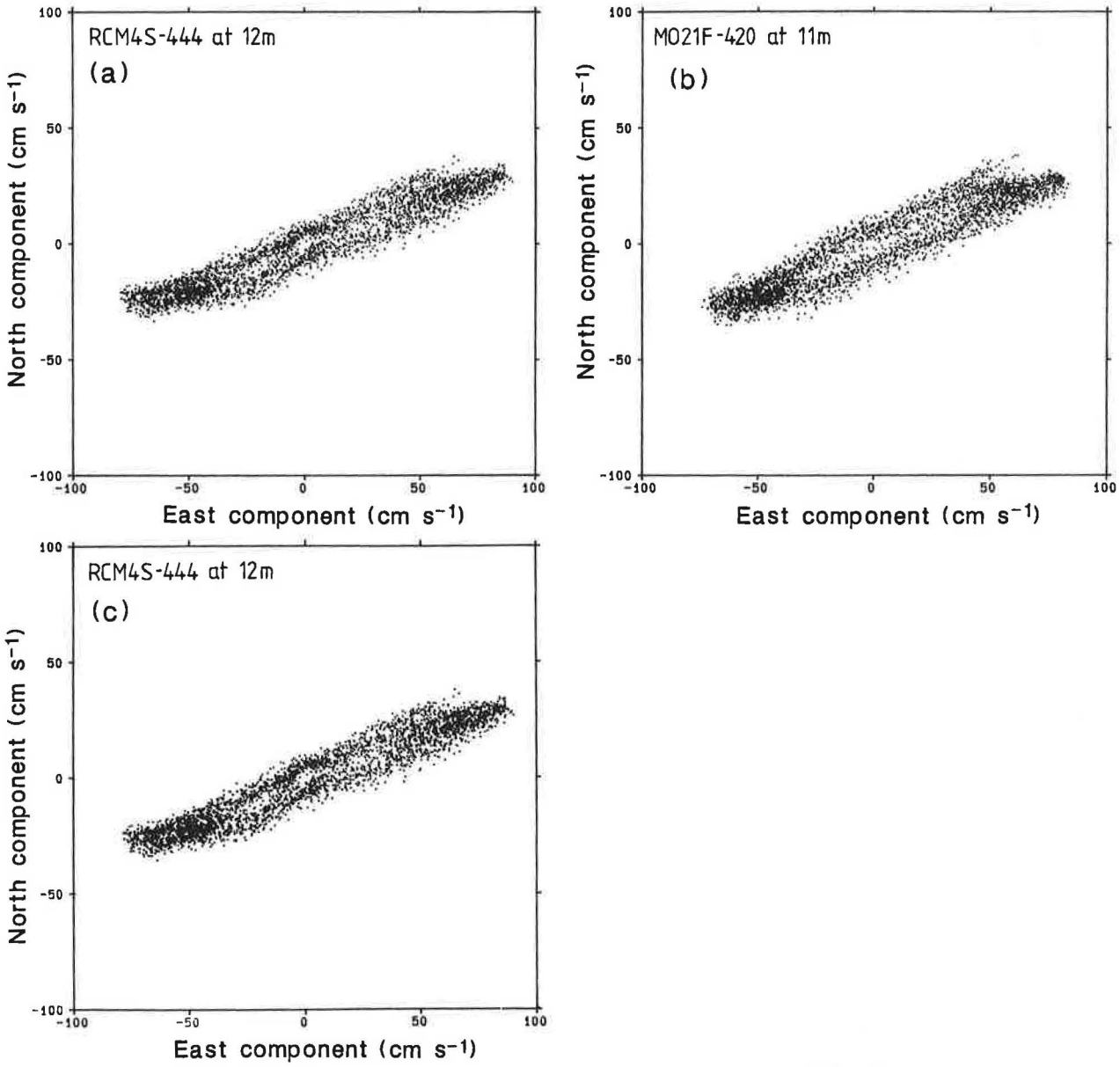

Figure 5. Scatter diagrams from the meter pair at mooring W5: (a) Aanderaa RCM4S before adjustment; (b) Plessey M021F; (c) Aanderaa RCM4S after adjustment of compass correction between 225° and 315°.

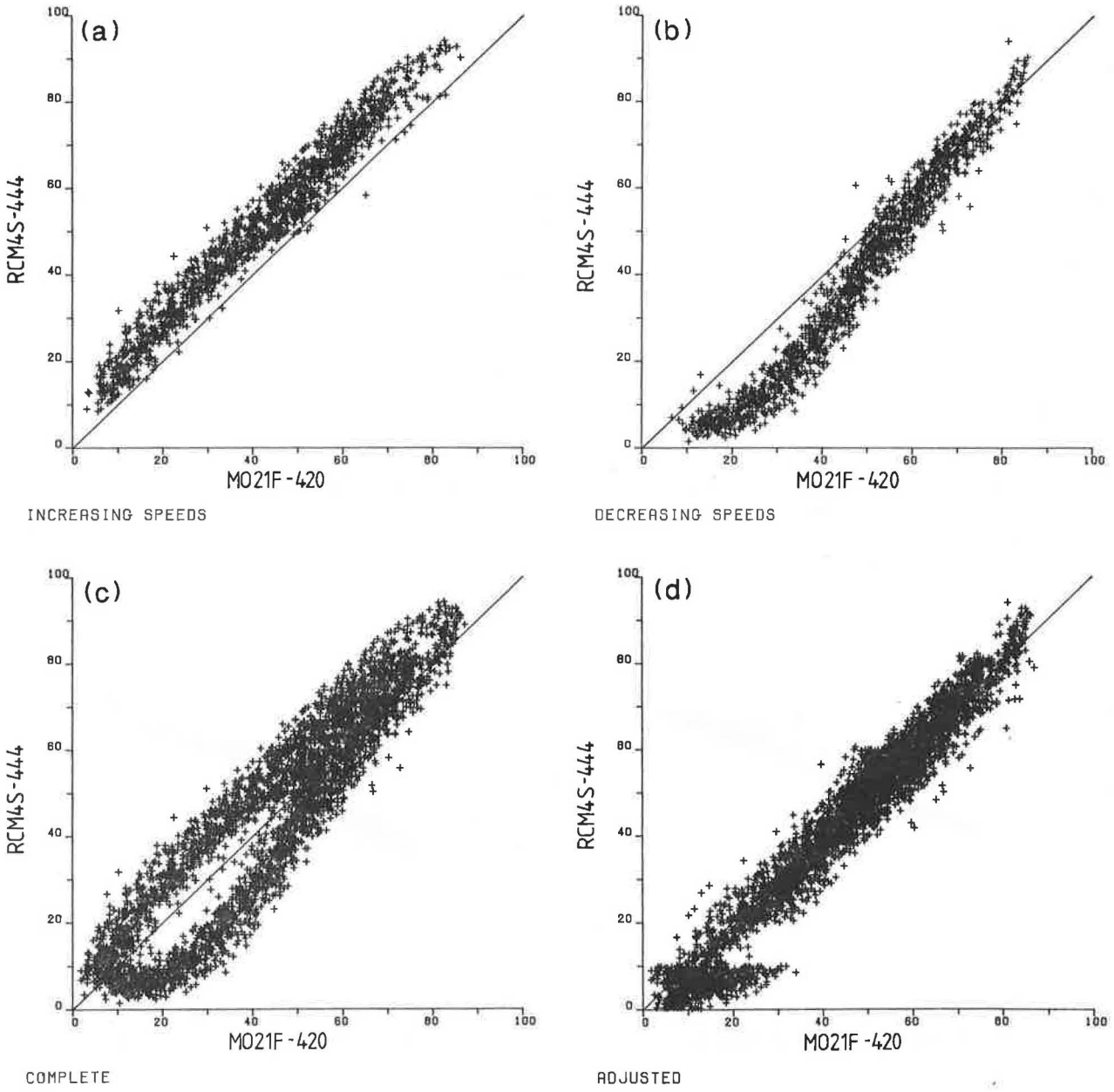

Figure 6. Comparative plots of speed values from the meter pair at mooring W5: (a) RCM4S vs M021F increasing speeds; (b) RCM4S vs M021F decreasing speeds; (c) composite of (a) and (b); (d) composite after adjustment of speed equation of RCM4S.

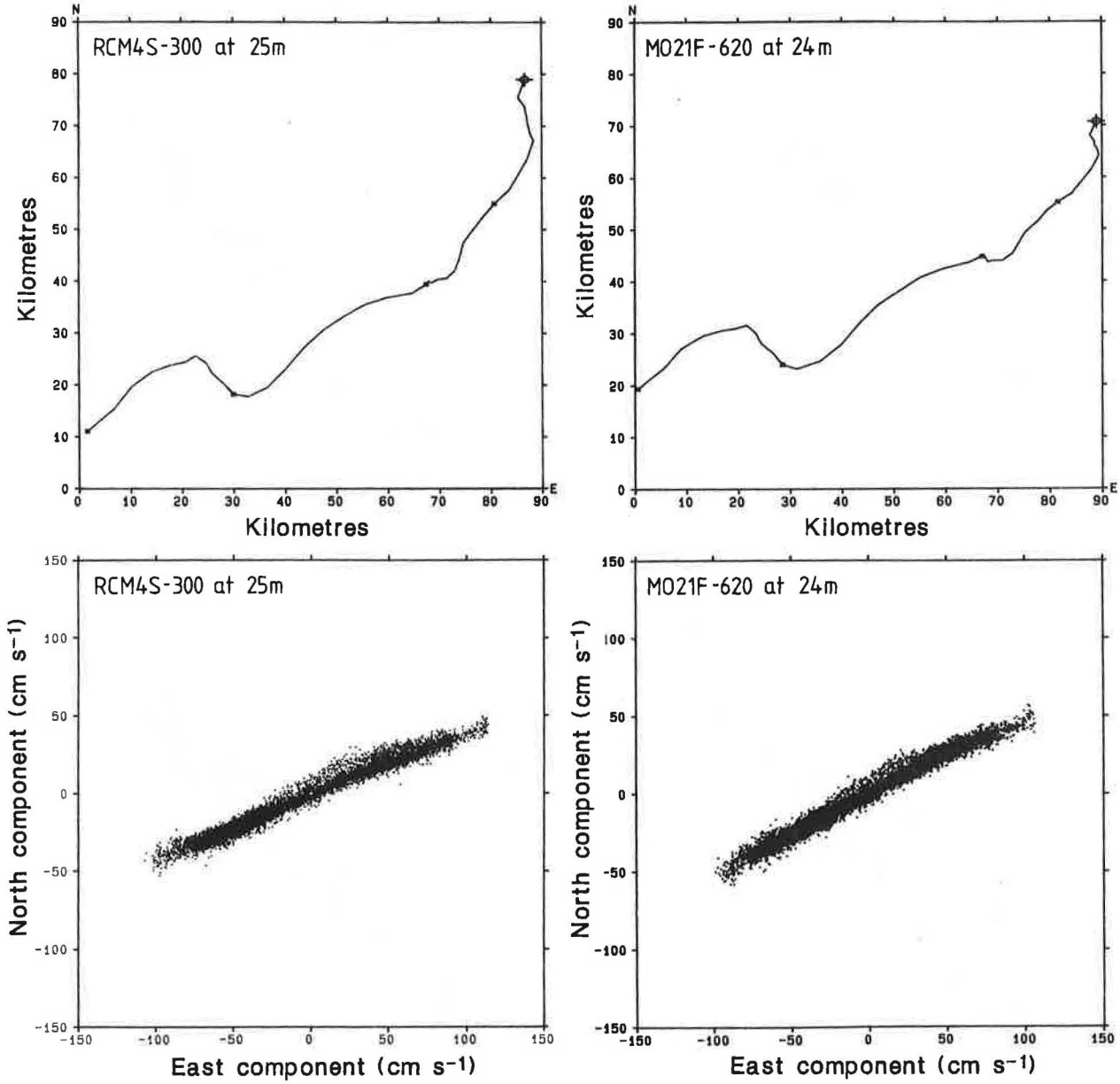

Figure 7. Progressive vector diagrams and scatter diagrams from the meter pair at mooring U5.

AN INTERCOMPARISON OF NEAR-SURFACE CURRENT MEASUREMENTS OFF SOUTHWEST NOVA SCOTIA

Peter G. Smith and Donald J. Lawrence
Physical and Chemical Sciences
Dept. of Fisheries and Oceans
Bedford Inst. of Oceanography
P.O.Box 1006
Dartmouth, Nova Scotia B2Y 4A2, Canada

1. INTRODUCTION

Accurate knowledge of the current field near the ocean surface is important in a number of scientific investigations, such as studies of transport and dispersion of buoyant fish eggs and larvae, as well as practical applications, as in the prediction of the movement of surface oil slicks. Such knowledge is difficult to obtain, however, because surface currents are highly variable in both space and time. In addition to pressure forces which drive tidal and geostrophic currents, surface winds inject momentum directly into the upper layer where it is distributed by turbulent mixing processes and produces strong vertical shear in the horizontal current field. The structure of the near-surface currents in the "wind-drift" layer is often modelled by analogy with turbulent flow over a rough surface (e.g., Churchill and Csanady, 1983). Immediately below the free surface is a very thin layer with constant shear (Wu, 1975):

$$\frac{\partial u}{\partial z} = \frac{u_*^2}{\nu_e} \quad , \quad u_*^2 = \tau_o/\rho \tag{1}$$

where τ_o is the surface wind stress, ρ is the water density and ν_e is an effective viscosity. To depths of order 1 m, the velocity is found to vary logarithmically, which implies

$$\frac{\partial u}{\partial z} = \frac{u_*}{kz} \tag{2}$$

where k (≈ 0.4) is Karman's constant. Lagrangian measurements by Churchill and Csanady (1983) suggest that under moderate winds the logarithmic layer extends over a depth range of 1 to 60 cm, below which the shear is reduced. Thus the most intense shear is expected to occur near the surface under strong wind forcing. Although the maximum velocity in the "wind drift" layer is commonly esti-

mated at 3% of the 10 m wind speed, U_{10} (LeBlond and Mysak, 1978), field and laboratory observations range from 2.6% to 5.5% U_{10} (Lange and Huhnerfuss, 1978).

Atmospheric forces at the sea surface also generate gravity waves whose energy propagates horizontally and decays with depth over a scale proportional to the dominant wavelength. The presence of waves complicates the observation of surface currents since, even in the simplest case of linear, irrotational waves, where the average Eulerian current is zero, the vertical migration of particles in the sheared velocity field results in a second-order Lagrangian current ("Stokes drift") in the direction of wave propagation given by:

$$u_s(z) = \frac{2}{g} \int_0^{2\pi f_c} \sigma^3 \, \phi(\sigma) \, e^{-\frac{2\sigma^2 z}{g}} \, d\sigma \qquad (3)$$

where σ is the frequency (rad s^{-1}), $\phi(\sigma)$ is the heave spectrum, and f_c is a cut-off frequency (Hz) designed to limit the influence of high frequency noise. Churchill and Csanady (1983) point out that even in moderate wave fields [H_s=O(1m)], the magnitude of the velocity shear associated with (3) is similar to that of (2) under moderate winds over the same depth range. In addition, viscosity produces a free-surface boundary layer whose vorticity diffuses downward and results in a surface current exceeding the Stokes drift component for fully-developed waves. As wind and wave energies increase, nonlinear interactions and breaking of waves lead to strong turbulent mixing of the surface layers which will modify the wave drift profile and (possibly) support secondary Eulerian mean flows such as Langmuir cells (Garrett, 1976). Laboratory experiments (Lange and Huhnerfuss, 1978) demonstrate that wind and wave drift currents cannot be simply superimposed, but rather that the presence of waves appears to retard (enhance) the wind-induced currents at low (high) wind speeds. Thus the meteorological forcing at the air-sea interface feeds energy into surface currents both directly as wind drift and indirectly via surface waves and horizontal pressure gradients. The adequate observation of wind-driven surface currents therefore requires simultaneous independent measurements of both Eulerian and Lagrangian current fields, surface wave amplitude and direction, and wind speed and direction.

In order to improve our understanding of surface currents in the coastal ocean and our ability to measure accurately, scientists from the Bedford Institute of

Oceanography (BIO) conducted an 8-day intercomparison of current measurement techniques off Cape Sable, N.S., during C.S.S. Dauson Cruise 84-043, 14-27 November, 1984. The experiment included Eulerian measurements with various types of current meters, surface current mapping by HF radar (CODAR), and Lagrangian measurements with both drogued and undrogued drifters. In addition, the program provided frequent measurements of wind velocity, the 2-D surface wave spectrum, and *in situ* current profiles. This report is focussed on analysis of the moored Eulerian and CODAR measurements. A summary of the salient results of previous intercomparison experiments is given in Section 2, followed by a description of the relevant aspects of the Cape Sable Intercomparison (Section 3). Section 4 will intercompare the moored results and CODAR, followed by a discussion and conclusions in Section 5.

2. PREVIOUS WORK IN THE FIELD

Records from conventional moored current meters that employ a Savonious rotor to measure speed (e.g., standard Aanderaa SRCM) are notoriously susceptible to contamination due to rectification of high-frequency surface wave and mooring motion (Smith *et al.*, 1984a). This leads to current estimates which are biased upward at all frequencies including the mean. The problem is mitigated considerably by vector-averaged sampling procedures (e.g., as in the AMF-VACM instrument). However, intercomparison studies (Beardsley *et al.*, 1977) show that the level of contamination has such a complex dependence on the sampling scheme, mooring configuration and signal-to-noise ratio that it is not possible to use independent data (such as surface wave energy or mooring tilt) reliably to correct for these effects.

Recent technological innovations have considerably improved the capability for making near-surface current measurements in the upper ocean. The vector-measuring current meter (VMCM), for example, uses biaxial dual propellers to sense orthogonal components of horizontal velocity (Weller and Davis, 1980). The main advantage of the propeller sensors is their linear response to Cartesian velocity components which isolates the surface layer and mooring motion contamination at high frequencies rather than distributing it over the spectrum as the "polar" sensors do. Similarly, a vector-averaging acoustic current meter (ACM) measures the velocity-dependent phase differences between two signals transmitted in opposite directions along orthogonal sound paths. Intercomparisons in both the laboratory (Weller and Davis, 1980) and the field (Halpern *et al.*, 1981) indicate that at low signal-to-noise ratios, the ACM and the VMCM under-

respond to the flow, in contrast to the VACM which over-responds. In order to relate field and laboratory results, Beardsley (1986) used the ratio of VMCM vector-mean speed, S_m, to a characteristic surface wave velocity at instrument depth, W (derived from the difference between squared VACM rotor and vector-mean speeds, i.e. $W^2=R_a^2-S_a^2$) as a measure of the signal-to-noise ratio. Based on that relationship, he then concluded that with respect to the true velocity, the VMCM under-responds by 5-6% and the VACM over-responds by 10-20% in the range: $0.5 \leq S_m/W \leq 2.0$.

Electromagnetic current meters (EMCM) have traditionally been plagued by biological fouling, zero offset drift and higher levels of flow-induced and electrical noise. However, tests of a new design spherical EMCM, the S4 (Inter-Ocean Systems Inc., San Diego, CA), indicate that these problems have been substantially overcome to provide a stable, robust current measurement, with linear speed and cosinusoidal directional responses, suitable for use near the surface. Beardsley et al. (1986) compared an S4 to an adjacent VMCM on a surface-following mooring and found that the S4 speed response in the range $0.5 \leq S_m/W \leq 2.0$ was greater by 8-10% while direction differences showed no particular bias. Assuming the VMCM under-responds by 6% in that range, they concluded that the S4 over-responds by only 3%. In an earlier field test against an acoustic (ACM) and a standard Aanderaa (SRCM), Pashinski (1985) also discovered an over-response of 9-12% in the S4 which he attributed to a difference in calibrations. He also found the response of the SRCM to be different from the others at low-energy forcing, based on a loss of coherence when the variance in a particular frequency band dropped below 10 cm^2s^{-2}.

The poor performance of the "polar"-type SRCM in the presence of high frequency fluctuations has been attributed to three factors (Smith et al., 1984a): 1) "overspeeding" of the rotor caused by a difference between the rates of acceleration and deceleration in oscillatory flow (Fofonoff and Ercan, 1967); 2) "rotor pumping", by which vertical oscillations of the instrument cause the rotor to spin (Gaul, 1963; Kalvaitis, 1974); and 3) the large time constant of the SRCM vane (Saunders, 1976). To improve the rotor response, Aanderaa Instruments have recently developed a modified rotor design consisting of a straight-vaned, six-bladed "paddlewheel", which is half-enclosed by a semicircular shield that deflects the current from one side of the rotor. The response to the one-sided current forcing is expected to be more symmetric in accelerating and decelerating flows and immune to pumping by vertical oscillations. Hammond et al. (1986) have shown that although the calibration of the new rotor is

slightly nonlinear, the "paddlewheel" Aanderaa (PRCM) shows a reduced tendency to over-respond in the presence of high-frequency wave noise [<5% (PRCM) versus >20% (SRCM) for $S/W \leq O(1)$].

Progress in the development of moored current meters has been matched by advances in the remote detection of ocean currents. The Coastal Ocean Dynamics Application Radar (CODAR) is an HF radar system (25 mHz) capable of mapping near-surface currents to ranges of 30 to 50 km by measuring the current-induced Doppler shift of the first-order Bragg scattering echo from surface waves. Barrick et al. (1977) found crude agreement (rms speed differences of 27 cm s^{-1}) between CODAR and Lagrangian drift measurements in the Gulf Stream off Florida. Holbrook and Frisch (1981), on the other hand, found differences of only 7 cm s^{-1} and 10^0 in vector-mean speeds and directions between CODAR and 4 m VACMs in the Strait of Juan de Fuca. Recently, the Centre for Cold Ocean Resources (C-CORE, St. John's, Newfoundland) tested a CODAR system in the Strait of Belle Isle by comparing with SRCM and VACM measurements from a depth of 15 m (Lawrence and Smith, 1986). They achieved reasonable agreement of 5-10 cm s^{-1} in radial currents with at least part of the differences arising from shear over the upper water column.

Collar et al. (1986) have compared a similar HF system, called Ocean Current Surface Radar (OSCR), with an experimental EMCM and VMCM moored at 0.4 m and 3.0 m and with Lagrangian measurements from floats drogued at 0.5 m and 1.0 m. They noted exceptional agreement between OSCR and the 0.4 m EMCM except when the wind/wave driven surface currents were opposed to the underlying tidal currents, suggesting a complex shear profile may lead to nonlinear modification of the wave phase velocity. The OSCR-VMCM and EMCM-VMCM differences were consistently in the wind direction, so that the effective depth of the radar measurements was certainly less than 3 m. [Stewart and Joy (1974) have used simple current profiles in a perturbation theory to derive an effective depth of $\lambda/4\pi$, where $\lambda(\approx$ 11 m) is the transmitted wavelength, whereas Ha (1979) found a smaller value of 0.022λ for a logarithmic profile.] Furthermore, a linear regression suggested that the magnitude of the OSCR-VMCM current difference was roughly 0.5% of the radial component of the wind speed. The motions of the 0.5 m and 1.0 m drogues exhibited very little vertical shear and overall mean differences between float and OSCR measurements were found to be quite small ($\leq$ 1 cm s^{-1}). However, a standard deviation of 3 cm s^{-1} was ascribed to considerable horizontal variability at scales of order 100 m.

It is clear from the above discussion that in order to interpret the differences between various types of surface current measurement techniques, it is necessary to make the measurements in close proximity to one another and to obtain contemporaneous, independent observations of the local wind speed and direction and the two-dimensional surface wave field. The Cape Sable Intercomparison Experiment was designed to do this.

3. THE CAPE SABLE INTERCOMPARISON EXPERIMENT

The primary goal of this study was to evaluate various techniques for measuring current in the top metre of the water column. The Eulerian instruments best suited to this task are the Cartesian vector-averaging types (e.g., VMCM, S4, ACM) which minimize surface layer contamination. The CODAR system, operating at 25 mHz, is also designed to give a horizontally-averaged estimate of the current at a depth less than one metre. Similarly, surface drifters with drafts less than one metre, developed at BIO for tracking oil spills, were used to measure Lagrangian surface currents. A secondary objective was to intercompare remote and *in situ* current measurements over the remainder of the water column. For this purpose, conventional (SRCM) and modified (PRCM) Aanderaa and VACM instruments; a ship-borne acoustic Doppler profiler (ADCP;Ametak Straza DCP-4400,300 kHz); and drogued Lagrangian drifters were employed. The third objective of the program was to explore various methodologies for tracking Lagrangian drifters. Apart from visual and/or satellite tracking, selected buoys were tracked acoustically using an array of bottom-mounted transponders and ship-borne hydrophones. In addition, when the drifters moved out of range of the fixed array, several ship-based tracking methods were tested (Smith *et al.*, 1984b).

The final element of the program was an airborne remote sensing study conducted jointly be researchers from the Canadian Centre for Remote Sensing (CCRS) and the RADARSAT Project Office of the Deptartment of Energy, Mines and Resources. The objective of this phase of the experiment was to obtain spatially-averaged measurements of the surface wind and wave fields with instruments such as synthetic aperture radar (SAR) and the microwave scatterometer (SCAT) for direct comparison against *in situ* observations.

The intercomparison was conducted during C.S.S. Dawson Cruise 84-043, 14-28 November. The location chosen for the experiment was the strong tidal regime off Cape Sable, N.S., (Figure 1) where long-term measurements of the current field were available from previous investigations (Smith, 1983). In addition to the

current observations, accurate shipboard measurements of wind speed and direction were made to define the atmospheric forcing function for the surface layer and for estimating the force balances on the Lagrangian drifters. Furthermore, measurements of the directional wave spectrum were made to aid in the interpretations of wave-induced drift in the Lagrangian data and of the high-frequency contamination of the current meter data. Full details of the field program are contained in the account of Dawson Cruise 84-043 (Smith et al., 1984b). This report is focussed on the analysis and evaluation of the moored instrumentation and CODAR with reference to the wind and wave data. Before discussing the results, the salient features of these systems will be outlined below.

3a. MOORED INSTRUMENTATION

The mooring site CS ($43^0$12'N, $65^0$49'W; Figure 1) selected for the intercomparison study lies on the 60 m isobath just west of the main mooring line for the earlier Cape Sable Experiment (Smith, 1983) and well within the anticipated CODAR range (35 km). The current meter mooring configuration initially consisted of two surface (671, 672) and one deep (669) moorings surrounded by a triangular array of guard buoys (1 km on a side) to ward off fishing vessels (Figure 2, inset). However, shortly after deployment, mooring 671 parted between the 5 m and 8 m instruments resulting in the loss of the float and top two instruments, VMCM(1) and VACM(5). Subsequently, the deeper portion of the mooring was recovered by dragging, refurbished and redeployed beneath a guard buoy as mooring 682. The deep, taut wire mooring (669), suspended beneath a float at 26 m, was intended to be a "quiet" mooring, whereas the 4-ft steel spheres on 671 and 672 and the guard buoy (5-ft steel sphere with mast above and ballast arm below the waterline) on 682 follow the free surface and thereby transmit energy to the deeper instruments.

The various types of current meters used in the experiment are described in Table 1 along with manufacturers specifications for accuracy and precision of the current sensors. In addition to measuring the current profile, the concentration of instruments in the surface layer was intended to yield several intercomparisons of closely-spaced instruments of different types on the same mooring or of the same type on adjacent moorings. Unfortunately, many of these intercomparisons were thwarted by generally poor data return due to instrument malfunction or damage. The latter was often traceable to the harsh environment of the

surface layer. Table 2 provides the deployment histories and performance summaries for all instruments. Notable failures include the complete loss of the ACM and all but one of the VACM records. The central shaft of the VMCM on mooring 672 appears to have been broken on recovery so that the data are not impaired, but the broken fin on the PRCM at 31 m apparently contaminated the entire record (see below). These events led to the conclusion that the mechanical and acoustic sensors are too delicate to survive wintertime conditions at the surface.

A two-minute sampling interval was set for all moored instruments except the VACM whose interval of 1.88 min (112.5 s) is constrained to be an even multiple of 3.516 s. To facilitate comparisons with other data types, the VACM data were interpolated to 2-min. intervals and all records were then filtered to 10-min. intervals using a 7-point running mean. Plots of the 10-min. data reveal the dominant tidal oscillations in the current field and at times in the temperature, salinity and density fields. Figure 3 indicates that the thermal and density stratification in the water column is highly variable, especially on tidal time scales and the semidiurnal currents sweep tidal fronts and other gradients past the moorings. Nevertheless, the small thermal contrast between VACM (12 m) and VMCM (1.5 m) suggests that the surface layer was relatively homogeneous at least over the latter half of the experiment.

In the remainder of this report, the records from individual moored instruments, or the instruments themselves, will be designated by the code in Table 2 (column 4).

3b. CODAR

The CODAR system for mapping surface currents was operated from shore for a 14-day period (13-26 November) surrounding the cruise by C-CORE. The CODAR stations (Figure 1) were established on Seal Island ($43^0$23'43"N, $66^0$00'48"W) and Cape Sable Island ($43^0$23'25"N, $65^0$37'24"W) and after some start-up problems over the first five days, operated satisfactorily until the end of the program at 1900Z on 26 November. The stations were scheduled to collect data simultaneously for 9-minute intervals starting at the top of every hour. However, some runs were started later within the hour or missed because of minor malfunctions of the equipment or loss of power at the site. In total, 286 (297) samples were collected at the Sea Island (Cape Sable) site over the 14-day period, representing a loss rate of 12% (8%).

For comparison with other current measurements at or near the mooring site, CODAR radial currents from the twelve (nominal) 1.2 km grid points surrounding the site, i.e., within a radius of 2.4 km, were averaged to give a spatial-mean radial component over an area of roughly 18.1 km^2. To improve data quality, the standard deviation (σ_r) about the mean was computed and used to reject outliers which were removed from the mean by more than $n\sigma_r$ (n = 1,2). The statistics of the reduced data set were then recomputed. Error estimates for the radial current components were derived from the standard deviations about the spatial mean. Comparisons of the $1\sigma_r$ and $2\sigma_r$ CODAR data against current meter and drifter results have indicated no significant improvement is achieved by the more stringent $1\sigma_r$-analysis. Therefore the CODAR results presented here are derived from the $2\sigma_r$-analysis. Unfortunately, the set of radial components collected from Seal Island is reduced because the effective range of the radar at that site was occasionally less than the anticipated 35 km.

3c. WIND AND WAVE DATA

During the cruise, local wind was regularly measured at a height of roughly 12.5 m using a Gill anemometer mounted on a mast at the bow. At each station, the bow was turned into the wind and that heading was maintained as much as possible while the relative speed and direction were recorded over a 10-min. interval. Unfortunately, under high winds and heavy seas, the ship's head could not be maintained to better than $\pm 38^0$ (worst case). Therefore the wind direction and to some extent the speed data are contaminated by high frequency noise.

In addition to the wind measurements, a Datawell WAVEC pitch-and-roll buoy was used to collect hourly directional wave data at the mooring site (Figure 2). Figure 4 shows the time series of wind speed and direction and orbital wave velocity, U_w, defined by,

$$U_w = 4\pi^2 \int_{f_L}^{f_N} f^2 \, \phi(f) \, df \qquad (4)$$

where f_N=.64 Hz (Nyquist frequency) and f_L=.01 Hz span the energetic portion of the heave spectrum, $\phi(f)$. [$\phi(f)$ is contaminated by instrument noise at frequencies lower than f_L.] The winds are predominantly <u>toward</u> the south and east, as is normal for this time of year on the Scotian Shelf, and the wind speed and wave orbital velocity are generally well correlated. Both wind and wave energy achieve minima on November 23 and at the end of the experiment.

4. RESULTS

4a. MOORED INSTRUMENTS

Eulerian statistics (Table 3) and progressive vector plots (Figures 5a-c) of the currents in the upper half of the water column reveal a strong tidal oscillation superimposed on a weak mean current. Both the vector-mean and standard deviation of the S4 currents exceed those of the VMCM by 27% and 12%, respectively. Deeper in the water column, the current variance is reduced and the mean current rotates clockwise to flow against the surface current near the bottom. The mean currents estimated from the complete records at mid-depth (27-30 m; Table 1) agree to within $\pm 5\%$ in magnitude and $\pm 5^0$ in direction. However, the shorter records from VACM(12) and PRCM(31) appear to have anomalous mean currents [with respect to VMCM(1.5) and SRCM(30), respectively] suggesting that those measurements were impaired in some way.

A comparison between the 10-min. current speeds and directions of the S4(1) and VMCM(1.5) (Figure 6a) reveals that the speed differences are greater when the magnitudes are large and approach zero when the current is slack. On the other hand, the PRCM(31) speed is consistently lower than that of the SRCM(30) (Figure 6b), whereas the speeds of PRCM(28) and SRCM(27) from the subsurface moorings are virtually identical (Figure 6c). Though noisy, the direction records from the Aanderaa pairs are generally in agreement, but significant discrepancies between the S4 and VMCM directions are evident, particularly during the latter portions of the records. These differences of order $20\text{-}30^0$ are sporadic, but appear to be most pronounced when the current speed is high and directed westward (i.e., into the Gulf of Maine). The smoothness and consistency of the VMCM direction signal suggests that it is the truer measure. VACM(12) speeds are generally smaller than those of VMCM(1.5) and both speed and direction signals at the VACM appear to lead by small amounts (Figure 6d).

Scatter plots of the 10-min. current speeds and directions (Figure 7) indicate that high correlations exist between the speeds measured at adjacent instruments on a given mooring. On the subsurface mooring, a linear regression of SRCM(27) on PRCM(28) speed (Table 4) is virtually indistinguishable from the 1:1 identity line (Figure 7b), and accounts for 99% of the variance. Differences between these two speeds are more pronounced when the magnitudes are low, whereas direction differences are rather uniformly distributed over the range $0\text{-}360^0$ (Figure

7g). On the other hand, though the regression of S4(1) on VMCM(1.5) accounts for a similarly high fraction of the variance, the slope of this line indicates that the S4 speeds are scaled upwards by 15% (Figure 7a). As suggested by the time series plots, the differences tend to zero with the speed itself and are maximum when the speed is high. S4-VMCM direction differences are concentrated at the dominant ebb and flood directions of the tide (Figure 7f).

The comparison of SRCM(30) versus PRCM(31) speed (Figure 7c) lies entirely above the 1:1 line confirming the under-response of the deeper "paddlewheel" instrument. The deviations are generally greater at low speed (except at the very lowest), and reduced but still significant at high speed. A linear regression accounts for 99% of the variance indicating that the speed offsets are consistent over the entire range, but differences in direction (Figure 7h) appear to be associated with the turning of the tide. Comparisons of the mid-depth records to the VMCM (Figures 7d,e,i,j) reveal a loss of coherence in the vertical, an average vertical shear of order 0.10 ms^{-1} over the upper half of the water column, and a relative enhancement of the mid-depth currents at low speeds.

Scatter plot comparisons of speeds and directions from instruments at nearly the same depth on adjacent moorings (Figure 8) shows reduced coherence of currents over horizontal scales ranging from 0.5 to 1.0 km. Nevertheless, there is evidence of contamination of the SRCM(30) measurements on the surface mooring as indicated by enhanced speeds relative to those from SRCM(27) and PRCM(28) in the range, $S \leq 0.5$ ms^{-1} (Figures 8b,c). The "paddlewheel" instrument, PRCM(31), also shows this behaviour versus PRCM(28) over a somewhat reduced range ($S \leq 0.25$ ms^{-1}; Figure 8a), but the entire distribution is shifted toward higher PRCM(28) speeds because of the apparent malfunction (under-response) of the PRCM(31). No consistent pattern was found in the direction scatter plots for these instruments (Figures 8f,g,h).

The deviations of VACM(12) speeds from those of the surface instruments, VMCM (1.5) and S4(1), on an adjacent mooring (Figures 8d,e) are larger than those at mid-depth. At least part of this discrepancy may be related to a difference in the semidiurnal tidal phase at the two locations, which is suggested by the direction scatter plot and confirmed by tidal analysis. [The "looping" of the direction pairs about the 1:1 line in Figure 8i, for instance, is consistent with the clockwise-rotating tidal current at VACM(12) leading that at VMCM(1.5) by 6^0 as observed.] In addition, there appears to be an average shear of order 0.05 ms^{-1} between the VMCM(1.5) and VACM(12) instruments.

The frequency dependence of the current variance may be investigated by rotary spectral analysis. The kinetic energy spectrum for the S4(1) currents exceeds that of the VMCM(1.5) by 20-30% at low frequencies (periods > 6 hr.) and by even greater amounts at high frequency (Figure 9a). By contrast, the spectra from SRCM(27) and PRCM(28) on the subsurface mooring agree to within 10% at the low frequencies and show a very similar behaviour at high frequencies (Figure 9b). However, both the Aanderaa records contain considerably more energy in the high frequency bands (by factors of 3-10) than those of either of the vector-averaging devices. On the surface mooring, the mid-depth SRCM(30) has low-frequency energy just slightly in excess of those on the subsurface mooring, but at high frequency, the SRCM(30) energies are higher by factors of 3-5. However, the PRCM (31) spectra are uniformly lower by 50% than those of SRCM(30) throughout the low-frequency range. This is equivalent to a 22% difference in the low-frequency current amplitude which is somewhat larger than may be inferred from the scatter plot (Figure 7c). Differences between the VMCM(1.5) and VACM(12) spectral energies are of order 20% and are found almost entirely in the low frequency bands.

The squared magnitude of the rotary correlation between the various instrument pairs (Figure 10) indicates that vector coherence at low frequencies is generally high out to periods approaching 6 hrs. At higher frequencies, the correlations fall precipitously except for the mid-depth pair on the subsurface mooring, SRCM(27) and PRCM(28). The coherence of that pair remains significant at 95% out to periods shorter than 1 hr., whereas the others are significant only in limited bands near 2- and 4-hours. The loss of coherence at high frequencies has been attributed to the excess noise of the S4 instrument in this range by Beardsley et al.(1986). The same may be said for the SRCM(30) measurements, whereas the VACM-VMCM correlation probably results from the physical separation of the instruments.

Finally, to examine the dependence of the speed and direction differences on the local signal-to-noise ratio (S/N) and the surface, fractional speed and direction differences,

$$FSDX = \frac{S_x - m}{S_m} \quad \text{and}$$

$$DDX = D_x - D_m$$

where m = VMCM and x = s(S4) or a (VACM), were computed by averaging the 10 min. difference data over one hour (centered on the mid-point of the WAVEC spectral calculation), and plotting against the ratio, S_m/U_w, where U_w is a measure of the orbital wave velocity defined by equation (4). [Note that if the speed, S_x, were simply a scaled version of S_m, e.g., $S_x = (1+\alpha)\ S_m$, then FSD = α.] At large S/N, the fractional speed difference for the S4 record (Figure 11a) asymptotes to roughly 0.15, consistent with the scale factor suggested by the linear regression of S_s on S_m (Table 4). At low S/N, however, the FSDS4 shows more scatter and its value approaches zero indicating that the over-response of the S4 is diminshed in the range, $S_m/U_w \leq 3.0$. For the VACM, the FSDVA appears to asymptote to a small negative value (as in a sheared tidal current), but shows a high degree of scatter in the range, $S_m/U_w \leq 5.0$ (Figure 11b). Direction differences for the S4 have extremes which fall well outside the estimated accuracy of that measurement ($\pm 7^0$) and show no consistent variation with S_m/U_w (Figure 11c). The VACM direction differences also show large, predominantly positive values at low signal-to-noise levels (≤ 4.0) and approach zero as S_m/U_w increases (Figure 11d).

4b. CODAR VERSUS NEAR-SURFACE MOORED INSTRUMENTS

To facilitate comparison with the CODAR spatially-averaged radial current components, the near-surface measurements from the S4 and VMCM were resolved along and across the radial directions from each site to the mooring (Figure 1). Comparison of the CODAR and current meter time series (Figure 12) shows that except for a few obvious errors, the Cape Sable radial velocity components agree with the 10-min. VMCM(1.5) equivalent quite well. The Seal Island measurements, however, which reflect a stronger tidal signal, are noisier and more sparse, primarily because of the difficulties encountered in achieving the full 30 km range to the mooring from that particular site. Scatter plots (Figure 13) confirm the superior quality of the Cape Sable measurements, but reveal no consistent pattern in the Seal Island discrepancies. Linear regression analysis (Table 4b) indicates that the CODAR signals account for 80% and 67%, respectively, of

the radial VMCM current variances at the mooring site along 215^0 (Cape Sable) and 146^0 (Seal Island). Further comparisons of the CODAR data against Lagrangian surface drift measurements have been described by Lawrence and Smith (1986).

5. DISCUSSION AND CONCLUSIONS

One of the primary conclusions of this study is that current meters intended to measure near the surface in harsh winter environments must be very robust. The high rate of instrument failure during the Cape Sable Intercomparison Experiment may be traced, in part, to 1) the difficultires involved in maneuvering the ship to place the moorings in high seas and strong currents, and 2) the stress acting on the mechanical parts of the instruments in the surface mooring configuration. The VACM Savonious rotors appear to be particularly susceptible to damage as is the entire sensor assembly of the ACM. Despite the problem with a leaky compass, the S4 instrument appears to be the most physically robust for this type of application.

The observed over-response of the S4(1) with respect to the VMCM(1.5) may have a number of different causes. Perhaps the simplest explanation is an inaccurate calibration of this particular instrument, which was on loan from the manufacturer. A linear regression analysis of the tow-tank test data for the original calibration (J. Trageser, InterOcean Systems Inc., pers.comm.) gives a slope of the S4 versus carriage speed of 1.055. Hence the original calibration appears to inflate the S4 currents by 5.5%. Another possible cause is flow distortion associated with the mooring configuration. To achieve an average depth of 1 m below the surface, the S4 was shackled directly to the 4 ft. steel float which supported the mooring such that its sensing elements were a distance of only 1/4 float diameter from the underside of the sphere. In a laminar, irrotational flow field, the current at this distance from a fully-immersed sphere is accelerated by 14% above its free stream value and 10% above that at the VMCM, which is just beyond one diameter from the center of the float (Batchelor, 1967). Thus, the combination of calibration inaccuracies and fluid dynamic effects of the mooring configuration are capable of explaining the upward scaling of the S4 currents by 15%.

It is worth pointing out as well that the S4 over-response is <u>not</u> consistent with wind-induced vertical shear. Since the maximum 10 m wind speed during the experiment was approximately $U_{10} \approx 15$ ms^{-1} (Figure 5), the vertical shear produced at z = 1 m according to (2) is

$$\frac{\partial u}{\partial z} = \frac{u_*}{kz} \approx 0.08 \ s^{-1},$$

where $u_* = (\varrho_a C_D/\varrho_o)\ U_{10}$, ϱ_a=1.3 kg m^{-3}, ϱ_o=10^3 kg m^{-3}, and $C_D \approx 3.5 \times 10^{-3}$, so that the maximum speed difference between the S4 and VMCM would be,

$$S_s - S_m \approx \Delta z \frac{\partial u}{\partial z} \approx 0.04 \ ms^{-1}$$

This difference is equivalent to the scatter about the regression line in Figure 7a, but much smaller than the observed differences at high speeds. Furthermore, since the speed variations are controlled primarily by tidal currents, it is expected that wind-induced shear on a longer time scale would produce a small <u>offset</u> of the S4 with respect to the VMCM rather than a scale factor.

The fractional speed difference comparisons (Figure 11) confirm the over-response of the S4 by 15-20% at high signal-to-noise ratio, but the interpretation is less clear in the range $S_m/U_w \leq 2.0$. Beardsley <u>et al</u>. (1986) have found that a 9% over-response of the S4 vs. VMCM in that range could be partially accounted for by a 6% under-response of the VMCM with respect to the true speed. Therefore, they concluded that the S4 over-responds by only 3($\pm$7)% for $S_m/U_w \leq 2.0$. Figure 11a shows similar behaviour in the lower range, but asymptotes to a higher value ($\approx$ 0.15) rather than zero as S_m/U_w increases. Further study of these effects is required.

The 27% difference between the S4 and VMCM mean speeds over the experiment (Table 3) may be partly explained by the over-response of the S4. However, the rest of the discrepancy is probably caused by the "sticky" S4 compass, which produced directions that were biased toward the southwest during peak flood currents (Figure 6a). The incomplete cancellation of the rotary tidal component could easily contribute such a small difference to the vector mean current.

Finally, the attempt to evaluate the performance of the new Aanderaa "paddlewheel" rotor was frustrated by the failure of the PRCM(31) on the surface mooring. The observed under-response of PRCM(31) is not inconsistent with the damage to the fin and the resulting imbalance of the instrument. If the loss of the counterweight on the fin had caused the instrument to tilt at the limit allowed by the gimbal (27^0) and the rotor had a cosine response, the PRCM(31) would have under-responded by the factor, 0.89. This difference is compatible with the observations in the range $S \leq 0.5$ ms^{-1} (Figure 7c). At lower speeds, the SRCM(30) appears to over-respond, as expected, with respect to the "adjusted"

PRCM(31). In addition, the SRCM(30) speed enhancements with respect to instruments on the subsurface mooring seem to occur over a wider range of low speeds than for the PRCM(31) (Figures 8a-c). Thus it appears that the PRCM(31) rejects some of the mooring motion which contaminates the SRCM(30). The differences are very difficult to quantify, however, because of uncertainties about the performance of the PRCM(31).

ACKNOWLEDGEMENTS

The authors would like to acknowledge the assistance and support of members of the Coastal Oceanography Division, PCS, DFO, especially R.R. Lively, A.J. Hartling, and T.R. Foote. This work was supported (in part) by the Canadian Federal Panel on Research and Development.

REFERENCES

Barrick, D.E., Evans, M.W. and Weber, B.L. 1977. Ocean surface currents mapped by radar. Science, 198:139-144.

Batchelor, G.K. 1967. An Introduction to Fluid Dynamics. Cambridge Univ. Press, Cambridge, UK, 615 pp.

Beardsley, R.C. 1987. A comparison of the Vector-Averaging Current Meter and new Edgerton, Germeshausen and Grier, Inc., Vector-Measuring Current Meter on a surface mooring in Coastal Ocean Dynamics Experiment I. J. Geophys. Res.,92: 1845-1859.

Beardsley, R.C., Scott, J. and Boicourt, W. 1977. CMICE 76: A current meter intercomparison experiment conducted off Long Island in February-March 1976. Technical Report 77-62, Woods Hole Oceanographic Institution, Woods Hole, MA, 123 pp.

Beardsley, R.C., Briscoe, M., Signell, R., and Longworth S. 1986. A VMCM-S4 current meter intercomparison on a surface mooring in shallow water. In Proceedings of the IEEE Third Working Conference on Current Measurement. Eds. G.F. Appell and W.E. Woodward, 7-12.

Churchill, J.H. and Csanady, G.T. 1983. Near-surface measurements of quasi-Lagrangian velocities in open water. J. Phys. Oceanogr., 13:1669-1680.

Collar, P.G., Howarth, M.J., and Millard, N.W. 1986. An intercomparison of HF radar observations of surface currents with moored current meter data and displacement rates of acoustically tracked drogued floats. In: Advances in Underwater Technology, Ocean Science and Offshore Engineering. Graham & Trotman Ltd., Vol.6:163-182.

Fofonoff, N.P. and Ercan, Y. 1967. Response characteristics of a Savonious rotor current meter. Technical Report 67-33, Woods Hole Oceanographic Institution, Woods Hole, MA, 36 pp.

Garrett, C. 1976. Generation of Langmuir circulations by surface waves: A feedback mechanism. J. Mar. Res., 34:117-130.

Gaul, R.D. 1963. Influence of vertical motion on the Savonious rotor current meter. Technical Report 63-4T, Texas A&M University, College Station, Texas, 29 pp.

Halpern, D., Weller, R.A., Briscoe, M.G., Davis, R.E. and McCullough, J.R. 1981. Intercomparison tests of moored current measurements in the upper ocean. J. Geophys. Res., 86:419-428.

Ha, E-C. 1979. Remote sensing of ocean surface current and current shear by HF backscatter radar. PhD Dissertation, Stanford University.

Hammond, T.M., Pattiaratchi, C.B., Osborne, M.J. and Collins, M. 1986. Field and flume comparisons of the modified and standard (Savonious rotor) Aanderaa self-recording current meters. Dt. Hydrogr. Z., 2:41-63.

Holbrook, J.R. and Frisch, A.S. 1981. A comparison of near-surface CODAR and VACM measurements in the Strait of Juan de Fuca, August, 1978. J. Geophys. Res., 86:10908-10912.

Kalvaitis, A.N. 1974. Effects of vertical motion on vector-averaging (Savonious rotor) and electromagnetic type current meters. Tech. Memo NOAA-TM-NOS-NOIC-3, Nat. Oceanic and Atmos. Admin., Rockville, Md.

Lange, P. and Huhnerfüss, H. 1978. Drift response of monomolecular slicks to wave and wind action. J. Phys. Oceanogr., 8:142-150.

Lawrence, D.J. and Smith, P.C. 1986. Evaluation of HF ground-wave radar on the east coast of Canada. IEEE J. Oceanic Engin., OE-11:246-250.

LeBlond, P. and Mysak, L.A. 1978. Waves in the Ocean. Elsevier Sci. Publ. Co., Amsterdam, 602 pp.

Pashinski, D.J. 1985. Comparison of current meters in a tidally dominated flow. MTS-IEEE, Oceans 85 Proc.:938-941.

Saunders, P.M. 1976. Near-surface current measurements. Deep-Sea Research, 23: 249-258.

Smith, P.C. 1983. The mean and seasonal circulation off southwest Nova Scotia. J. Phys. Oceanogr., 13:1034-1054.

Smith, P.C., Lively, R.R. and Brown, K.C. 1984a. An intercomparison of near-surface measurements with Aanderaa and AMF-VACM current meters in strong tidal currents. Can. Tech. Rep. Hydrogr. Ocean Sci., 48, 36 pp.

Smith, McKeown, D.L. Milligan, T.G. Whitman, J. Belliveau, D. and Freeman, N. 1984b. Report on Dawson Cruise - 84-043. Unpublished manuscript.

Stewart, R.H. and Joy, J.W. 1974. HF radio measurements of surface currents. Deep-Sea Research, 21:1030-1049.

Weller, R. and Davis, R.E. 1980. A vector-measuring current meter. Deep-Sea Research, 27:565-582.

Wu, J. 1975. Wind-induced drift currents. J. Fluid Mech., 68:49-70.

TABLE 1 Moored Instrumentation Employed During the Cape Sable Intercomparison Experiment, 14-27 November, 1984

NAME	DESIGNATION	MANUFACTURER'S SPECIFICATIONS	range	resolution	accuracy
Standard Aanderaa Recording Current Meter	SRCM	Speed(cm s^{-1}):	2-250.	0.04	±1 or 2%
		Direction:	0-360°	0.4°	±5°-7.5°
Modified Aanderaa "Paddlewheel" Rotor	PRCM	Speed(cm s^{-1}):	2-250.	0.04	±1 or 2%
		Direction:	0-360°	0.4°	±5°-7.5°
EG&G Vector Measuring Current Meter	VMCM	Speed(cm s^{-1}):	1-400.	0.08	±1%
		Direction:	0-360°	1.4°	±5°
EG&G Vector Averaging Current Meter	VACM	Speed(cm s^{-1}):	3-309.	0.04	±0.3
		Direction:	0-360°	2.8°	±5°
InterOcean S4 Electromagnetic Current Meter	S4	Speed(cm s^{-1}):	0-350.	0.2	±1 or 2%
		Direction:	0-360°	0.5°	±2°
Neil Brown Instruments Smart Acoustic Current Meter	ACM	Speed(cm s^{-1}):	0-360.	0.1	±1 or 3%
		Direction:	0-360°	1.4°	±5°

TABLE 2 Performance of Moored Instrumentation at Site CS during Cape Sable Intercomparison Experiment, 14-27 November, 1984

MOORING (DEPTH,m)	N. LAT., W. LONG.	DEPLOY/RECOVER TIME(GMT),DATE	INSTRUMENT (DEPTH,m)	PERFORMANCE
669(57)	43°11.1′	0102,Nov 17/	SRCM(27)	satisfactory
	65°49.5′	1452,Nov 26	PRCM(28)	"
			SRCM(38)	"
			SRCM(48)	"
671(61)	43°10.9′	1341,Nov 18/	VMCM(1)	lost after 2 hr.
	65°48.9′	1820,Nov 22	VACM(5)	"
			VACM(8)	on bottom after 2 hr., compass defective
			VACM(12)	on bottom after 2 hr., rotor broken on deployment
			VACM(16)	on bottom after 2 hr., rotor broken on deployment
672(58)	43°10.9′	1502,Nov 18/	S4(1)	oil leak from compass
	65°49.3′	1312,Nov 26	VMCM(1.5)	shaft broken on recovery
			ACM(5)	acoustic sensors damaged, no data
			SRCM(30)	satisfactory
			PRCM(31)	broken fin, rotor fails after 67^{+} hr.
682(63)	43°11.0′	1545,Nov 23/	VACM(5)	rotor lost after 15 hr.
	65°48.6′	1627,Nov 26	VACM(8)	rotor lost after 1 hr.
			VACM(12)	post-calibration indicates compass out of spec.
WAVEC1	43°11.4′	2255,Nov 16/	WAVEC	satisfactory
	65°48.7′	1350,Nov 22		
WAVEC2	43°11.3′	1408,Nov 22/	WAVEC	nylon mooring line parted
	65°49.5′	1415,Nov 26		on recovery

TABLE 3 Eulerian Current Statistics for the Cape Sable Intercomparison

MOORING NO.	INSTRUMENT (DEPTH,m)	NO. OF 2-MIN SAMP.	EASTWARD CURRENT MEAN (cm s^{-1})	EASTWARD CURRENT STD.DEV (cm s^{-1})	NORTHWARD CURRENT MEAN (cm s^{-1})	NORTHWARD CURRENT STD.DEV (cm s^{-1})
672	S4(1)	5703	-12.0	84.9	-16.0	33.4
672	VMCM(1.5)	"	-12.0	75.3	-10.1	30.9
669	SRCM(27)	"	-5.0	66.7	-3.6	23.1
669	PRCM(28)	"	-4.7	66.5	-4.2	28.3
672	SRCM(30)	"	-4.8	66.3	-4.7	30.1
669	SRCM(37)	"	1.8	54.5	-1.0	30.6
669	SRCM(47)	"	4.9	47.3	3.8	28.6
Short Records:						
672	VMCM(1.5)	2085	-5.7	75.1	-9.3	27.8
682	VACM(12)	"	-8.4	68.2	1.8	29.4
672	SRCM(30)	2024	-1.6	65.2	-1.8	29.1
672	PRCM(31)	"	0.3	55.2	0.4	19.4

TABLE 4a Linear Regression Coefficients for 10-Min. Speed Comparisons

$$y = a_o + a_1 x$$

SPEED VARIABLES x	y	REGRESSION CONSTANTS $a_o \pm s_o^*$	$a_1 \pm s_1^*$	SQUARED REGRESSION COEFFICIENT: r^2
VMCM(1.5)	S4(1)	-0.023±.003	1.148±.004	.986
PRCM(28)	SRCM(27)	-0.023±.002	1.006±.003	.990
PRCM(31)	SRCM(30)	0.215±.003	0.883±.004	.991
PRCM(31)	VMCM(1.5)	0.237±.014	1.008±.024	.818
SRCM(30)	VMCM(1.5)	0.074±.012	1.023±.017	.767
PRCM(31)	PRCM(28)	0.077±.007	1.051±.012	.947
SRCM(30)	SRCM(27)	-0.163±.006	1.169±.008	.945
SRCM(30)	PRCM(28)	-0.113±.006	1.130±.009	.938
VACM(12)	VMCM(1.5)	0.082±.012	0.971±.016	.893
VACM(12)	S4(1)	0.081±.016	1.107±.022	.860

4b Linear Regressions for Current Meter/CODAR Radial Component Comparisons

VMCM146	CODARSI2	-0.040±.026	0.927±.047	.674
VMCM215	CODARCS2	0.027±.010	0.798±.031	.798

*a_o, a_1 are the standard errors of the regression constants

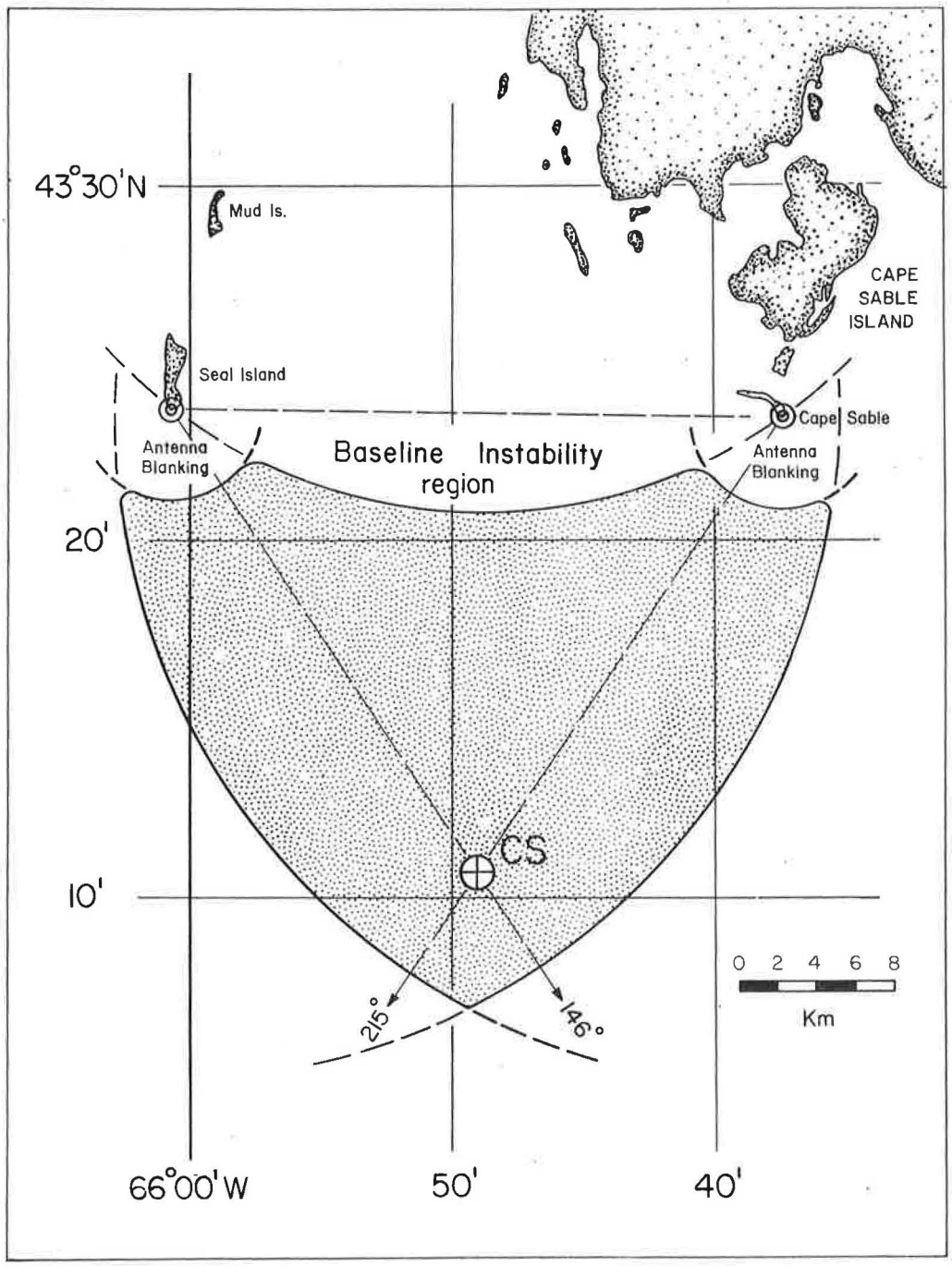
43°30'N
Mud Is.
CAPE
SABLE
ISLAND
Seal Island
Cape Sable
Antenna
Blanking
Baseline Instability
region
Antenna
Blanking
20'
CS
10'
0 2 4 6 8
Km
215°
146°
66°00'W
50'
40'

FIGURE 1

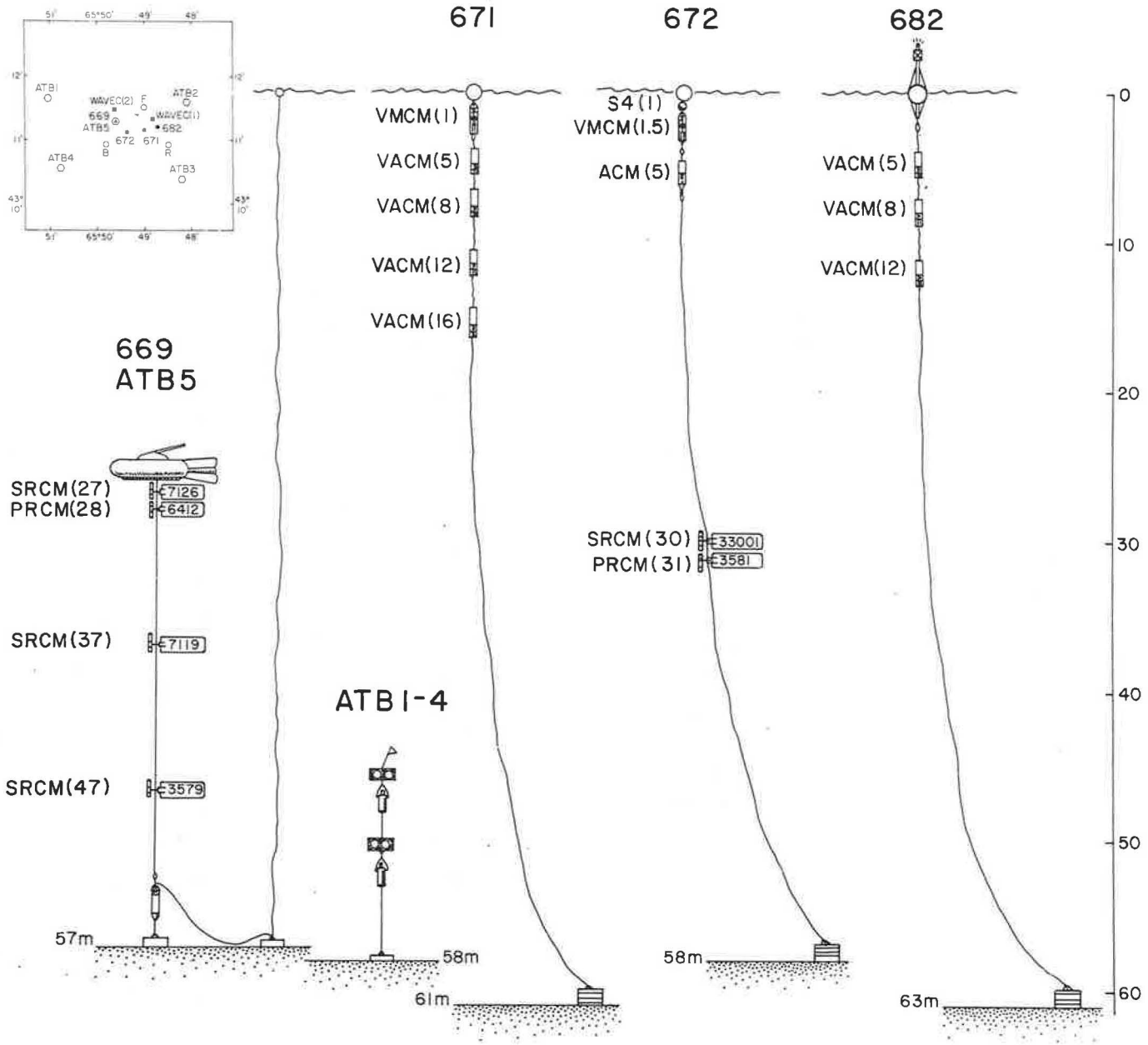
671
672
682
669
ATB5
ATB1-4
ATB1
ATB2
ATB3
ATB4
WAVEC(2)
WAVEC(1)
669
672
671
682
B
R
VMCM(1)
VACM(5)
VACM(8)
VACM(12)
VACM(16)
S4(1)
VMCM(1.5)
ACM(5)
VACM(5)
VACM(8)
VACM(12)
SRCM(27)
PRCM(28)
7126
6412
SRCM(37)
7119
SRCM(47)
3579
SRCM(30)
33001
PRCM(31)
3581
57m
58m
61m
58m
63m
0
10
20
30
40
50
60

FIGURE 2

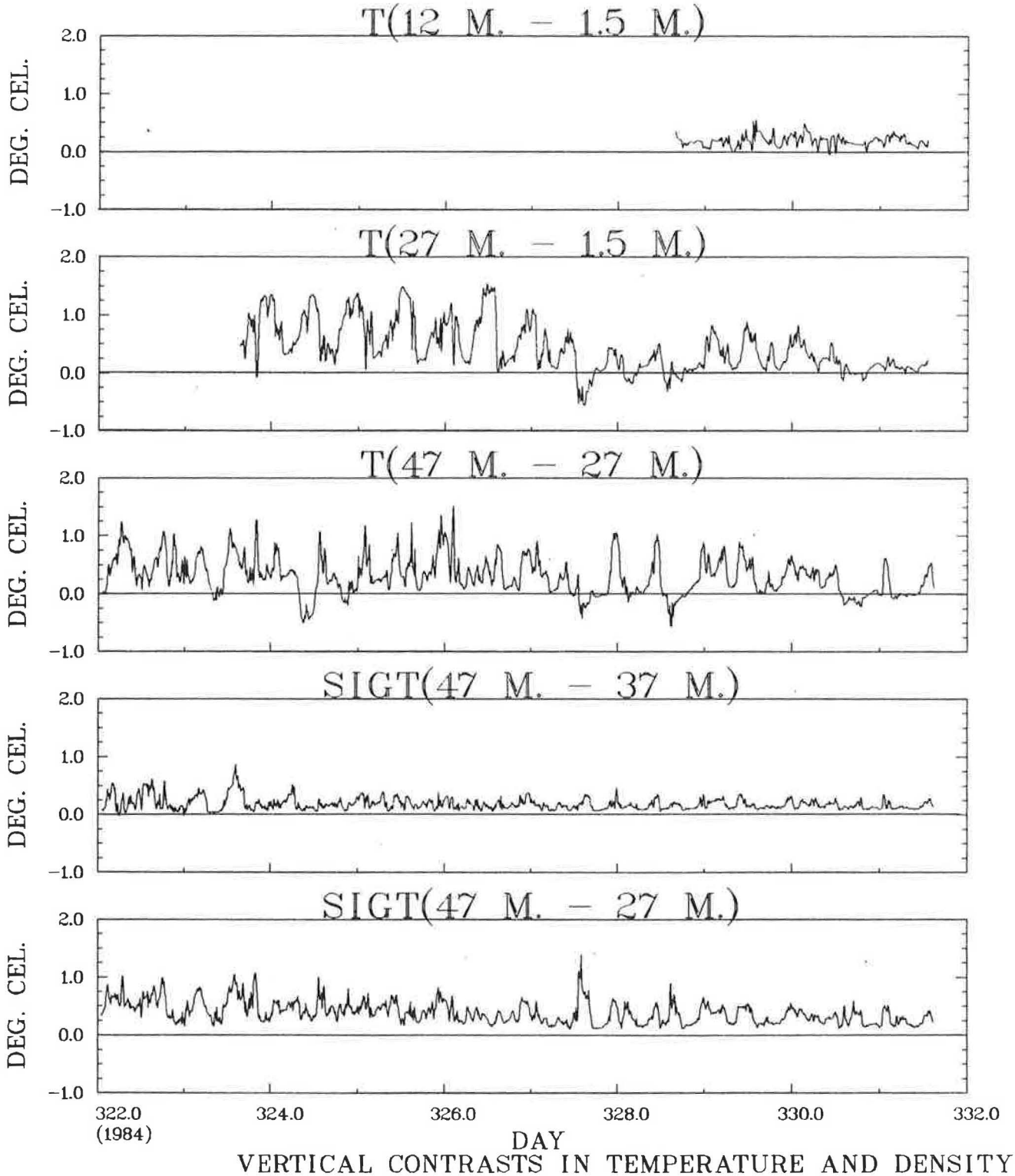

VERTICAL CONTRASTS IN TEMPERATURE AND DENSITY

FIGURE 3

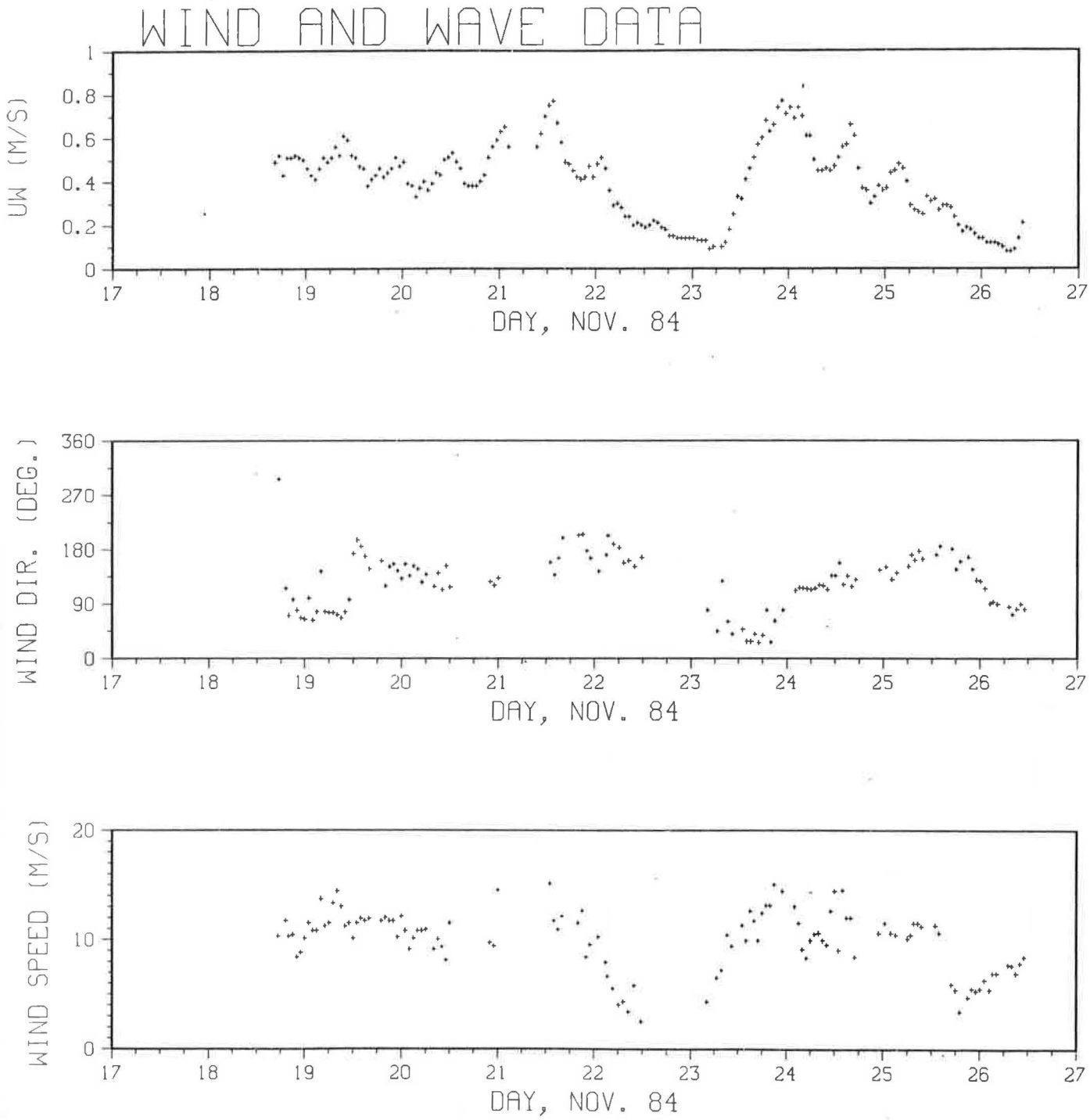
WIND AND WAVE DATA
UW (M/S)
1
0.8
0.6
0.4
0.2
0
17
18
19
20
21
22
23
24
25
26
27
DAY, NOV. 84
WIND DIR. (DEG.)
360
270
180
90
0
17
18
19
20
21
22
23
24
25
26
27
DAY, NOV. 84
WIND SPEED (M/S)
20
10
0
17
18
19
20
21
22
23
24
25
26
27
DAY, NOV. 84

FIGURE 4

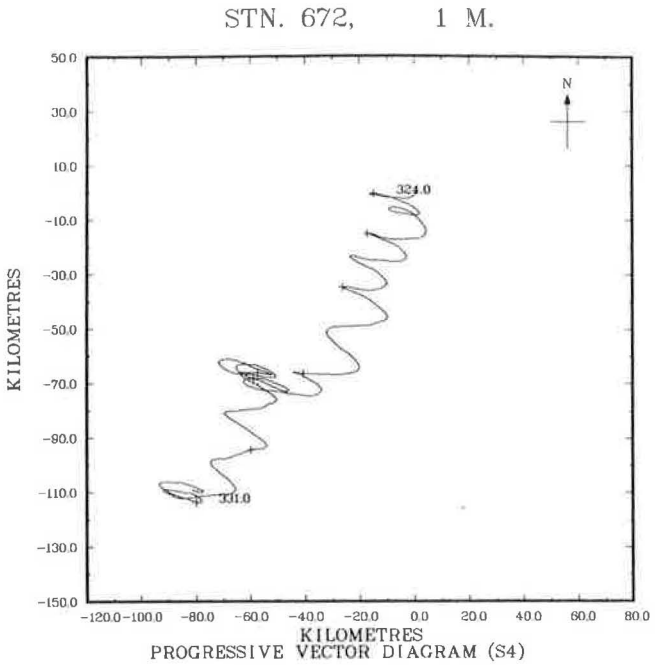
STN. 672, 1 M.
KILOMETRES
KILOMETRES
PROGRESSIVE VECTOR DIAGRAM (S4)
N
324.0
331.0

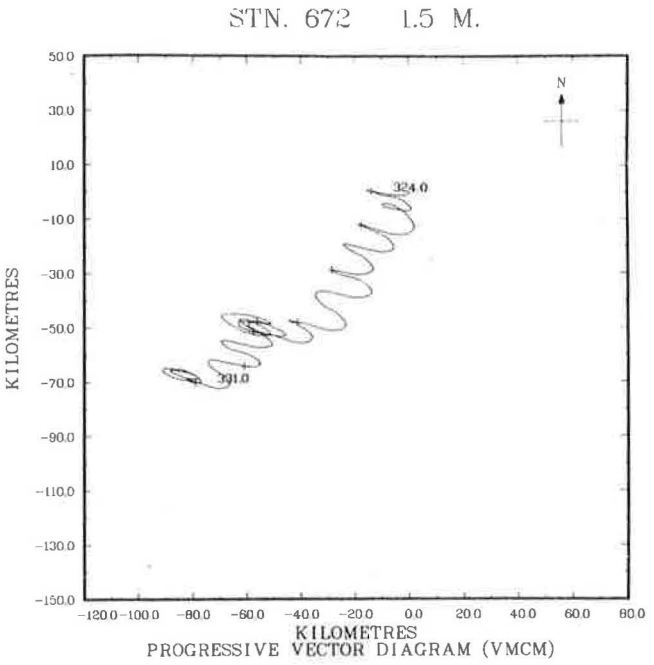
STN. 672 1.5 M.
KILOMETRES
KILOMETRES
PROGRESSIVE VECTOR DIAGRAM (VMCM)
N
324.0
331.0

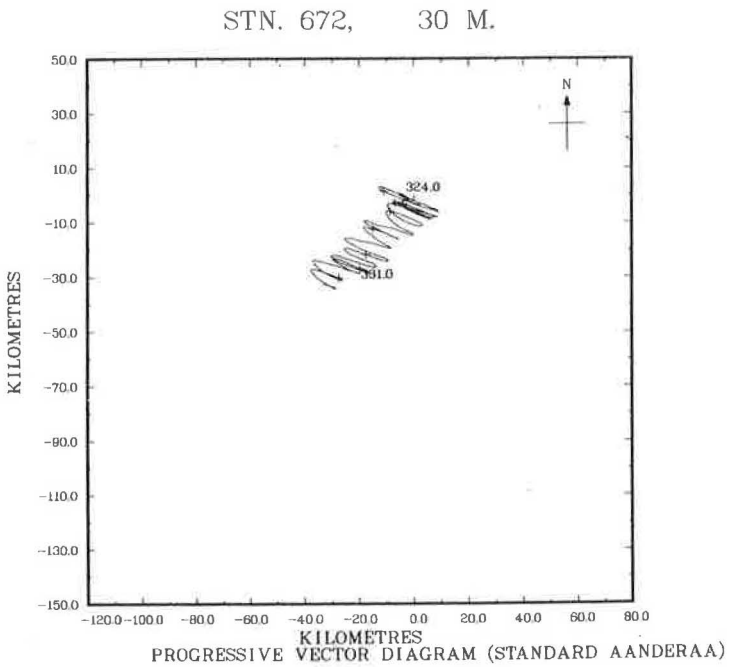
STN. 672, 30 M.
KILOMETRES
KILOMETRES
PROGRESSIVE VECTOR DIAGRAM (STANDARD AANDERAA)
N
324.0
331.0

FIGURE 5 (a)

STN. 669, 27 M.

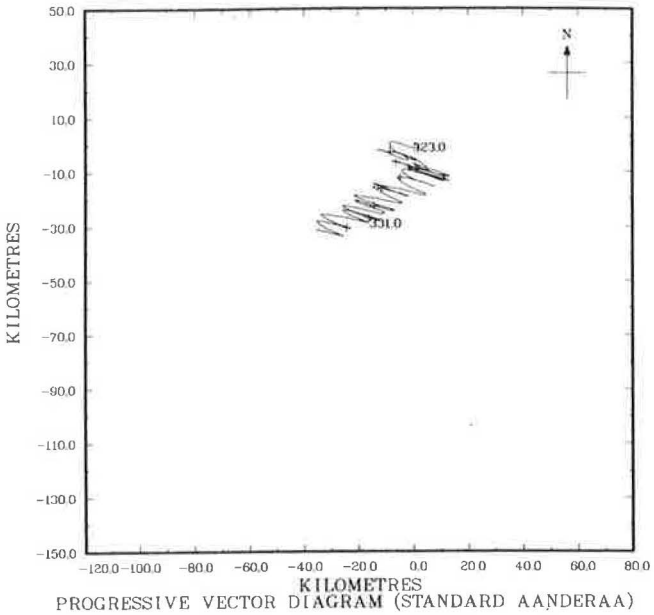

PROGRESSIVE VECTOR DIAGRAM (STANDARD AANDERAA)

STN. 669, 28 M.

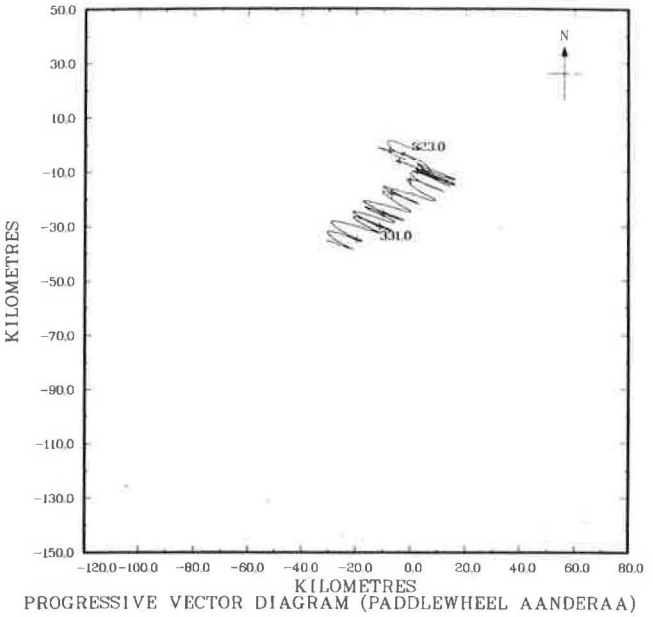

PROGRESSIVE VECTOR DIAGRAM (PADDLEWHEEL AANDERAA)

STN. 669, 37 M.

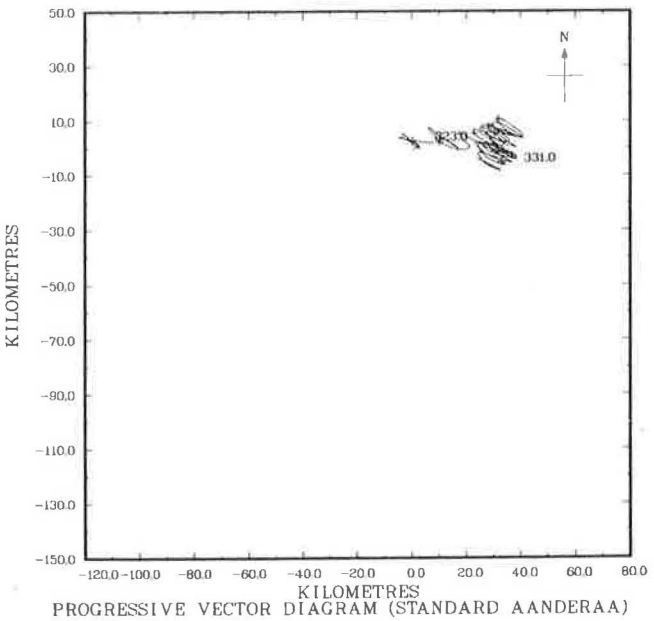

PROGRESSIVE VECTOR DIAGRAM (STANDARD AANDERAA)

STN. 669, 47 M.

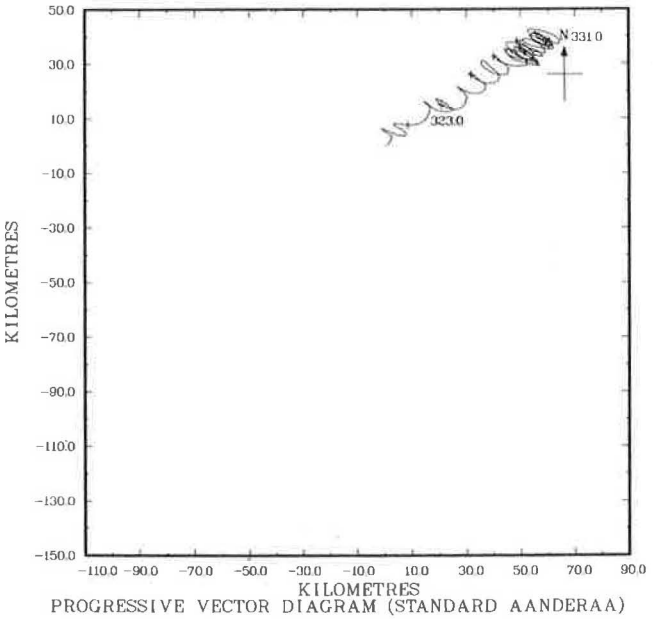

PROGRESSIVE VECTOR DIAGRAM (STANDARD AANDERAA)

FIGURE 5 (b)

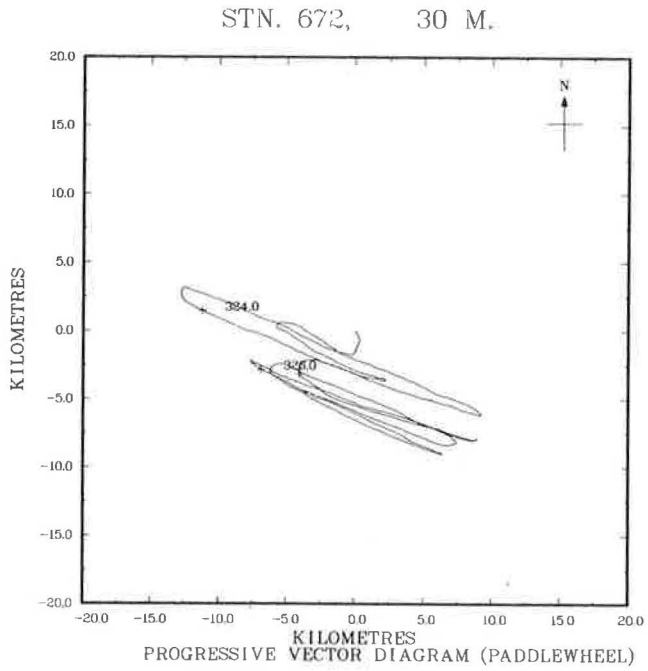
STN. 672, 30 M.
KILOMETRES
KILOMETRES
PROGRESSIVE VECTOR DIAGRAM (PADDLEWHEEL)

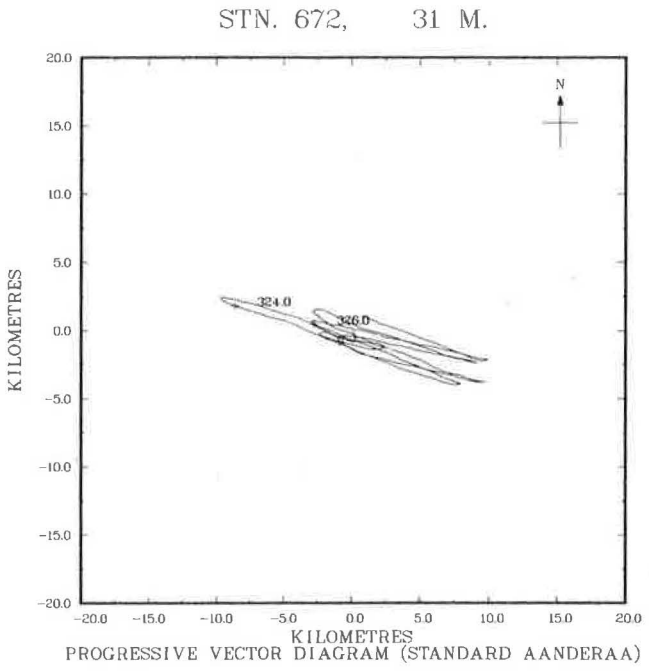
STN. 672, 31 M.
KILOMETRES
KILOMETRES
PROGRESSIVE VECTOR DIAGRAM (STANDARD AANDERAA)

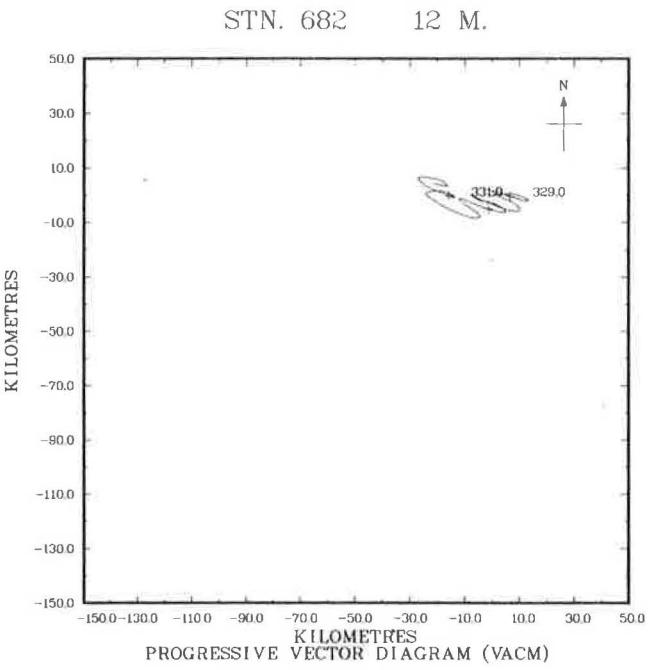
STN. 682 12 M.
KILOMETRES
KILOMETRES
PROGRESSIVE VECTOR DIAGRAM (VACM)

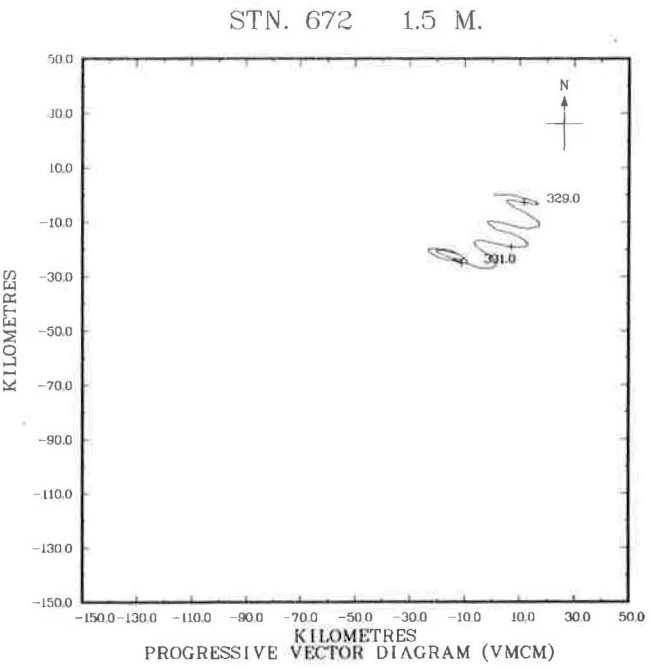
STN. 672 1.5 M.
KILOMETRES
KILOMETRES
PROGRESSIVE VECTOR DIAGRAM (VMCM)

FIGURE 5 (c)

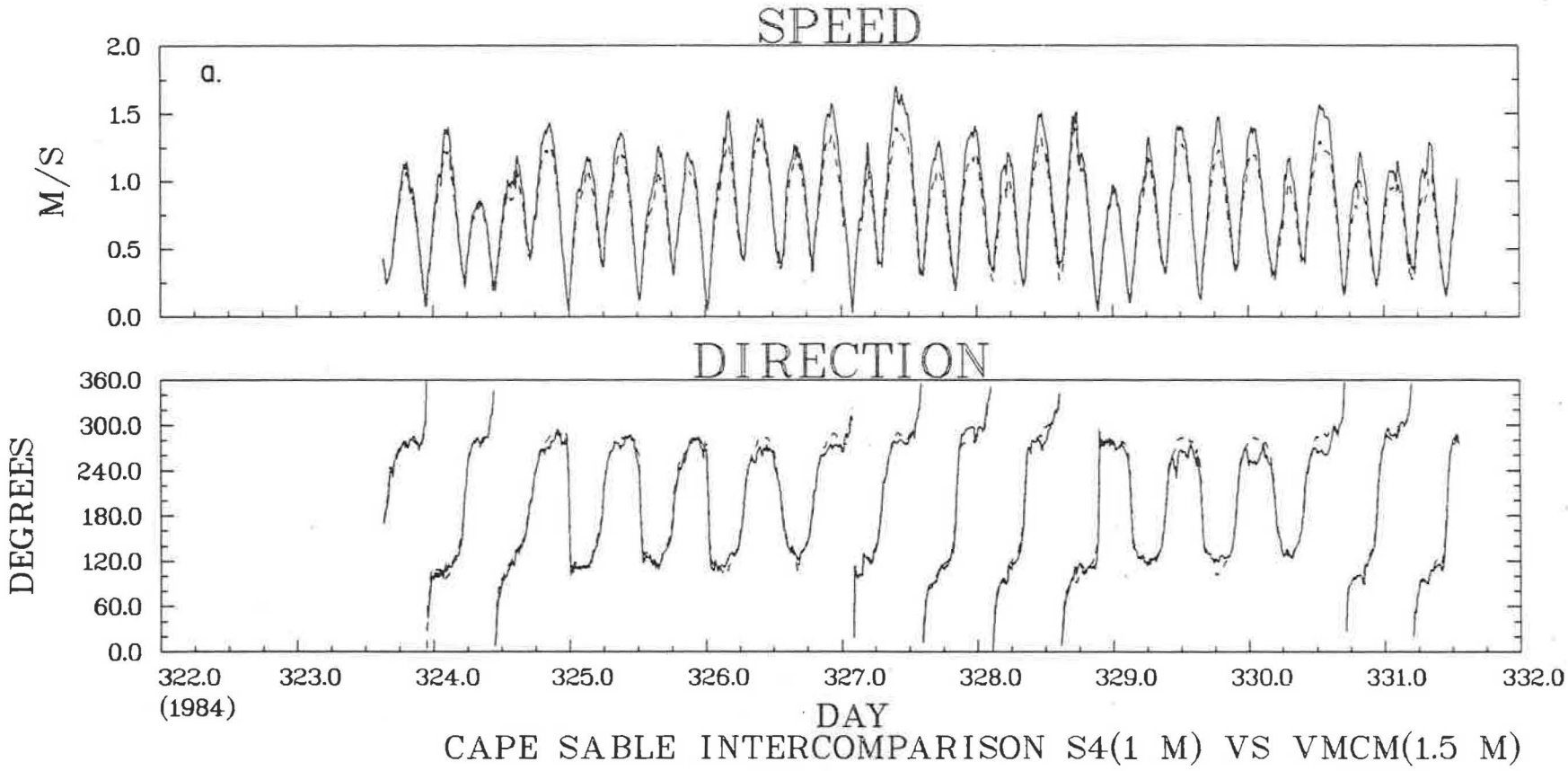
SPEED
a.
2.0
1.5
1.0
0.5
0.0
M/S
DIRECTION
360.0
300.0
240.0
180.0
120.0
60.0
0.0
DEGREES
322.0
(1984)
323.0
324.0
325.0
326.0
327.0
328.0
329.0
330.0
331.0
332.0
DAY
CAPE SABLE INTERCOMPARISON S4(1 M) VS VMCM(1.5 M)

FIGURE 6 (a)

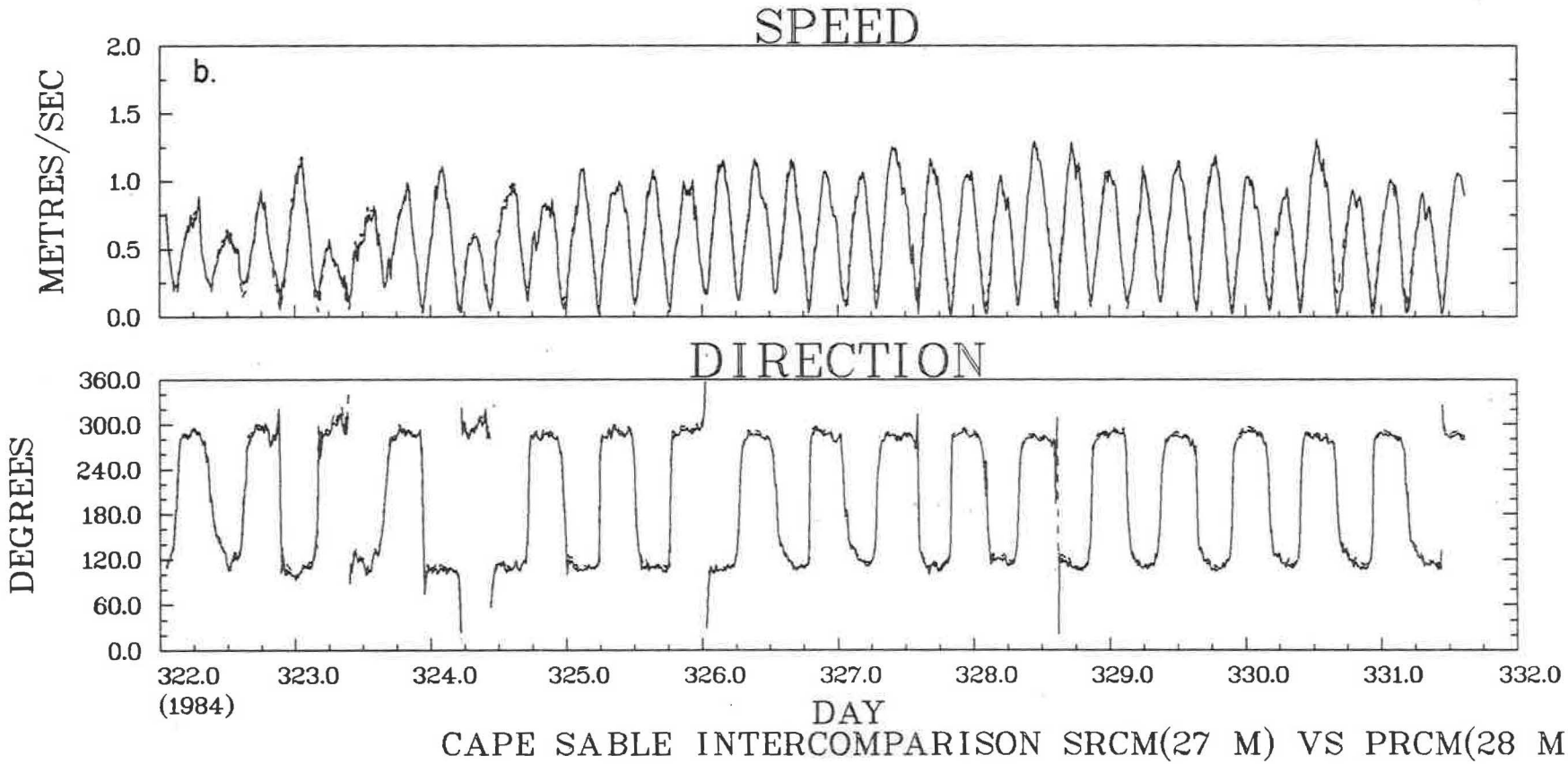
SPEED
b.
METRES/SEC
2.0
1.5
1.0
0.5
0.0
DIRECTION
DEGREES
360.0
300.0
240.0
180.0
120.0
60.0
0.0
322.0
(1984)
323.0
324.0
325.0
326.0
327.0
328.0
329.0
330.0
331.0
332.0
DAY
CAPE SABLE INTERCOMPARISON SRCM(27 M) VS PRCM(28 M)

FIGURE 6 (b)

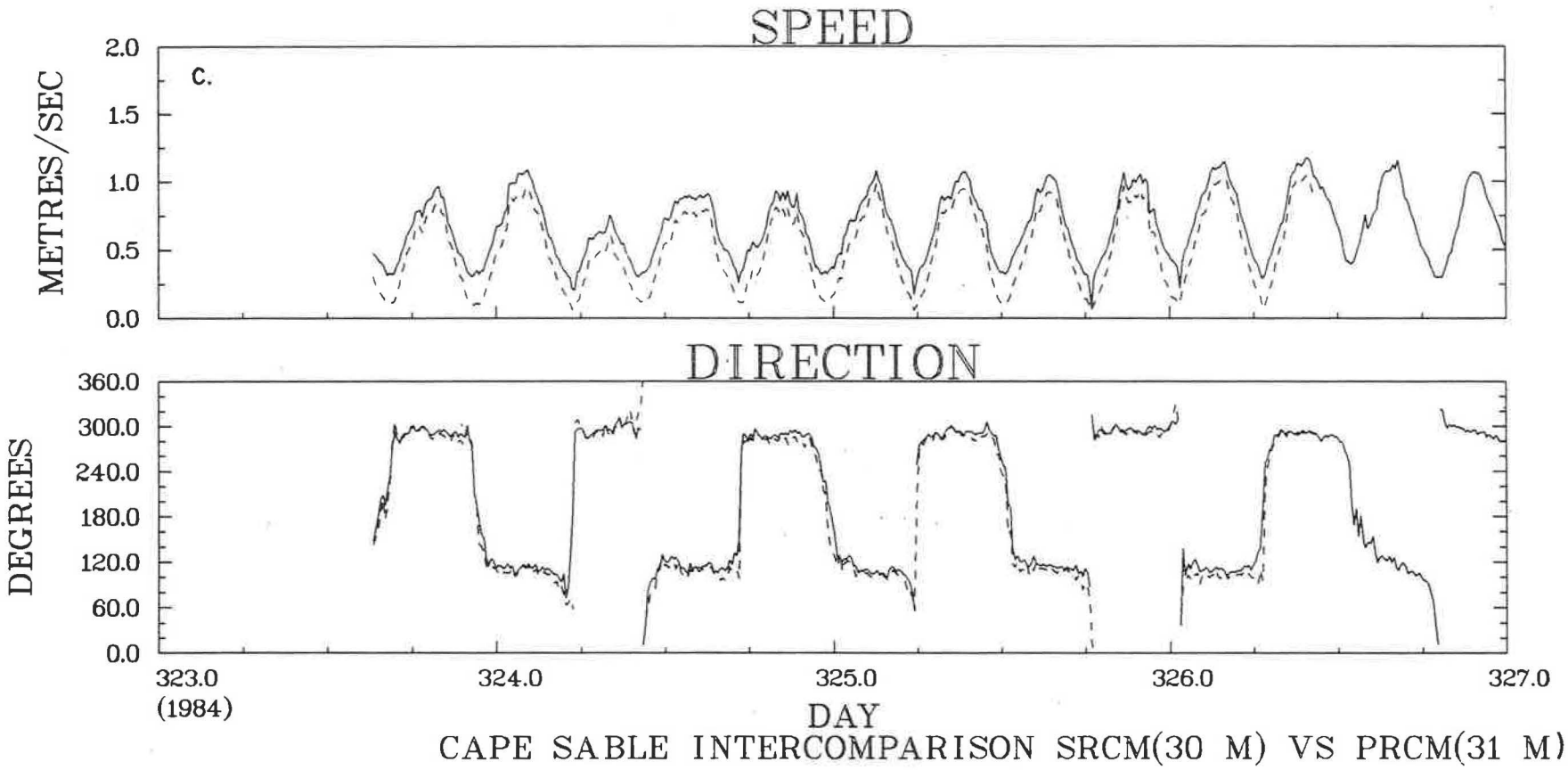
SPEED
c.
METRES/SEC
2.0
1.5
1.0
0.5
0.0
DIRECTION
DEGREES
360.0
300.0
240.0
180.0
120.0
60.0
0.0
323.0
(1984)
324.0
325.0
326.0
327.0
DAY
CAPE SABLE INTERCOMPARISON SRCM(30 M) VS PRCM(31 M)

FIGURE 6 (c)

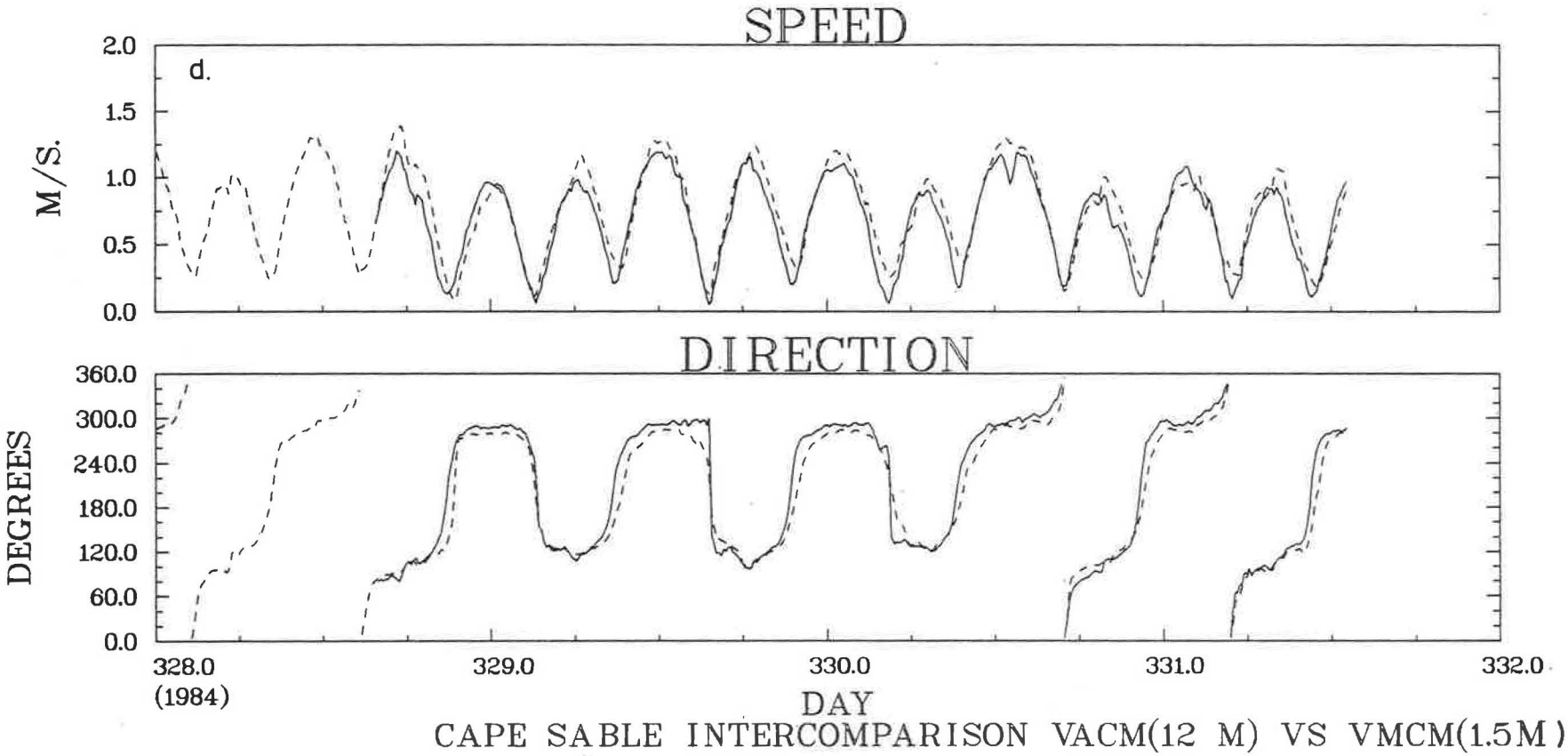
SPEED
d.
M/S.
2.0
1.5
1.0
0.5
0.0
DIRECTION
DEGREES
360.0
300.0
240.0
180.0
120.0
60.0
0.0
328.0
(1984)
329.0
330.0
331.0
332.0
DAY
CAPE SABLE INTERCOMPARISON VACM(12 M) VS VMCM(1.5M)

FIGURE 6 (d)

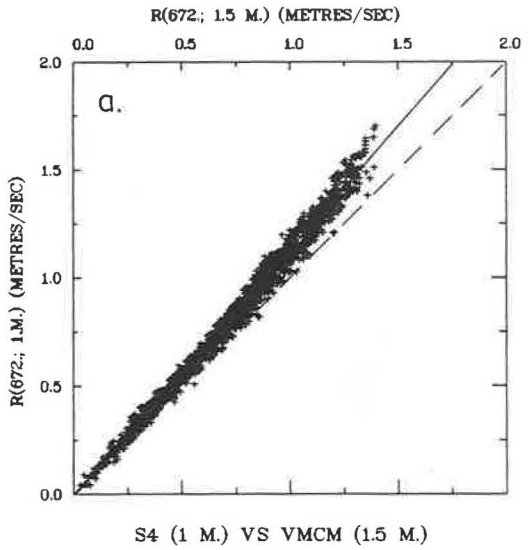
R(672.; 1.5 M.) (METRES/SEC)
a.
R(672.; 1.M.) (METRES/SEC)
S4 (1 M.) VS VMCM (1.5 M.)

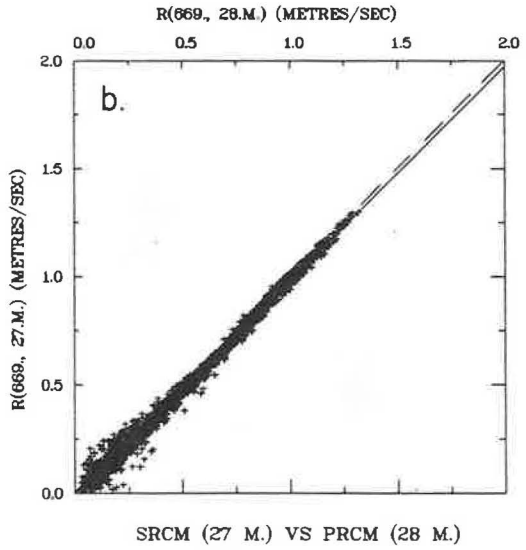
R(669., 28.M.) (METRES/SEC)
b.
R(669., 27.M.) (METRES/SEC)
SRCM (27 M.) VS PRCM (28 M.)

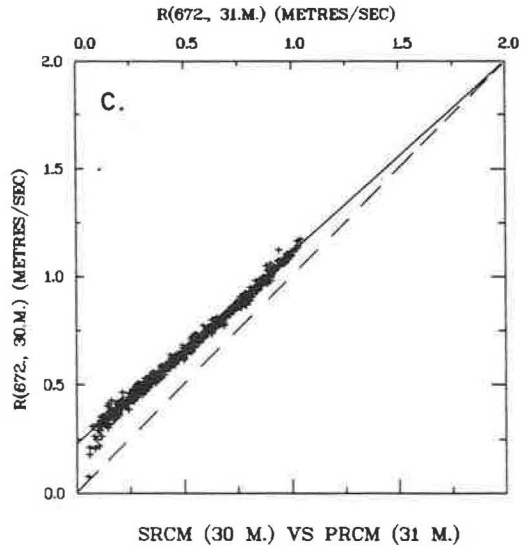
R(672., 31.M.) (METRES/SEC)
c.
R(672., 30.M.) (METRES/SEC)
SRCM (30 M.) VS PRCM (31 M.)

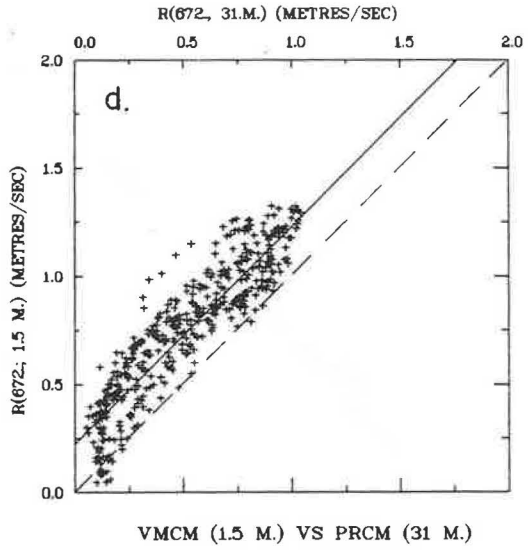
R(672., 31.M.) (METRES/SEC)
d.
R(672.; 1.5 M.) (METRES/SBC)
VMCM (1.5 M.) VS PRCM (31 M.)

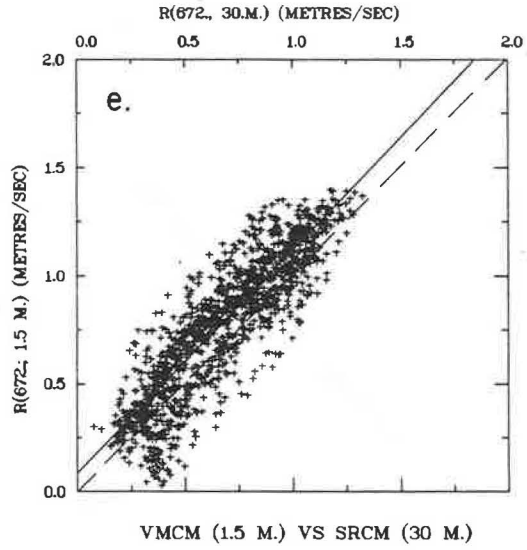
R(672., 30.M.) (METRES/SEC)
e.
R(672.; 1.5 M.) (METRES/SEC)
VMCM (1.5 M.) VS SRCM (30 M.)

FIGURE 7 (a-e)

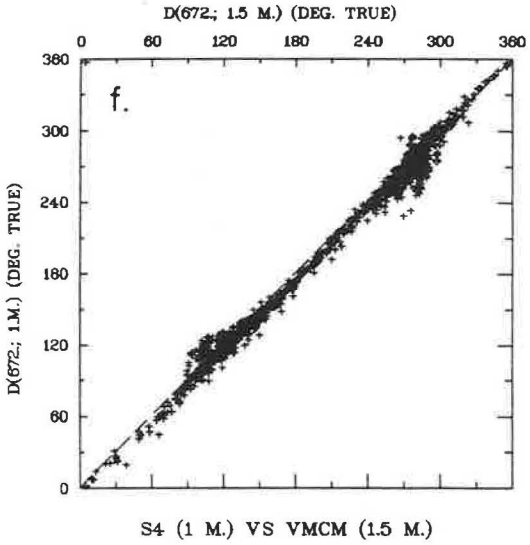
D(672., 1.5 M.) (DEG. TRUE)
f.
D(672., 1.M.) (DEG. TRUE)
S4 (1 M.) VS VMCM (1.5 M.)

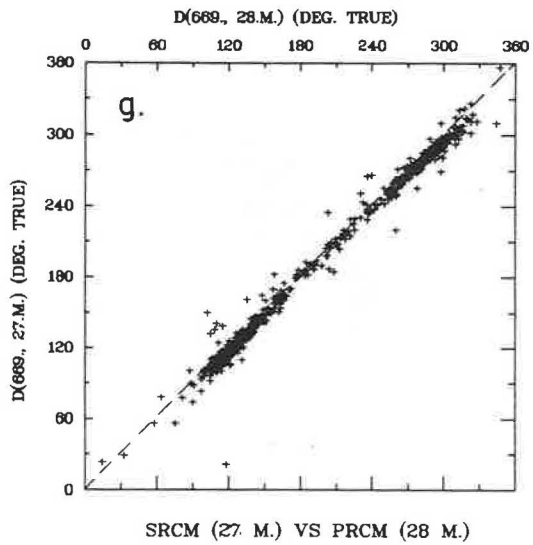
D(669., 28.M.) (DEG. TRUE)
g.
D(669., 27.M.) (DEG. TRUE)
SRCM (27. M.) VS PRCM (28 M.)

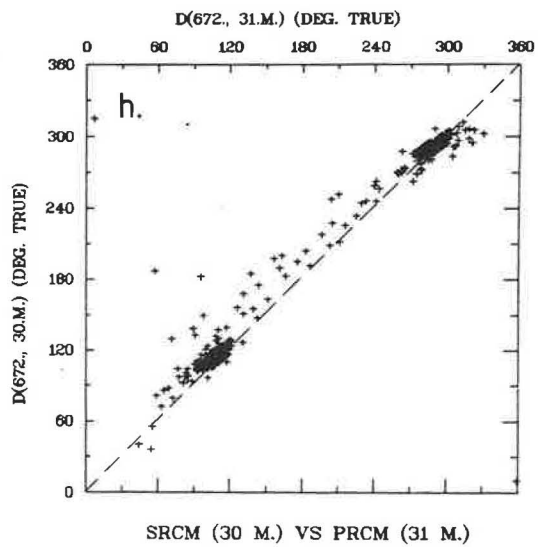
D(672., 31.M.) (DEG. TRUE)
h.
D(672., 30.M.) (DEG. TRUE)
SRCM (30 M.) VS PRCM (31 M.)

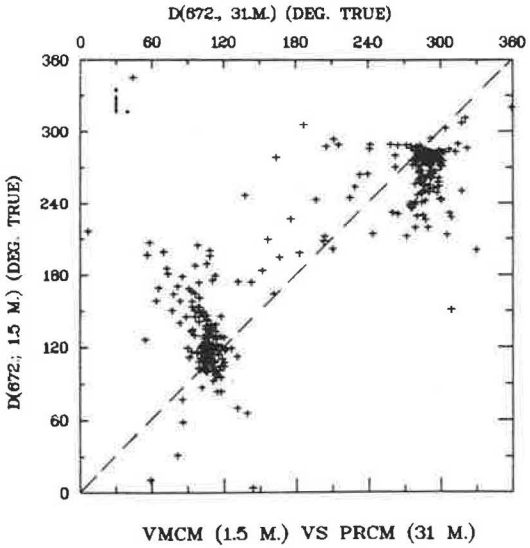
D(672., 31.M.) (DEG. TRUE)
i.
D(672., 1.5 M.) (DEG. TRUE)
VMCM (1.5 M.) VS PRCM (31 M.)

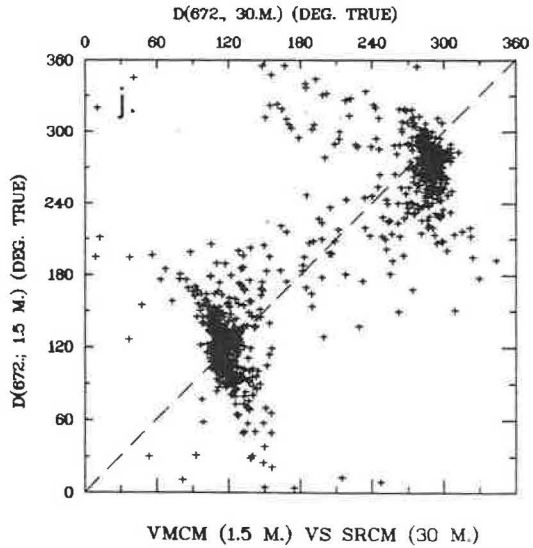
D(672., 30.M.) (DEG. TRUE)
j.
D(672., 1.5 M.) (DEG. TRUE)
VMCM (1.5 M.) VS SRCM (30 M.)

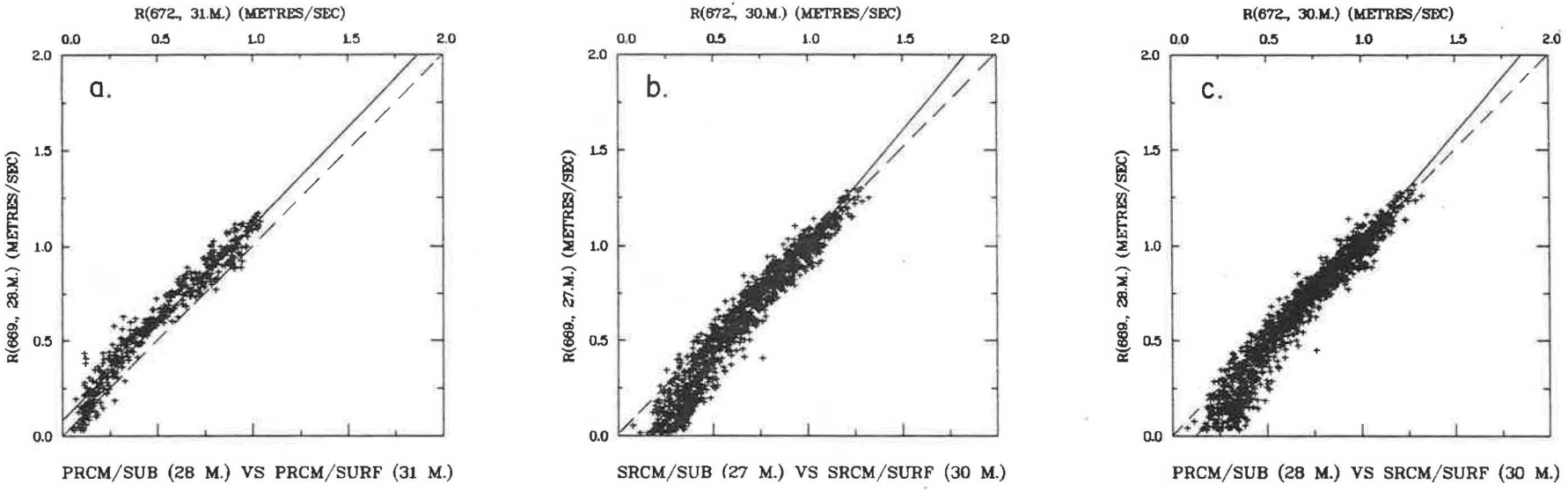
R(672., 31.M.) (METRES/SEC)
a.
R(669., 28.M.) (METRES/SEC)
PRCM/SUB (28 M.) VS PRCM/SURF (31 M.)
R(672., 30.M.) (METRES/SEC)
b.
R(669., 27.M.) (METRES/SEC)
SRCM/SUB (27 M.) VS SRCM/SURF (30 M.)
R(672., 30.M.) (METRES/SEC)
c.
R(669., 28.M.) (METRES/SEC)
PRCM/SUB (28 M.) VS SRCM/SURF (30 M.)
R(682., 12.M.) (METRES/SEC)
d.
R(672., 1.5 M.) (METRES/SEC)
VMCM/SURF (1.5 M.) VS VACM/SURF (12 M.)
R(682., 12.M.) (METRES/SEC)
e.
R(672., 1.M.) (METRES/SEC)
S4/SURF (1 M.) VS VACM/SURF (12 M.)

FIGURE 8 (a-e)

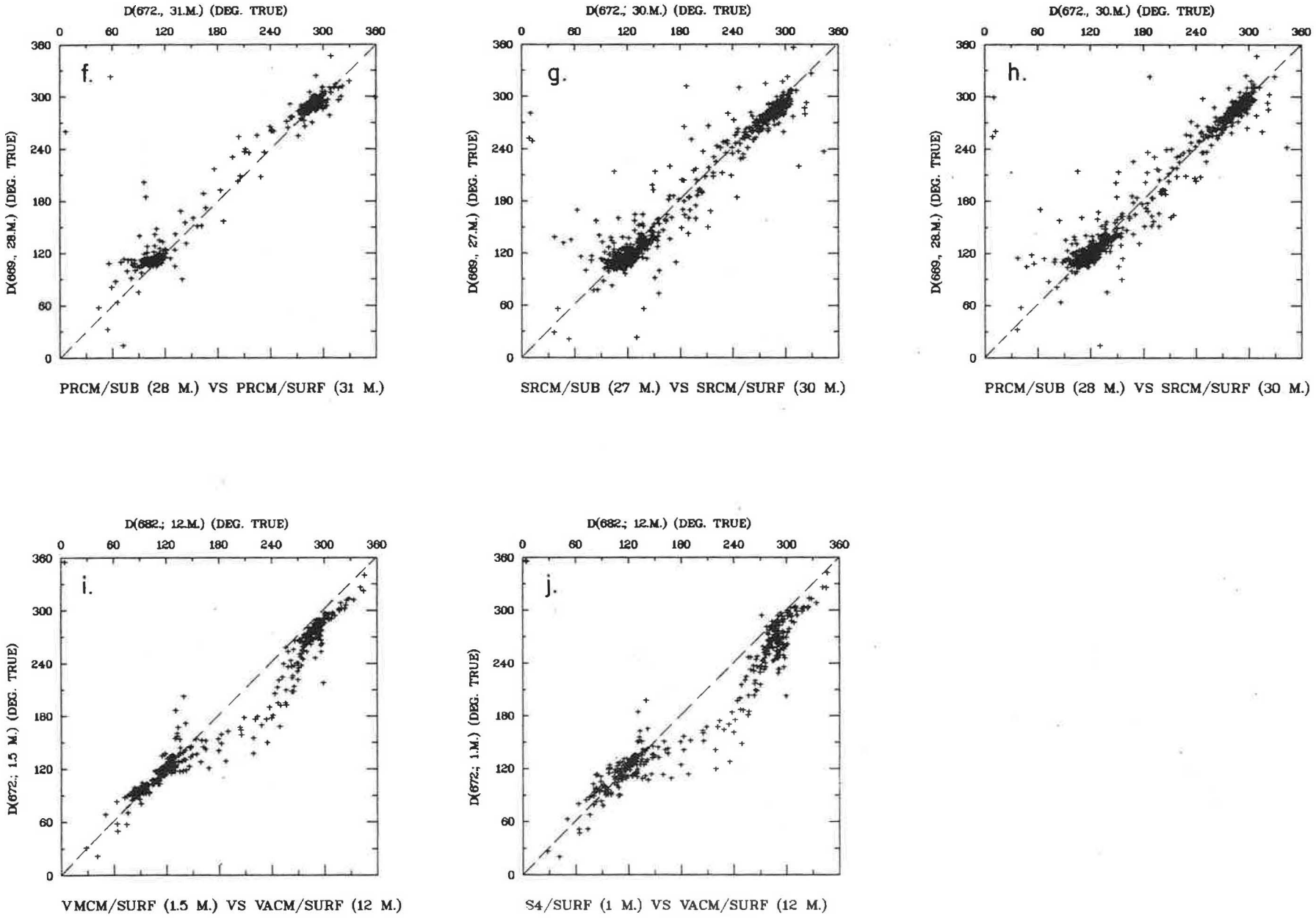
f.
D(672., 31.M.) (DEG. TRUE)
D(669., 28.M.) (DEG. TRUE)
PRCM/SUB (28 M.) VS PRCM/SURF (31 M.)
g.
D(672., 30.M.) (DEG. TRUE)
D(669., 27.M.) (DEG. TRUE)
SRCM/SUB (27 M.) VS SRCM/SURF (30 M.)
h.
D(672., 30.M.) (DEG. TRUE)
D(669., 28.M.) (DEG. TRUE)
PRCM/SUB (28 M.) VS SRCM/SURF (30 M.)
i.
D(682., 12.M.) (DEG. TRUE)
D(672., 1.5 M.) (DEG. TRUE)
VMCM/SURF (1.5 M.) VS VACM/SURF (12 M.)
j.
D(682., 12.M.) (DEG. TRUE)
D(672., 1.M.) (DEG. TRUE)
S4/SURF (1 M.) VS VACM/SURF (12 M.)
0
60
120
180
240
300
360

FIGURE 8 (f-j)

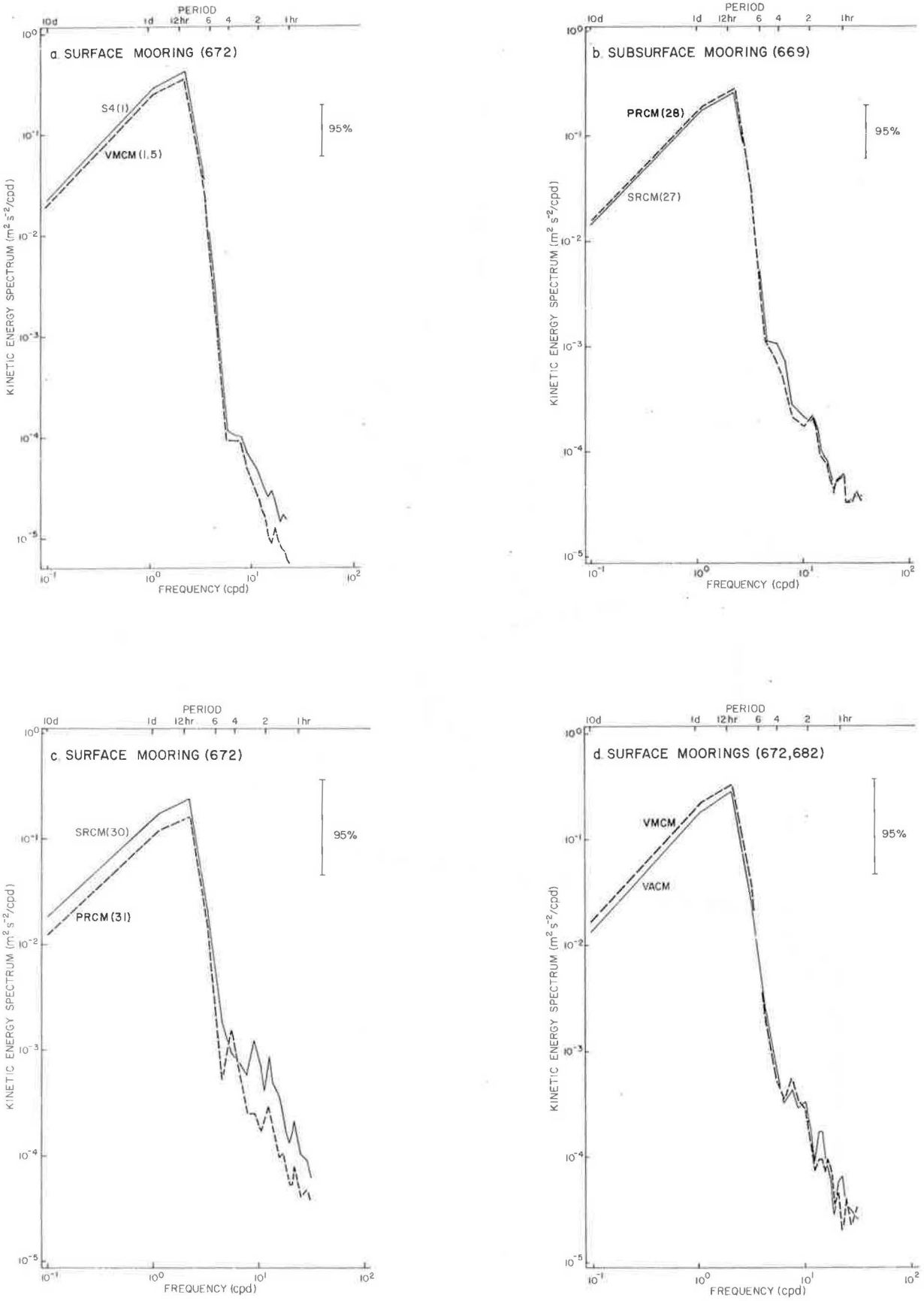
PERIOD
10d 1d 12hr 6 4 2 1hr
a. SURFACE MOORING (672)
S4(1)
VMCM(1,5)
95%
KINETIC ENERGY SPECTRUM (m² s⁻²/cpd)
FREQUENCY (cpd)
b. SUBSURFACE MOORING (669)
PRCM(28)
SRCM(27)
c. SURFACE MOORING (672)
SRCM(30)
PRCM(31)
d. SURFACE MOORINGS (672,682)
VMCM
VACM

FIGURE 9 (a-d)

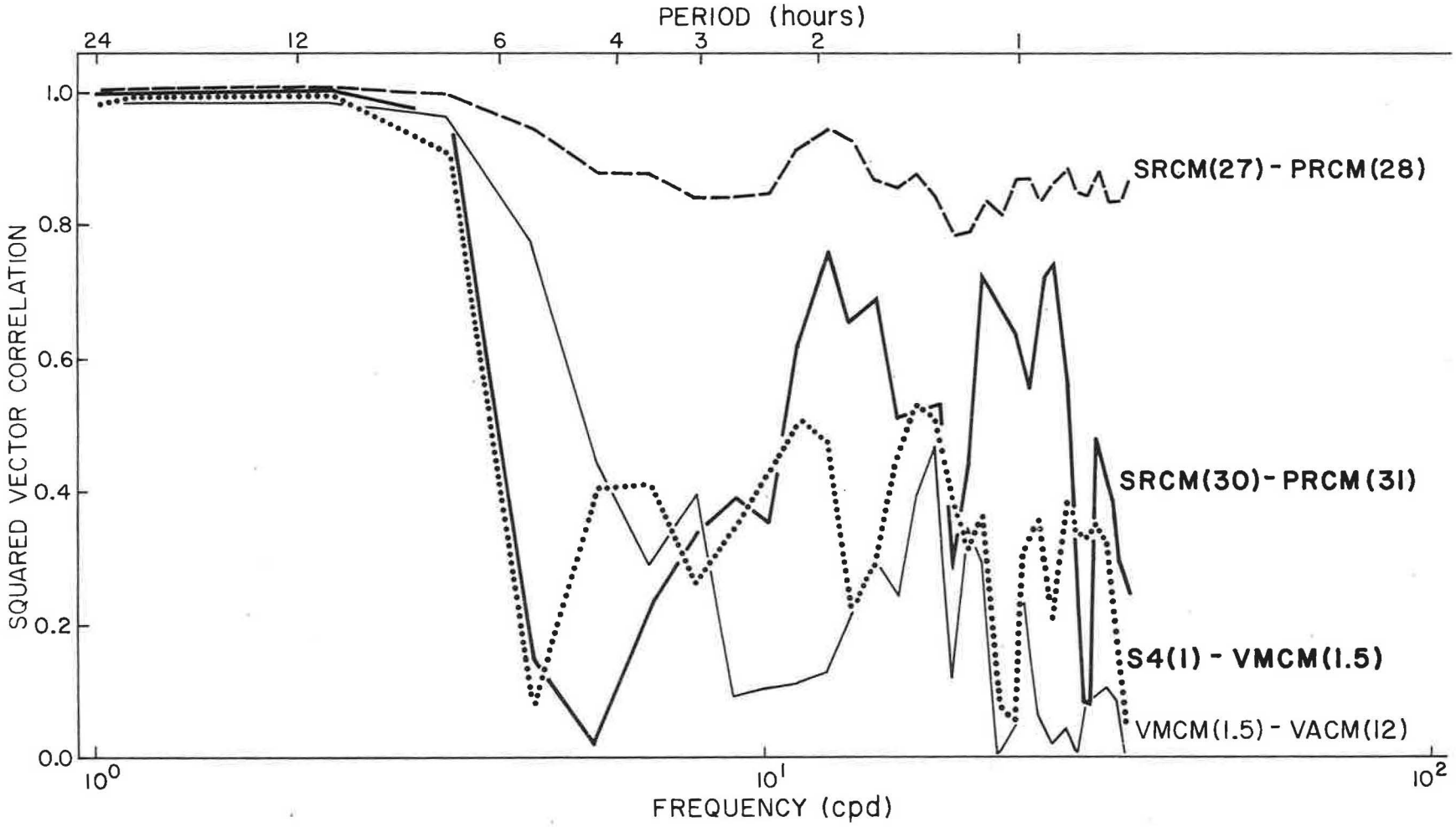
PERIOD (hours)
24
12
6
4
3
2
1
1.0
0.8
0.6
0.4
0.2
0.0
SQUARED VECTOR CORRELATION
SRCM(27) - PRCM(28)
SRCM(30) - PRCM(31)
S4(1) - VMCM(1.5)
VMCM(1.5) - VACM(12)
10^0
10^1
10^2
FREQUENCY (cpd)

FIGURE 10

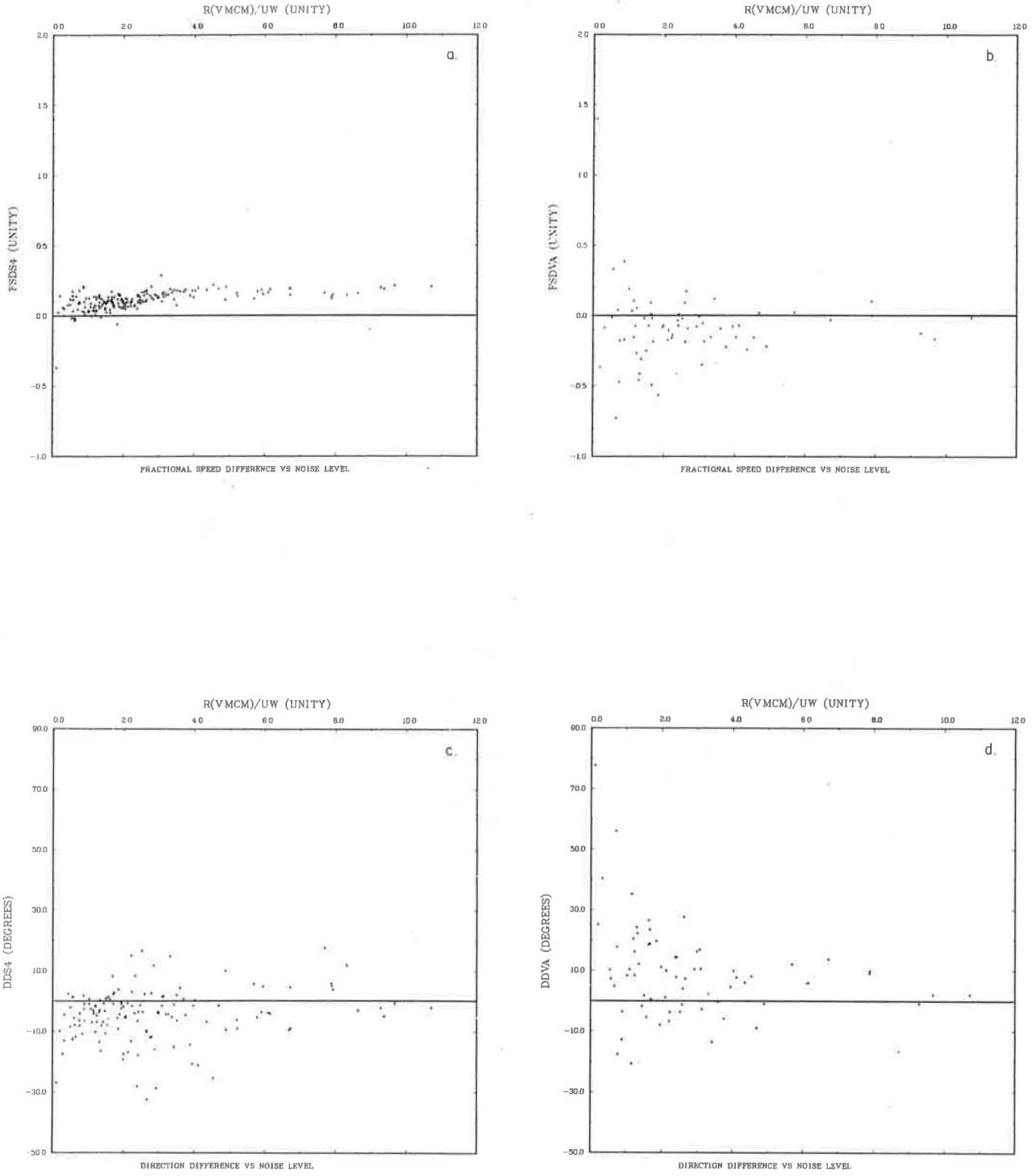
R(VMCM)/UW (UNITY)
a.
FSDS4 (UNITY)
FRACTIONAL SPEED DIFFERENCE VS NOISE LEVEL
R(VMCM)/UW (UNITY)
b.
FSDVA (UNITY)
FRACTIONAL SPEED DIFFERENCE VS NOISE LEVEL
R(VMCM)/UW (UNITY)
c.
DDS4 (DEGREES)
DIRECTION DIFFERENCE VS NOISE LEVEL
R(VMCM)/UW (UNITY)
d.
DDVA (DEGREES)
DIRECTION DIFFERENCE VS NOISE LEVEL

FIGURE 11 (a-d)

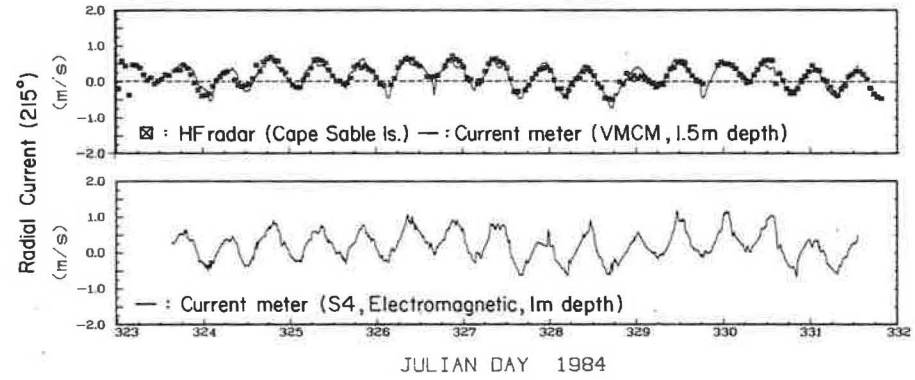
Radial Current (215°)
(m/s)
2.0
1.0
0.0
-1.0
-2.0
⊠ : HF radar (Cape Sable Is.) — : Current meter (VMCM, 1.5m depth)
— : Current meter (S4, Electromagnetic, 1m depth)
323
324
325
326
327
328
329
330
331
332
JULIAN DAY 1984

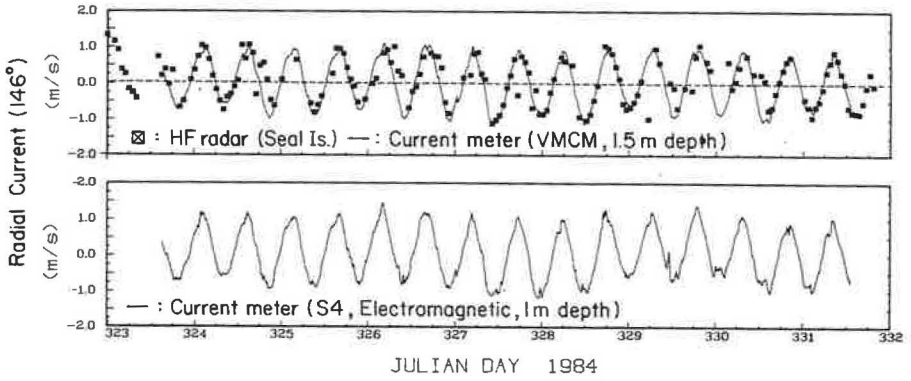
Radial Current (146°)
(m/s)
2.0
1.0
0.0
-1.0
-2.0
⊠ : HF radar (Seal Is.) — : Current meter (VMCM, 1.5 m depth)
— : Current meter (S4, Electromagnetic, 1m depth)
323
324
325
326
327
328
329
330
331
332
JULIAN DAY 1984

FIGURE 12

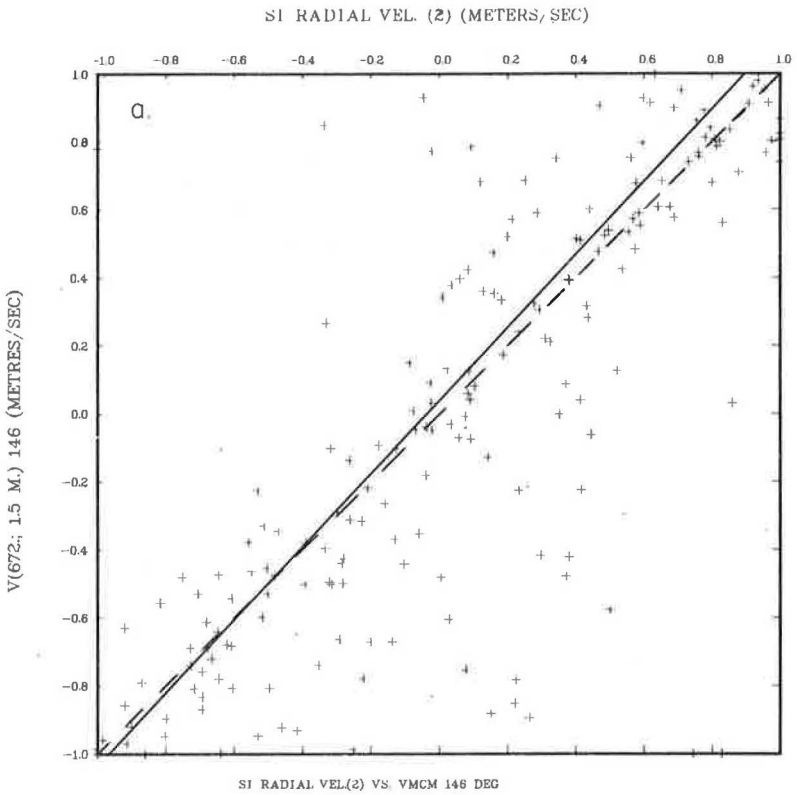
S1 RADIAL VEL. (2) (METERS/SEC)
a.
V(672.; 1.5 M.) 146 (METRES/SEC)
S1 RADIAL VEL(2) VS. VMCM 146 DEG

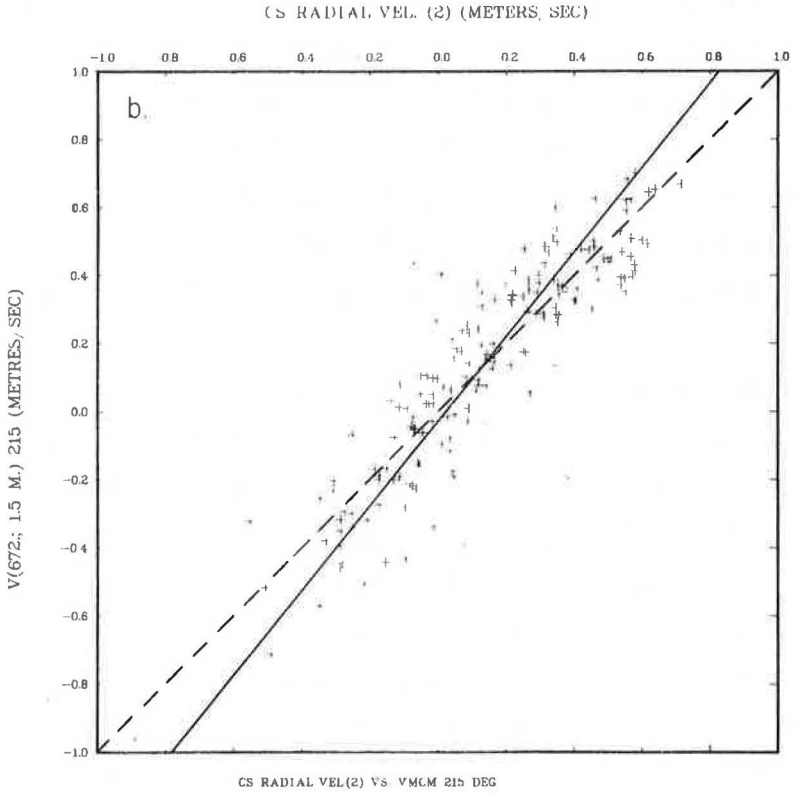
CS RADIAL VEL. (2) (METERS/SEC)
b.
V(672.; 1.5 M.) 215 (METRES/SEC)
CS RADIAL VEL(2) VS. VMCM 215 DEG

FIGURE 13 (a-b)

COMPARISON OF ADCP DATA AGAINST MOORED CURRENT METER DATA AND CALCULATED GEOSTROPHIC CURRENTS

Swein Østerhus[1] and Lars G. Golmen[2]
[1]Geophysical Institute, University of Bergen,
Allégaten 70, 5007 Bergen, Norway
[2]Norwegian Inst. for Water Research,
Breiviken 5, 5035 Bergen, Norway

1. INTRODUCTION

A joint Nordic oceanographic investigation in the area north of the Faroes was started in 1986. The main objective of this investigation is to get better estimates for the flux of Atlantic Water into the Norwegian Sea. The Faroe-Shetland Channel is assumed to be the main inflow route. Preliminary results from the present investigation indicate a substantial (eastward) flow of Atlantic Water also north of the Faroes (B. Hansen et al., 1986, 1988).

The primary basis for the present flow estimate is direct current measurements by current meters moored on the Faroe shelf slope. During the cruise in June 1986 a vertical north-to-south hydrographic section was made with the towed Sea-Soar undulator. The ship's towing track was close to the five current meter moorings C-G previously deployed (Figure 1.1). The ship mounted acoustic doppler current profiler (ADCP) was also actively sampling data during the Sea-Soar tow (Figure 1.2). The ADCP and Sea-Soar data sets were both collected mainly to resolve fine scale features of the hydrographic and current fields of the upper 300 metres. Also, one hoped to gain additional experience in the use of the very recently installed ADCP on board "Håkon Mosby". Deeper sections of additional lowered CTD profiles were made before and after the Sea-Soar/ADCP section.

The processing and analysis of ADCP data in our case requires additional information, especially from the ship's integrated navigation system. An accurate positioning system is crucial for the determination of the absolute current velocities when the ship is in deep water, with no doppler bottom contact. The quality of the data from the ship's navigation computer essentially determines the accuracy of the finally computed ADCP velocities. Other information, such as wind speed, direction, and waves may be important information when absolute velocities are to be determined. Due to our limited experience in the operation of the ADCP at the time of this particular cruise, such data may not have been systematically gathered. The synoptically gathered data from the moored current meters, as well as the Sea-Soar (hydrography) make possible an

inter-comparison among these three data sets. Possible error sources for the discrepancies among the data sets will be discussed, after a brief general presentation of the ADCP and hydrographic data.

2. THE FIELD PROGRAMME

2.1 CTD Measurements

On June 4 1986, a vertical hydrographic section was taken by means of the towed, undulating vehicle Sea-Soar. The section was taken from north to south, parallel with, and close to the line of current meter moorings previously described (Figure 1.1). The depth of the undulating Sea-Soar varied between approx. 40 metres and 350 metres. The undulation period was about 12 minutes, and the 175 km long section was completed in 13 hours. The Sea-Soar was equipped with a Neil Brown CTD. The CTD data were monitored (in practically real-time) on board the ship, and stored on digital tape for subsequent on-shore processing. Data from the ship's navigation system were merged in between the blocks of CTD data on the tape at regular time intervals (2 minutes). These navigation data provided the time-space base needed for the present analysis of the Sea-Soar as well as the ADCP data (see Chapter 3). For further details regarding the collection and monitoring of the Sea-Soar data on board "Håkon Mosby", see Golmen (1987). Additional lowered CTD data were collected along the same section both prior to and after the Sea-Soar tow. These data are not specifically reported on here.

2.2 The Acoustic Doppler Current Profiler

The R/V Håkon Mosby is equipped with a RD Instruments Acoustic Doppler Current Profiler System (ADCP). This ADCP operates by transmitting short acoustic pulses into the water from a hull mounted four beam transducer assembly. The transducer is transmitting at 150 kHz. The beams are each tilted 30^0 from the vertical, symmetrically in the athwartship, fore-aft directions. Backscattered sound is received by the transducer with a Doppler frequency shift proportional to the relative velocity between the scattering particles and the transducer. The vertical profile of frequency shift can be measured with a resolution of 128 depth bins. If the ship is operating in water depths shallower than approx. 500 metres, the ADCP measures ship velocity relative to the bottom. In deeper waters, only profiles of ship speed relative to the various backscattering layers are measured. For further details on the ADCP operation, see the RDI Operation and Maintenance Manual (RD Instruments 1985). During the present cruise the ADCP was operating with the optional depth resolution of 60 bins,

each bin corresponding to depth intervals of 8 metres. Water depth was generally far exceeding 500 metres, so only relative velocities were measured. The ADCP (raw) velocities are measured in the ship's coordinate system, but were automatically transformed into easting-northing coordinates by the ADCP system, after correction for ship's pitch, roll and heave, and taking into account the ship's gyro compass direction. 5-minutes vector averages of the velocities in each depth bin were calculated, and stored on diskettes for later processing.

2.3 Navigation System

The Nav-system on "Håkon Mosby" is an integrated system mainly consisting of TRANSSAT, Loran-C, DECCA and PULSE-8 receivers. Only Loran-C data were considered in the present data analysis, as these signals are strong near the Faroes. Accuracy is assumed better than 20 m. The 1-second values of Loran data were run through a "sliding mean" filter, and recorded on the Sea-Soar data tape at 2 min. intervals, together with other navigation information.

3. DATA PROCESSING

3.1 CTD Data

The CTD data consisted of one north-to-south section by Sea-Soar, plus several sections of lowered CTD data. The post-cruise processing of the Sea-Soar data is done in several steps. First the raw data tapes are run through a computer programme which does some editing and correcting of the CTD data, prior to low pass filtering and sub-sampling at 1-second intervals. The T-S curves of the profiles are finally checked, and possible bad data due to conductivity cell contamination are removed. The final and over all salinity calibration was based on lab-calibration of the conductivity sensor prior to and after the cruise. The CTD data of the Sea-Soar section are divided into "descending" and "ascending" profiles, each profile being given a unique station number. This method makes sorting and retrieval of Sea-Soar data easy, and the data are easily implemented in the standard CTD data base at the Geophysical Institute in Bergen. This method of organising the data implies only very small distortions of the mappings of the real T-S fields in vertical sections (a slight misinterpretation of horizontal gradient sizes may occur) (Golmen, 1987). Only data from Sea-Soar descents are analysed here. The data are coupled with (interpolated) navigation data to get the true positions of the start of each

Sea-Soar descent. This enables computation of distances between descents, and computation of geostrophic currents. The distance between each descent was typically around 3 km.

3.2 ADCP Data

After the cruise the 5-min. averages of ADCP profiles were merged with the separately collected navigation data. As the NAV data were stored at 2 min. intervals, interpolation of these data had to be done in order to get the best estimates of the positions of the ADCP profiles. Each ADCP profile was then given an unique number, and assigned a (mean) value of ship speed (absolute) and heading, as calculated from the navigation data. East and north components of absolute ADCP velocities were then calculated by subtracting the ship velocity from each depth bin's relative velocity value. The "station" profiles were then stored in the same format as regular lowered CTD stations, and the velocity field can be presented e.g., as vertical computer contoured sections. In periods when the ship was changing direction or speed, the merging of ADCP and NAV data as explained above had its definite shortcomings. This resulted systematically in large and unexpected deviations in the ADCP velocities, relative to profiles from before and after these periods. Slowing down of the ship was done at regular intervals, in order to let the Sea Soar sink down into the deep water for calibration purpose. Also some course changes were deliberatedly made, in order to approach the current metre rigs as close as possible. Due to the resulting errors, we have chosen certain criteria for flagging an ADCP profile as good or bad. In the present case, profiles sampled while the ship had been subject to a speed or course change greater than 10 cm/s (.2 knots) or 2^0 respectively, were rejected. Thus some areas will have less data coverage than others.

4. DATA PRESENTATION

4.1 Sea-Soar Data

Figure 4.1 (upper two frames) shows computer contoured vertical sections of temperature and salinity, as observed by Sea-Soar. The most prominent feature is the wedge of Atlantic Water, stretching about 100 kilometres northwards from the northern Faroe shelf break. Sub-surface fronts may be seen within the Atlantic Water, with associated upwelling features and smaller patches of anomalous water in the frontal region. These patches are not resolved in the lowered CTD sections. The highest core values of salinity in the Atlantic Water slightly

exceeded 35.25, with core depths around 100 metres (Sta. 817-818). The bottom depth at these two profiles is around 430 metres. A second high salinity core with salinities near 35.23 is found farther north, at a bottom depth of 800 metres (Sta. 519.801). Two distinct cores, one above the other, are observed close to the main front, at about $63^0$30'N. The upper one represents a distinct salinity minimum, with values near 34.87 at 150 m depth. This water must be of Arctic and/or Icelandic origin, from north of the Sub-Arctic Front. The lower core has salinity values slightly exceeding 34.93. Possibly this can be a northward extending filament of water from the front proper, intersecting the large scale dome of low salinity water. The lowest salinity values are found at Sta. 810, with values below 34.70 at 300 m depth. This cold, and low salinity water intersects the wedge of Atlantic Water vertically through the whole column.

Figure 4.1 also shows the vertical section of derived geostrophic velocity. Negative values (-dotted lines) represent a westward flow. Two distinct regions with high values (30-50 cm/s) of eastward flow is seen, at $63^0$05'N and $63^0$25'N respectively. The magnitude of the velocities are comparable to the geostrophic velocities as computed from other lowered CTD sections from during the investigation. Also the two distinct geostrophic "jets" seem to have been a permanent feature during the 10 day investigation period.

4.2 ADCP data

Figure 4.2 shows arrow plots of ADCP velocities at 50m, 100m and 200m respectively. ADCP profiles from periods of course or speeed change have been sorted out (see para. 3.2). The heavy arrows indicate the measured current velocities by moored Aanderaa current meters, at the time when the ship was close to the mooring.

The most prominent feature of the measured ADCP velocities is the vertical homogeneity, i.e. small changes in speed or direction with depth. This is further demonstrated in Figure 4.3, where vertical sections of ADCP speed, east component and vertical comp. are presented. The whole transect shows significant eastward velocity components, also in the area north of the main front (Figure 4.1). Close to the main front, at $63^0$30'N, the ADCP shows a relative minimum in speed. Unfortunately several ADCP profiles were rejected in this area, due to irregular ship motion (see para. 3.2), so the very minimum values are probably not resolved in the plots. A second region of lower speed values is seen around 63^0N. The ADCP speed typically range from 20 to 50 cm/s. There is a tendency

towards larger southward velocity components in the southern part of the transect. The vertical velocity component of the ADCP is shown in Figure 4.3, lower frame. Values in mm/s. The data quality of velocity component is sensitive to calibration (ship's ballasting), and these data generally are not reported. According to the RDI manual (RD Instruments 1985), positive values are downwards. The vertical velocities as shown in Figure 4.3 range between 0 and 10 mm/s downwards, with generally the higher values found at depth. A more recent RDI ADCP manual says the vertical velocity is positive upwards. When overlying the hydrographic sections with the vertical velocity section, even the relative values of our vertical velocities indicate a sign error in our data. Upwelling hydrographic features near the main front coincides with maximum downward velocities.

5. DISCUSSION

A comparison of the section of geostrophic velocity (Figure 4.1) against the observed ADCP east component (Figure 4.3) shows a general consistency. However, the two distinct geostrophic "jets" around 63.5^0 and 63^0N does not exactly coincide with the ADCP "jets". The two main ADCP jets are found some 5-15 km south of the corresponding geostrophic jets. Possible trivial causes for this discrepancy have been sought for, as e.g. difference in the time bases for the data sets, or different distance computations. No obvious errors have been found. The data seem to reflect an observed spatial de-coupling of the geostrophic and ageostrophic current fields. Similar direct comparisons of deep water ADCP and geostrophic data are sparse among the literature. Shears have been compared, however, and results range from very bad correlation (Regier, 1982) to excellent (Chereskin et al. 1987). We have not included any shear calculations in this presentation.

The Aanderaa measured speed is generally smaller than the ADCP speed by 10 to 50 percent. The ADCP velocities are more easterly as compared with the Aanderaa velocities. The angle deviations are typically in the range 30 to 60 degrees. Generally the absolute accuracy of the ADCP is reckoned to be within 10 cm/s at a ship speed of 7 knots, (T.M. Joyce et al. 1982). An overall comparison of Aanderaa and ADCP speeds seem to indicate that this does not hold for our data. The angle deviations are unexpectedly large. There are several factors that influence the angle calculations. Uncertainties in transducer beam angle, misalignment of the ADCP transducer relative to the foreaft direction, as well as gyro compass error are obvious candidates. Mis-alignment is believed to be within +/- 1^0, and if so, will cause only a minor error. The gyro-compass was

not checked during our cruise, but experience has shown that the error may be as large as +/- 5^0. These possible errors may explain some of, but probably not the whole observed angle deviation. Our ADCP data suggest that an overestimation of the across-ship current component is done, as the cruising direction always was close to 180^0. During the cruise the wind had a westerly component. The gyro compensation while navigating is due to the combined effect of surface current and wind, which in our case both had east-going components. A positive deviation of the gyro leads in our case to an overestimation of the east component, as well as current speeds. The error in this component is expressed as U_s*sin a, where U_s is ship speed, and a is the deviation, or error in the momentary gyro reading. As U_s is of order 400 cm/s, a small value of a can cause significant errors in derived current components.

As a precaution against too much noisy ADCP data, we recommend to use autopilot with a constant GYRO heading, instead of attempting a predescribed sail direction. This will reduce the number of "bad" profiles due to temporary course changes. When sailing in regions of horizontal shear, the ship may experience sudden momentary course changes. The true zig-zag sail line is represented as a straight line when averaging (over e.g. 5 min.), which results in (some) underestimation of averaged ship speed.

REFERENCES

Chereskin, T.K., Halpern, D and Regier, L.A. 1987. Comparison of Shipboard Acoustic Doppler Current Profiler and Moored Current Measurements in the Equatorial Pacific. Journ. Atm. Ocean. Techn. Vol. 4, No. 4.

Golmen, L.G. 1987. Profiling the upper ocean by means of the towed vehicle Sea-Soar. ICES paper C.M.1987/C:2.

Hansen, B., Malmberg, S.A., Sælen O.H. and Østerhus, S. 1986. Measurements of flow north of the Faroe Islands June 1986. ICES paper C.M.1986/C:12.

Hansen, B., Sælen, O.H. and Østerhus, S. 1988. The passage of Atlantic Water east of the Faroe Islands. ICES paper C.M. 1988/C:29.

Joyce, T.M., Bitterman, D.S.,Jr. and Prada, K.E. 1982. Shipboard acoustic profiling of upper ocean currents. Deep Sea Res. Vol. 29, No. 7A.

RD Instruments 1985. RD-VM Acoustic Doppler Current Profiler Operation and Maintenance Manual. RDI, San Diego, Ca.

Regier, L. 1982. Mesoscale Current Fields Observed with a Shipboard Profiling Acoustic Current Meter. Journ. Phys. Ocean., Vol. 12.

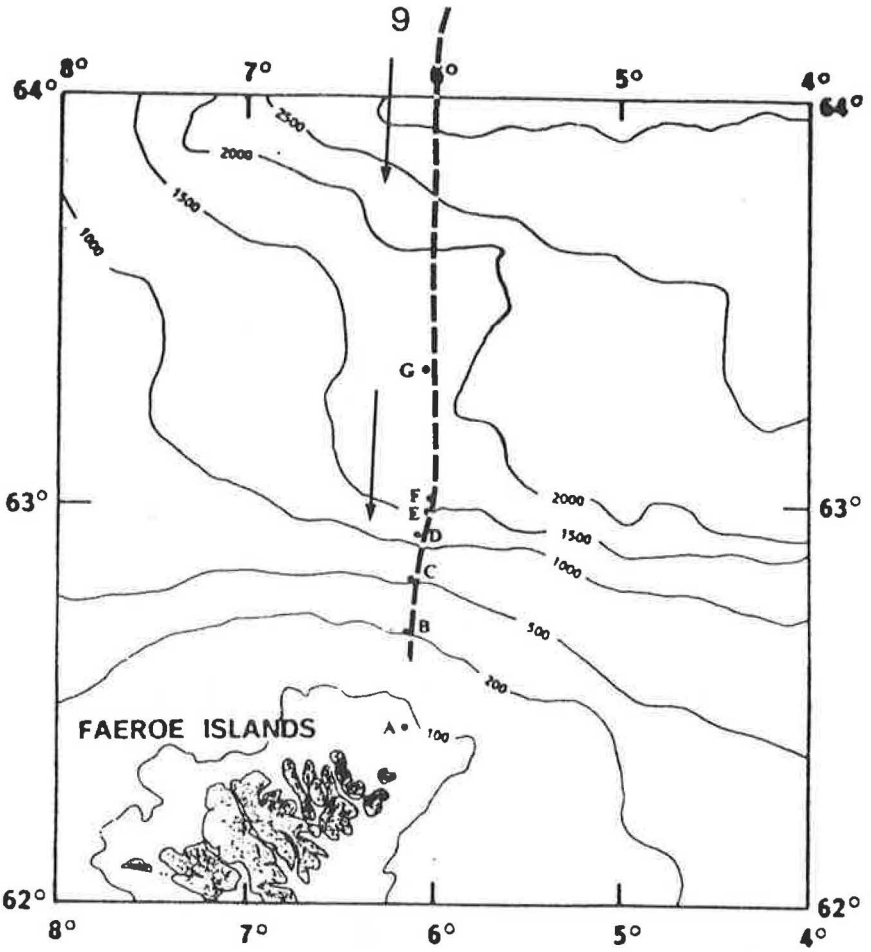

Fig. 1.1. Map of the investigation area, with bottom depth contours indicated. The dashed line shows the ship's cruising track. Arrows indicate cruising direction. Dots show positions of the current meter rigs.

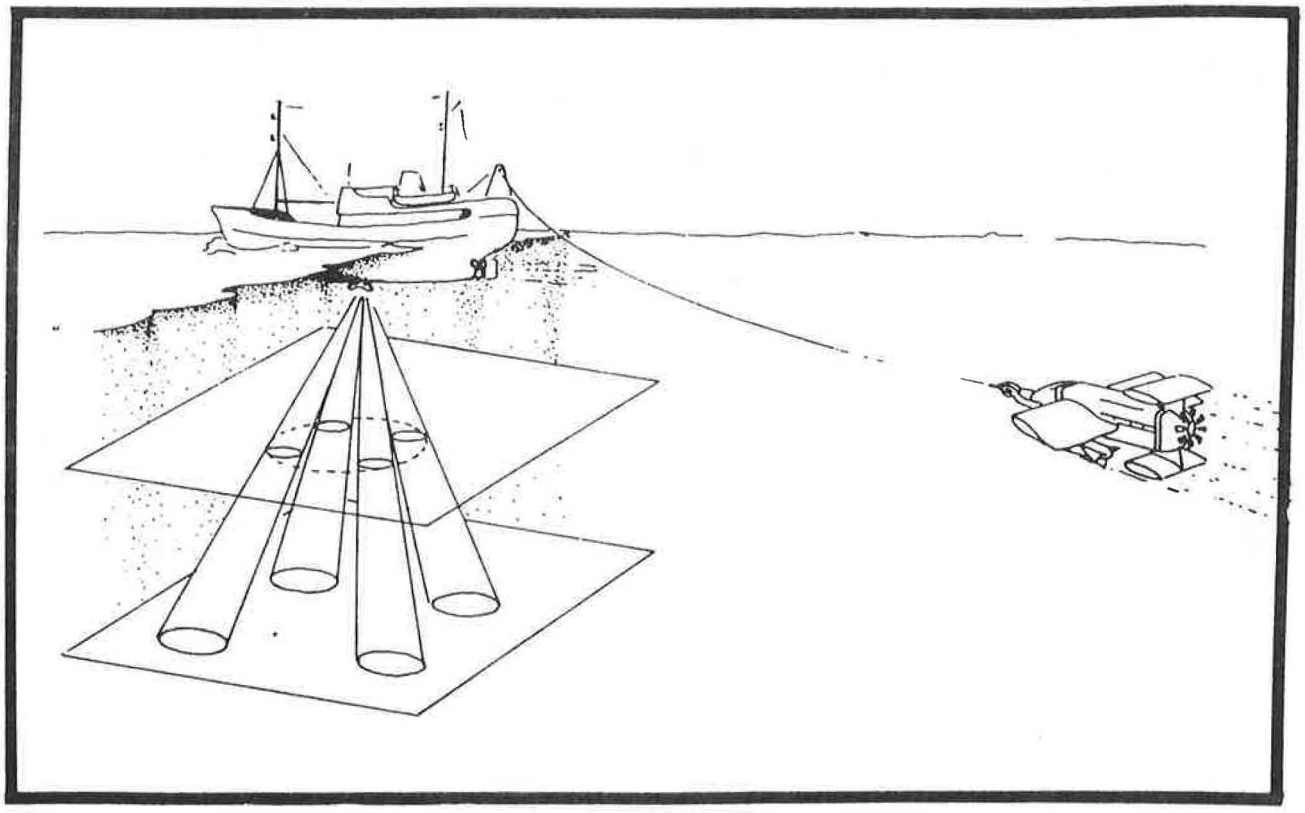

Fig. 1.2. Scetch of the ADCP and Sea-Soar in operation.

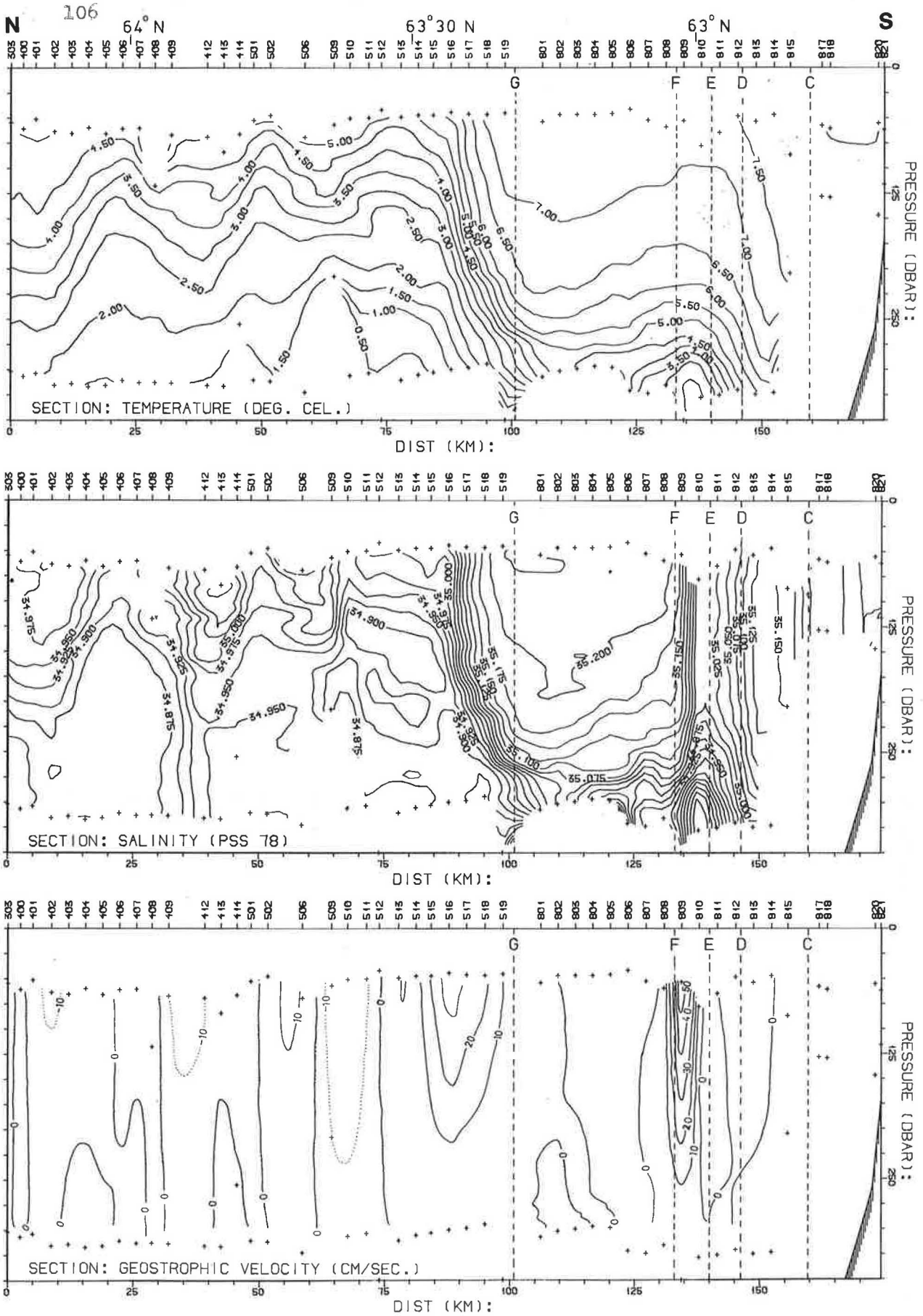

Fig. 4.1. Vertical sections of temperature, salinity and calculated geostrophic velocity, as observed by Sea-Soar. The "+" signs indicate minimum and maximum observation depths. Vertical lines show position of current meter rigs.

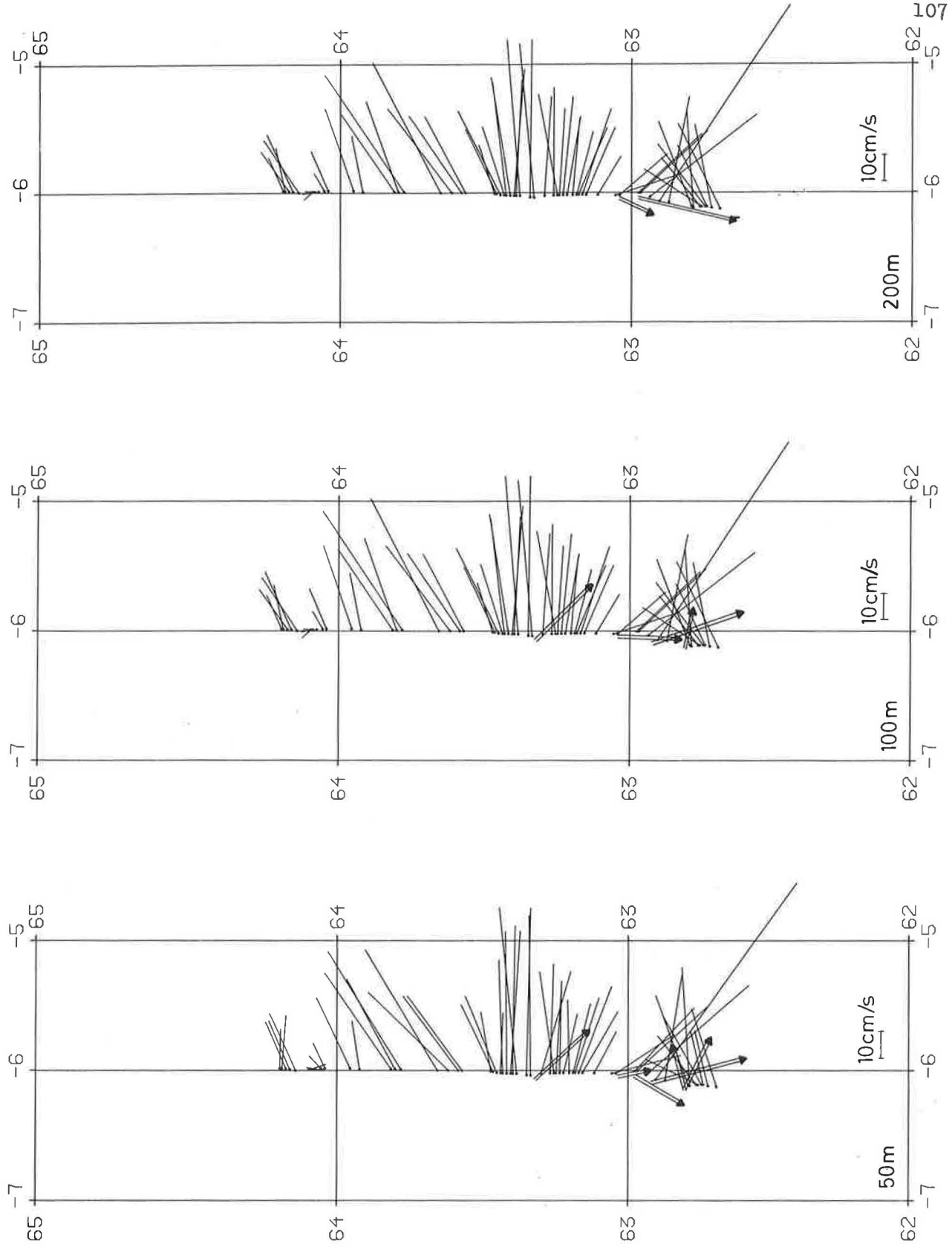

Fig. 4.2. Arrow plots of ADCP velocities at 50m, 100m and 200 m. The heavy arrows show the corresponding measured current meter (Aanderaa RCM) velocities. ADCP velocities are rejected where the ship excessively changed course or speed (see text).

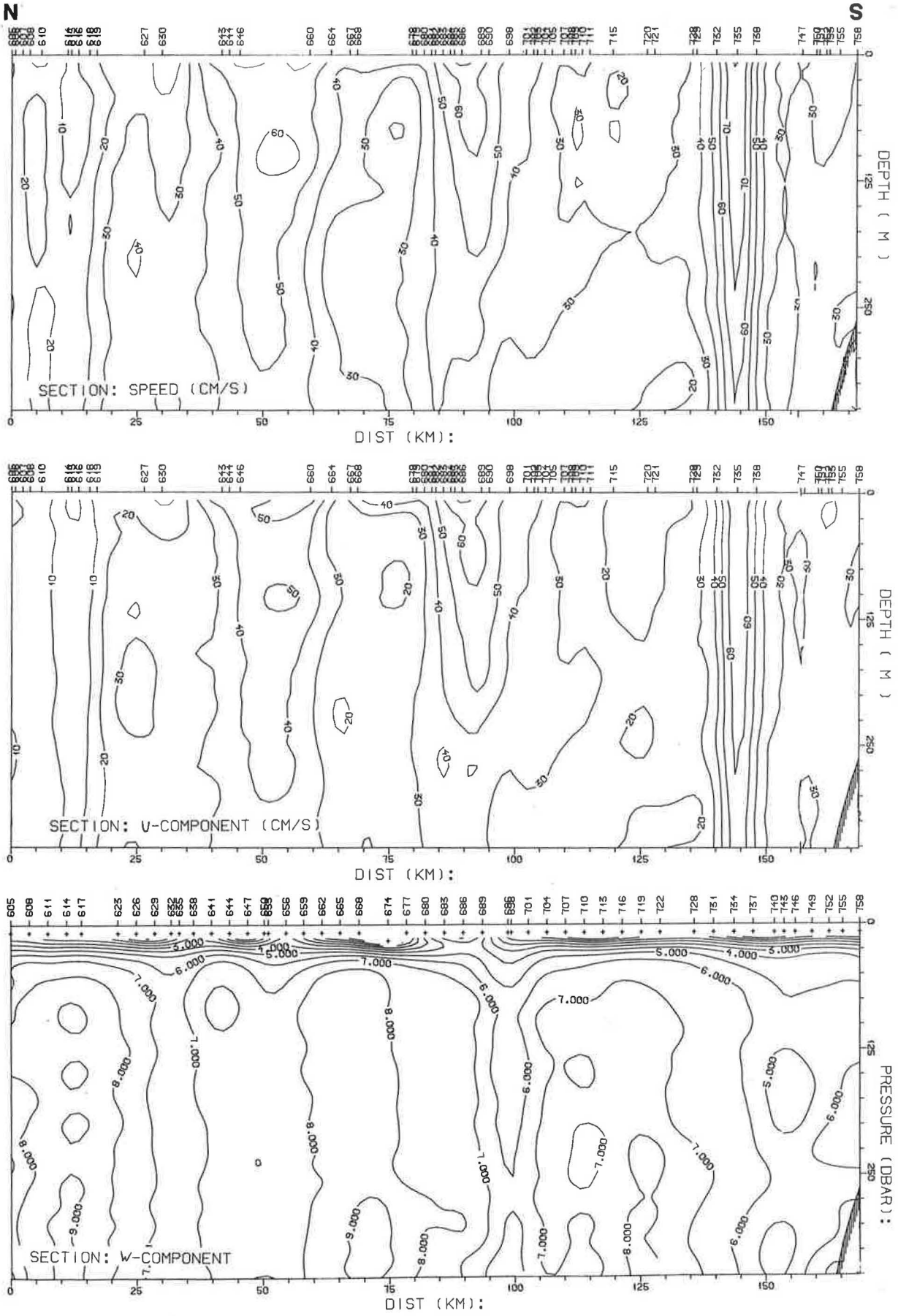

Fig. 4.3. Vertical sections of computer contoured ADCP current speed, east (U) component and vertical (W, mm/s, positive down) component Numbers on top of frames indicate individual ADCP profiles.

Indication of spine colours

Reports of the Advisory Committee on Fishery Management	Red
Reports of the Advisory Committee on Marine Pollution	Yellow
Fish Assessment Reports	Grey
Pollution Studies	Green
Others	Black

-o-o-o-